

Copyright Undertaking

This thesis is protected by copyright, with all rights reserved.

By reading and using the thesis, the reader understands and agrees to the following terms:

- 1. The reader will abide by the rules and legal ordinances governing copyright regarding the use of the thesis.
- 2. The reader will use the thesis for the purpose of research or private study only and not for distribution or further reproduction or any other purpose.
- 3. The reader agrees to indemnify and hold the University harmless from and against any loss, damage, cost, liability or expenses arising from copyright infringement or unauthorized usage.

IMPORTANT

If you have reasons to believe that any materials in this thesis are deemed not suitable to be distributed in this form, or a copyright owner having difficulty with the material being included in our database, please contact lbsys@polyu.edu.hk providing details. The Library will look into your claim and consider taking remedial action upon receipt of the written requests.

SENSORIMOTOR INTEGRATED EXO-NEUROMUSCULO-SKELETON (ENMS) WITH ELECTRO-VIBROFEEDBACK FOR WRIST/HAND REHABILITATION AFTER STROKE

LIN LEGENG

PhD

The Hong Kong Polytechnic University

The Hong Kong Polytechnic University

Department of Biomedical Engineering

Sensorimotor Integrated Exo-neuro-musculo-skeleton (ENMS) with Electro-vibro-feedback for Wrist/hand Rehabilitation after Stroke

Lin Legeng

A thesis submitted in partial fulfilment of the requirements for the degree of Doctor of Philosophy

December 2024

CERTIFICATE OF ORIGINALITY

I hereby declare that this thesis is my own work and that, to the best of my knowledge and belief, it reproduces no material previously published or written, nor material that has been accepted for the award of any other degree or diploma, except where due acknowledgement has been made in the text.

	(Signed)		
Lin Legeng	(Name of student)		

ts that nurtured me,	

ABSTRACT

Sensorimotor integration (SMI) is often disrupted after stroke, hindering the functional recovery effects of robot-assisted upper limb (UL) training. Although proprioception experiences could be provided in movement assisted by robots with pure mechanical actuation (pure robot), the rehabilitative effects on UL are still limited, especially for the distal joints, i.e., wrist/hand (W/H). Neuromuscular electrical stimulation (NMES) and mechanical robot hybrid system (NMES-robot) could lead to faster motor recovery for W/H joints than the pure robot. However, NMES as electrical stimulations is not applicable to flexor digitorum (FD) because it leads to pain, muscle fatigue, and higher muscle spasticity on FD in long-term usage.

Compared to NMES, focal vibratory stimulation (FVS) without causing muscle contraction holds the potential to be more suitable than NMES for somatosensory priming on FD, which usually has sufficient residual voluntary force after stroke. However, little is known about the differences between the transient neuromodulatory effects of FVS and NMES poststroke. Besides, little work has been done on the optimized integration of FVS and NMES in robot design for somatosensory priming of target muscles in rehabilitation after stroke. Furthermore, the feasibility and rehabilitative effects of the integrated device with somatosensory priming from NMES and FVS are still unclear in robot-assisted rehabilitation training.

Therefore, the main objectives of this study were: (i) to investigate and compare the immediate neuromodulatory effects of FVS and NMES at the cortical level in poststroke and unimpaired persons; (ii) to integrate FVS and NMES into a hybrid robotic system for W/H rehabilitation after stroke; (iii) to evaluate the effectiveness of the new system in W/H rehabilitation and analyze the neuroplastic mechanisms of functional recovery. The study was conducted as follows:

The first section investigated the immediate neuromodulatory effects of FVS and NMES at the cortical level after stroke. Cortical responses in persons with chronic stroke (N = 15) and unimpaired controls (N = 15) were measured by whole-brain electroencephalography (EEG) when FVS and NMES at different intensities were applied transcutaneously to the forearm muscles, i.e. extensor digitorum (ED) and FD. Results showed that both FVS and NMES effectively activated the sensorimotor cortex after stroke. However, FVS was particularly effective in eliciting transient involuntary attention, while NMES primarily fostered the cortical responses of the targeted muscles in the contralesional motor cortex.

The second section designed a novel electromyography (EMG)-driven exoneuromusculoskeleton with electro-vibro-feedback (ENMS-EVF) that integrates NMES on the ED and FVS on the FD into a wearable exoskeleton with soft pneumatic muscles for somatosensory priming in poststroke W/H rehabilitation. Participants with chronic stroke (N=7) were recruited to participate in a validation test and a preliminary training program containing 20-session rehabilitation training assisted by the new system. The evaluation outcomes were measured before and after the training program, as well as after the 10^{th} session of training, including sensorimotor clinical scores. The results validated the effectiveness of the system's design and parameter and task settings for the intended rehabilitative applications. The ENMS-EVF-assisted training program could facilitate sensorimotor improvement in the affected upper limb of the participants with chronic stroke.

The third section evaluated the long-term effectiveness of the ENMS-EVF system in W/H rehabilitation and analyzed the neuroplastic mechanisms of functional sensorimotor recovery after rehabilitation training. Participants with chronic stroke (N = 15) were recruited to undergo a 20-session rehabilitation training program assisted by ENMS-EVF. The evaluation outcomes were measured before, after, and three months after the training, including sensorimotor clinical scores and corticomuscular electrophysiological features. The results demonstrated that the system was feasible and

effective for improving UL sensorimotor functions in robot-assisted somatosensory priming after stroke because of sustained neuroplasticity of enhanced contralateral control of agonist muscles and ascending somatosensory feedback from antagonist muscles during W/H extension.

In conclusion, this study compared the immediate neuromodulatory effects of FVS and NMES, confirming the effectiveness of FVS for somatosensory stimulation and contributing to our understanding of their potential tailored applications in stroke rehabilitation. In addition, this study designed and validated the novel ENMS-EVF system, which is feasible and effective for assisting stroke patients in improving sensorimotor functions of UL after the training program. Moreover, long-term rehabilitation effects and neuroplasticity changes after ENMS-EVF-assisted training sheds light on the rehabilitative effects of robot-assisted somatosensory priming on sensorimotor functions and its underlying cortical and pathway-specific corticomuscular mechanisms after stroke, providing significant insights for developing more effective interventions toward SMI rehabilitation in the future.

PUBLICATIONS ARISING FROM THE THESIS

Journals:

- (1) <u>Lin, L.</u>, Qing, W., Huang, Y., Ye, F., Rong, W., Li, W., Jiao, J., & Hu, X. (2024). Comparison of Immediate Neuromodulatory Effects between Focal Vibratory and Electrical Sensory Stimulations after Stroke. *Bioengineering*, 11(3), 286. https://doi.org/10.3390/bioengineering11030286
- (2) <u>Lin, L.</u>, Qing, W., Zheng, Z., Poon, W., Guo, S., Zhang, S., & Hu, X. (2024). Somatosensory integration in robot-assisted motor restoration post-stroke. *Frontiers in Aging Neuroscience*, 16, 1491678. https://doi.org/10.3389/fnagi.2024.1491678
- (3) <u>Lin, L.</u>, Qing, W., Kuet, M.-T., Zhao, H., Ye, F., Rong, W., Li, W., Huang, Y., & Hu, X. (2025). Sensorimotor Integration (SMI) by Targeted Priming in Muscles with EMG-driven Electro-Vibro-Feedback in Robot-Assisted Wrist/Hand Rehabilitation after Stroke. *Cyborg and Bionic System*. Submitted.
- (4) Qing, W., Song, H., <u>Lin, L.</u>, Ye, F., & Hu, X. Cyber-paired telerehabilitation assisted by ankle-foot exoneuromusculoskeleton for poststroke patients: interventional study evaluating feasibility and efficacy. Under Preparation.
- (5) Kizyte, A*, Zhang, H.*, <u>Lin, L.</u>, Wang, R., & Hu, X. Advancing CMC analysis in stroke: EEG coupled with motor unit spike train data. Under preparation.

Conference publications and presentations:

(1) <u>Lin, L.</u>, Kuet, M.-T., Qing, W., Zhao, H., Ye, F., Huang, Y., & Hu, X. (2024). Effects of sensorimotor-integrated (SMI) wrist/hand rehabilitation on pathway-specific corticomuscular coherence poststroke. In *46th Annual International*

- Conference of the IEEE Engineering in Medicine and Biology Society (EMBC). Orlando, FL, USA.
- (2) <u>Lin, L.</u>, Kuet, M.-T., Qing, W., Zhao, H., Ye, F., Huang, Y., & Hu, X. (2024). Sensorimotor-integrated (SMI) wrist/hand rehabilitation assisted by hybrid soft robot with electro-vibro-feedback poststroke. In *11th World Congress on Bioengineering (WACBE)*. Hong Kong SAR, P. R. China.
- (3) <u>Lin, L.</u>, Kuet, M.-T., Qing, W., Zhao, H., Ye, F., Huang, Y., & Hu, X. (2024). Effects of sensorimotor-integrated (SMI) wrist/hand rehabilitation assisted by a hybrid soft robot poststroke. In 2024 International Convention on Rehabilitation Engineering and Assistive Technology (i-CREATe 2024). Shanghai, P. R. China. https://doi.org/10.1109/i-CREATe62067.2024.10776482
- (4) <u>Lin, L.</u>, Kuet, M.-T., Qing, W., Zhao, H., Ye, F., Huang, Y., & Hu, X. (2024). Hybrid soft robot with electro-vibro-feedback for sensorimotor-integrated (SMI) rehabilitation after stroke. In *Hong Kong Medical and Healthcare Device Industries Association (HKMHDIA) Student Research Award*. Hong Kong SAR, P. R. China.
- (5) Qing, W., Song, H., <u>Lin, L.</u>, Ye, F., & Hu, X. (2024). Self-help cyber-paired telerehabilitation assisted by an ankle-foot exoneuromusculoskeleton for patients with stroke. In *18th World Congress of the International Society of Physical and Rehabilitation Medicine (ISPRM)*. Sydney, Australia.
- (6) Qing, W., Song, H., <u>Lin, L.</u>, Ye, F., & Hu, X. (2024). Effects of exoneuromusculoskeleton-assisted lower limb telerehabilitation on poststroke muscular compensation. In *11th World Congress on Bioengineering (WACBE)*. Hong Kong SAR, P. R. China.
- (7) Song, H., Qing, W., <u>Lin, L.</u>, Ye, F., & Hu, X. (2024). Effects of exoneuromusculoskeleton (ENMS) assisted home-based self-help

- telerehabilitation on gait symmetry in chronic stroke. In 11th World Congress on Bioengineering (WACBE). Hong Kong SAR, P. R. China.
- (8) Qing, W., Song, H., <u>Lin, L.</u>, Ye, F., & Hu, X. (2024). Reorganization of undirected and directed cortico-muscular connectivity after exoneuromusculoskeleton-assisted telerehabilitation. In *2024 International Convention on Rehabilitation Engineering and Assistive Technology (i-CREATe 2024)*. Shanghai, P. R. China. https://doi.org/10.1109/i-CREATe62067.2024.10776416

Book chapter:

(1) <u>Lin, L.</u>, Nam, C., Hu, X. (2024). Chapter 7: Mobile upper limb robots for self-help telerehabilitation. In X. Hu (Ed.), *Automation in Tele-Neurorehabilitation*. CRC Press. In press.

ACKNOWLEDGEMENTS

First and foremost, I would like to express my deepest gratitude to my supervisor, Dr. HU Xiaoling. Your exceptional expertise, unwavering guidance, and rigorous approach to scientific research have profoundly influenced my academic and personal growth. Thank you for your continuous support, immense patience, and encouragement over the past three years. It has been a privilege and an honor to study under your supervision.

I am also sincerely thankful to my lab colleagues and collaborators for their invaluable contributions and support throughout my research. My heartfelt thanks go to Miss. QING Wanyi, Dr. HUANG Yanhuan, Dr. YE Fuqiang, Dr. ZHOU Sa, Dr. GUO Ziqi, Mr. KUET Man-Ting, Mr. ZHAO Hengtian, and Dr. JIAO Jiao for their assistance with experiments, clinical assessments, patient training, and data processing. I sincerely thank Mr. ZHOU Xingzhi, Mr. SONG Hantao, Miss. WANG Maner, Miss. ZHANG Hanxun, Mr. FAN Zhuyao, Mr. IP Winchun, Mr. TAN Fangning, Dr. NAM Chingyi, Mr. PAN Changjie, Miss. Asta Kizyte, Miss. FAN Yiming and Dr. YANG Bibo for their valuable suggestions and encouragement. I would also like to extend special thanks to Mr. RONG Wei and Mr. LI Waiming for their crucial technical support.

I owe a great deal to all the experimental participants whose willingness to contribute and share invaluable data formed the foundation of this research. Your participation has been indispensable.

Lastly, I would like to express my heartfelt appreciation to my family and partner. Your unwavering love, care, and encouragement have been my greatest source of strength throughout this journey. You have been my steadfast supporters and cheerleaders, and your sacrifices mean more to me than words can express. Thank you for always believing in me.

TABLE OF CONTENTS

CERTIFICATE OF ORI	IGINALITY
---------------------------	-----------

ABSTRACT	I
PUBLICATIONS ARISING FROM THE THESIS	IV
ACKNOWLEDGEMENTS	VII
TABLE OF CONTENTS	VIII
LIST OF FIGURES	XI
LIST OF TABLES	XVII
LIST OF ABBREVIATIONS	XVIII
LIST OF APPENDICES	XX
CHAPTER 1 INTRODUCTION	1
1.1 Background of wrist/hand rehabilitation after stroke	2
1.2 Sensorimotor integration in motor restoration after stroke	3
1.3 Rehabilitation robots for W/H training after stroke	5
1.4 Hybrid robotic systems with stimulation on UL distal muscles	7
1.5 Objectives	9
CHAPTER 2 COMPARISON OF IMMEDIATE NEUROMODU	LATORY
EFFECTS BETWEEN FOCAL VIBRATORY AND ELECTRICAL S	SENSORY
STIMULATIONS AFTER STROKE	11
2.1 Introduction	12
2.2 Materials and Methods	14
2.2.1 Participants	14
2.2.2 Experimental setup	16
2.2.3 Experimental protocol	18
2.2.4 EEG analysis	20
2.2.5 Statistical analysis	23
2.3 Results	26
2.3.1 Monofilament test and NMES thresholds	26

2.3.2 P300 in the ERP response to FVS and NMES	29
2.3.3 RSP response on the contralateral sensorimotor cortex	31
2.3.4 ERSP response on the bilateral sensorimotor cortex	35
2.3.5 Spatial distribution of ERD/ERS topography	37
2.4 Discussion	38
2.4.1 Altered perceptual sensitivity after stroke	38
2.4.2 Earlier P300 evoked by FVS than NMES	39
2.4.3 Spectral features of cortical responses to FVS and NMES	40
2.4.4 Topographical patterns of cortical responses to FVS and NMES	43
2.4.5 Limitations and future work	46
2.5 Periodic Summary	46
CHAPTER 3 HYBRID SOFT ROBOT WITH ELECTRO-VIBRO-FEEDE	BACK
FOR SENSORIMOTOR-INTEGRATED WRIST/HAND REHABILITA	TION
AFTER STROKE	48
3.1 Introduction	49
3.2 Methodology	52
3.2.1 System design of ENMS-EVF	53
3.2.2 Control design of ENMS-EVF	56
3.2.3 Evaluation of ENMS-EVF	57
3.2.4 Statistical analysis	62
3.3 Results	62
3.3.1 Validation test results of ENMS-EVF configuration	63
3.3.2 Feasibility and effects of ENMS-EVF-assisted training	64
3.4 Discussion	65
3.4.1 Design and validation of ENMS-EVF system	66
3.4.2 Short-term rehabilitative effects of ENMS-EVF	67
3.5 Periodic Summary	68
CHAPTER 4 LONG-TERM EFFECTS OF SENSORIMOTOR-INTEGRA	ATED
WRIST/HAND REHABILITATION ASSISTED BY THE ENMS-EVI	7 ON

SENSORIMOTOR FUNCTIONS AND NEUROPLASTICITY AFTER STROKE

	70
4.1 Introduction	71
4.2 Materials and Methods	74
4.2.1 Design of ENMS-EVF and experimental setup	74
4.2.2 Rehabilitation assisted by ENMS-EVF	76
4.2.3 Sensorimotor evaluation of training outcomes	79
4.2.4 Statistical analysis	84
4.3 Results	85
4.3.1 Sensorimotor functional changes in clinical assessments	85
4.3.2 Sensorimotor neurological changes in corticomuscular coupling	87
4.4 Discussion	89
4.4.1 Recovery of sensorimotor functions	90
4.4.2 Corticomuscular changes related to functional improvements	91
4.4.3 Limitations and future works	95
4.5 Periodic Summary	96
CHAPTER 5 CONCLUSIONS	98
APPENDICES	.102
REFERENCES	.121

LIST OF FIGURES

Figure 1.1 Sensorimotor integration process (adapted form Asan et al., 2021)4
Figure 2.1 (A) Experiment setup. (B) Identification of 5 intensities in FVS
schemes. (C) Identification of 3 intensities in NMES schemes according to
the perceptual and motor threshold. (D) Experimental protocol timing for a
target muscle. The 8 different schemes of FVS and NMES were randomly
delivered in 8 trials
Figure 2.2. (A) EEG electrode layout and channel assignment according to the
standard 10-10 system (Seeck et al., 2017). (B) Schematic placement of
NMES electrodes and FVS vibration motors on the forearm
Figure 2.3 Flow chart of EEG pre-processing and analysis
Figure 2.4 The logical flow of statistical analysis
Figure 2.5 Monofilament scores (A), and pulse widths of perceptual (B) and motor
(C) NMES thresholds on forearm muscle unions of the stroke and control
groups, presented as the mean with SE (error bar). Significant inter-group
differences based on muscle unions are indicated by "*" ($p < 0.05$, Mann-
Whitney U test). Significant intra-group differences between ECU-ED and
FCR-FD muscle unions, and between dominant and nondominant arms are
indicated by " \blacktriangle " and "#" ($p < 0.05$, Wilcoxon signed-rank Test). (AE,
affected ECU-ED; AF, affected FCR-FD; UE, unaffected ECU-ED; UF,

Figure 2.6 P300 in ERP averaged across subjects on the Fz, Cz, and Pz electrodes. The vertical dashed lines at 0s mean the onset of stimulations. (A) Intra-group comparisons among different schemes. (B) Inter-group comparisons among target arms of stroke and control groups based on stimulation scheme. The bold line means the significantly different periods between the amplitude of ERPs compared within a sliding time window (p < 0.05, cluster-based permutation test). The shading means P300 with statistical significance, of which the start and end time points were shown in blue. (C) Comparison of P300 peak amplitude and latency. Significant inter-group and intra-group differences are indicated by "*" and "#" (p < 0.05, independent t-test and

Figure 2.7 RSP averaged across subjects on the contralateral sensorimotor cortex in the theta, alpha, beta, and gamma bands during the period of interest. The RSP values are presented as the mean with SE (error bar). RSP comparison with respect to (A) the stimulation scheme, target arm, and group. Significant intra-group differences between schemes are indicated by "#" (p < 0.05, one-way ANOVA repeated measures with Bonferroni post hoc tests). Overall, significant inter-group differences are indicated by " \blacktriangle " (p < 0.05, two-way mixed ANOVA). Significant inter-group differences based on the target arm

Figure 2.8 RSP comparison with respect to target muscle union. Significant intergroup differences based on target muscle union are indicated by "*" (p<0.05, independent t-test). No significant intra-group difference between four muscle unions in each group (p > 0.05, two-way mixed ANOVA). Significant intra-group differences between arms in each group are indicated by "#" (p < 0.05, independent t-test).

Figure 2.10 (A) ERD/ERS topographies when stimulating the nondominant arm.

The blue and red color schemes denote the ERD and ERS, respectively. Peak
channels are indicated by the labels. (B) Differences of the topography
between stroke and control groups. The blue and red color schemes denote
the negative or positive differences, respectively. Significant differences
between stroke and control groups are indicated by " \times " for $p < 0.05$ and " \ast "
for $p < 0.01$ (cluster-based permutation test). The orange triangle indicates
stimulating the nondominant (left/affected) arms. The right hemisphere is
ipsilesional for the stoke group
Figure 3.1 Overview of the ENMS-EVF robotic design and experimental setup.
(A) ENMS-EVF system design. (B) ENMS-EVF worn on a mannequin. (C)
The design of the PCB mounted in the control box53
Figure 3.2 The design diagram of ENMS-EVF
Figure 3.3 The control scheme diagram of the ENMS-EVF with voluntory motor
effort detection by EMG56
Figure 3.4 Evaluation of ENMS-EVF. (A) Horizontal task. (B) Vertical task. (C)
Training program assisted by ENMS-EVF60
Figure 3.5 Immediate rehabilitation effects of ENMS-EVF assisted training on (A)
FMA scores, (B) ARAT scores, (C) WMFT scores, and (D) Monofilament
test scores. Sites 1-4 reflect glabrous skin and sites 5-6 hairy skin; sites 1-2
have median nerve innervation, 3-4 ulnar nerve, and 5-6 radial nerve
(Bowden et al., 2014). (E) MAS scores. Pre assessments were conducted

three times and averaged in statistical analysis. Results are presented as the
means with standard deviations in (A), (B), (C), and (D), and violin plots with
all data points in (E). Significant differences are indicated as "*" for $p < 0.05$
and "**" for $p < 0.01$ (paired t-test in (A), (B), (C), and (D); Wilcoxon's
signed-rank test in (E))65
Figure 4.1 (A) Experimental setup for rehabilitation training assisted by ENMS-
EVF. (B) Positions of EMG+NMES electrodes on ED and a reference
electrode on the olecranon. (C) Positions of EMG electrodes on FD75
Figure 4.2 Timeline of the 20-session training program assisted by the ENMS-
EVF and assessments before (Pre), after (Post), and 3 months after (3-month
follow-up, 3MFU) the training sessions. In the Pre assessment, three times of
clinical assessments were conducted over 2 weeks
Figure 4.3 Signal processing flow chart
Figure 4.4 Results of clinical assessments on (A) FMA scores, (B) ARAT total and
subscale scores, and (C) Monofilament test scores. Sites 1-4 reflect glabrous
skin and sites 5-6 hairy skin; sites 1-2 have median nerve innervation, 3-4
ulnar nerve, and 5-6 radial nerve (Bowden et al., 2014). (D) MAS scores. Pre
assessments were conducted three times and averaged in statistical analysis.
Results are presented as the means with standard deviations in (A), (B), and
(C), and violin plots with all data points in (D). Significant differences are
indicated as "*" for $p < 0.05$ and "**" for $p < 0.01$ (One-way ANOVA with

repeated	d measures	and Turkey's	post hoc test	in (A), (B)	, and (C); F	Friedman
test witl	n FDR corr	rection in (D)).				86

Figure 4.5 Results of corticomuscular assessments and their correlation with clinical assessments. (A) Grand averaged topography changes of significant CMC between sensorimotor cortex and ED/FD during extension/flexion of all participants (N = 15). Peak channels are indicated as "*" with corresponding labels on the top right corner of each topography. (B) LI changes of significant CMC topography with the agonist muscles. Results are presented as the means with standard deviations. Significant changes are indicated as "*" (p < 0.05, One-way ANOVA with repeated measures and Turkey's post hoc test). Significant dCMC between the peak CMC channel and four UL muscles during W/H extension (C) and felxion (D). Results are presented as box and whisker plots with all data points. Significant changes are indicated as "*" (p < 0.05, Friedman test with FDR correction). Pearson's correlation of changes of the significant ascending dCMC with FD during W/H extension (Post-Pre and 3MFU-Pre periods) vs. (E) FMA W/H subscore, (F) ARAT total score, and (G) ARAT pinch sub-score, together with the least-squares fit line and its 95% confidence bands for both periods pooled

LIST OF TABLES

Table 2.1 Demographic data of the participants.	.15
Table 2.2 Clinical scores of the stroke participants.	.15
Table 2.3 Levels and abbreviation labels of the protocol.	.19
Table 2.4 Monofilament scores on target muscle unions.	.28
Table 2.5 Pulse widths of perceptual NMES threshold on target muscle unions	.28
Table 2.6 Pulse widths of motor NMES threshold on target muscle unions	.29
Table 2.7 The amplitude and latency of P300 peaks	.31
Table 3.1 Demographic information of participants.	.63
Table 3.2 Validation of ENMS-EVF configuration.	.64
Table 4.1 Demographic information of participants	.85

LIST OF ABBREVIATIONS

Abbreviation Full Term

3MFU 3-Month Follow-Up

A/D Analog-to-Digital

ANOVA Analysis of Variance

AR Autoregressive

ARAT Action Research Arm Test

BIC Biceps Brachii

CNS Central Nervous System

CMC Corticomuscular Coherence

CST Corticospinal Tract

DALY Disability-Adjusted Life-Year

dCMC directed Corticomuscular Coherence

ECU Extensor Carpi Ulnaris

ED Extensor Digitorum

EF Effect Size

EEG Electroencephalography

EMG Electromyography

ENMS Exoneuromusculoskeleton

ERP Event-Related Potential

ERD Event-Related Desynchronization

ERS Event-Related Synchronization

ERSP Event-Related Spectrum Perturbation

EVF Electro-Vibro-Feedback

FCR Flexor Carpi Radialis

FD Fxtensor Digitorum

XVIII

FDR False Discovery Rate

FMA Fugl-Meyer Assessment

FVS Focal Vibratory Stimulation

ICA Independent Component Analysis

LI Laterality Index

MAS Modified Ashworth Scale

MCU Microprocessor-Based Control Unit

MCP Metacarpophalangeal

M1 Primary Motor Cortex

MMSE Mini-Mental State Examination

MVC Maximal Voluntary Contraction

NMES Neuromuscular Electrical Stimulation

PMC Premotor Cortex

RM Repeated Measure

ROM Range of Motion

RSP Relative Spectral Power

S1 Primary Somatosensory Cortex

S/E Shoulder/Elbow

SMA Supplementary Motor Area

SMI Sensorimotor Integration

TRI Triceps Brachii

UL Upper Limb

VME Voluntary Motor Effort

W/H Wrist/Hand

WMFT Wolf Motor Function Test

LIST OF APPENDICES

Appendix A: Comparison of RSP for the factors of the scheme and the stimulated
muscle in Chapter 2
Appendix B: Comparison of RSP for the factors of the scheme and the target arm
in Chapter 2102
Appendix C: Comparison of RSP for the factors of the intensity and the group in
Chapter 2
Appendix D: RSP during stimulating by different intensities of FVS and NMES in
Chapter 2
Appendix E: RSP during stimulating each target arm of stroke and control groups
in Chapter 2105
Appendix F: RSP of stroke and control group during FVS and NMES in Chapter
2
Appendix G: WMFT score and consumed time results in Chapter 4 (One-way
ANOVA with repeated measures and Turkey's post hoc test)
Appendix H: Mini-mental State Examination (MMSE)108
Appendix I: Modified Ashworth Scale (MAS)
Appendix J: Fugl-Meyer Assessment for UL (FMA-UL)
Appendix K: Action Research Arm Test (ARAT)
Appendix L: Wolf Motor Function Test (WMFT)
Appendix M: Consent Form for Chapter 2, 3 and 4

CHAPTER 1

INTRODUCTION

This chapter is adapted from

Lin, L., Qing, W., Zheng, Z., Poon, W., Guo, S., Zhang, S., & Hu, X. (2024). Somatosensory integration in robot-assisted motor restoration post-stroke. *Frontiers in Aging Neuroscience*, 16, 1491678. https://doi.org/10.3389/fnagi.2024.1491678

1.1 Background of wrist/hand rehabilitation after stroke

Stroke has an increasing incidence and widespread prevalence worldwide. It is the second leading cause of death, and the third leading cause of death and disability combined (as expressed by disability-adjusted life-years (DALYs) lost) around the world (Valery L Feigin et al., 2021). There are 12.2 million new strokes per year, meaning 1 in 4 people above age 25 years old will have a stroke in their lifetime; 101 million people are living with stroke after-effects (Valery L Feigin et al., 2021; Feigin et al., 2022). In 2019, the global prevalence of stroke was 101.5 million people (Virani et al., 2021). From 1990 to 2019, the absolute number of poststroke people has almost doubled, with a 143% increase in DALYs (Valery L Feigin et al., 2021; Feigin et al., 2022). The number is expected to become worse due to population growth and aging.

Stroke is also one of the major causes of chronic disability worldwide. It is also one of the leading reasons for serious long-term disabilities, and more than 2% of people reported that they had disabilities because of stroke (Mane et al., 2020). Around 80% of stroke survivors suffer from motor impairments (Bao et al., 2020) and somatosensory deficits are estimated to be present in more than 50% of them (Kessner et al., 2016). More than 70% of stroke survivors are affected by upper limb (UL) impairments resulting from a combination of motor, sensory, and cognitive problems (Lawrence et al., 2001). This results in challenges and reduced independence in daily activities, impacting overall quality of life and further increasing burdens on society.

The hand and wrist are the most dexterous parts of the human body. Their function is essential for post-stroke patients' daily tasks (Lin et al., 2021). Since the hand and wrist are on the distal of the UL, the rehabilitation of them requires a large amount of time, money, and workload in traditional physical therapy. For example, more than 80% of stroke survivors experienced moderate to severe motor impairments in the UL, particularly the hand, even after receiving routine rehabilitation (Timmermans et al.,

2010). Recent years have seen the development of robotic devices assisting wrist/hand (W/H) rehabilitation after stroke. However, the developing robotic technologies of W/H rehabilitation are still not effective enough to serve the expanding stroke population because of lacking modulation in the ascending pathways.

1.2 Sensorimotor integration in motor restoration after stroke

Motor relearning after stroke depends on integrated sensorimotor practices in the paralyzed limbs with high repetitions, and significant motor functional improvements could be obtained even in the chronic stage (Pan et al., 2018). Sensorimotor integration (SMI) incorporates somatosensation (mainly tactile, proprioceptive, thermal, and pain) from the body and the external environment to shape movement in a closed-loop mode (Wolpert et al., 1998; Asan et al., 2021). In the SMI process (Figure 1.1), somatosensory information from the periphery is transmitted to the spinal cord and then relayed to sensory centers in the brain of the central nervous system (CNS) along the dorsal column—medial lemniscus pathway. The CNS predicts the motor movements based on the sensory inputs to minimize errors through feedforward control when somatosensory feedback updates the forward model to fine-tune motor plans, resulting in faster and more precise motor output commands to target muscles through the corticospinal tract (CST) (Asan et al., 2021). This SMI coordination enables the execution of skilled tasks, learning of new skills (Wolpert et al., 2011), or relearning skills by neuroplasticity after neurological disorders, such as stroke (Papale and Hooks, 2018).

Disruption of SMI after a stroke is a key barrier to motor restoration. More than 50% of stroke survivors experience sensory impairments on their hemiplegic side, which impedes SMI and exacerbates motor function impairments (Edwards et al., 2019). It has been reported that the poststroke sensorimotor process exhibited weakened descending motor outputs to target muscles due to diverse compensatory neuroplasticity with disturbance of involuntary spasticity and overwhelmed ascending

somatosensory feedback from a target muscle against those from the compensatory muscles (Zhou et al., 2021a), which could lead to abnormal movement patterns with muscular compensation and learned disuse in the long term (Hu et al., 2006; Jones, 2017).

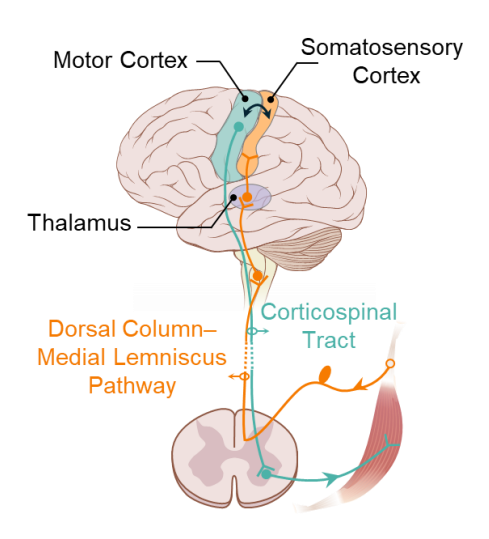


Figure 1.1 Sensorimotor integration process (adapted form Asan et al., 2021).

In poststroke rehabilitation, integrating somatosensory input into motor relearning is crucial for effective W/H functional restoration. Among major perceptual modalities of somatosensation, tactile and proprioceptive sensations are particularly important for guiding W/H movements (Hartmann, 2009). Somatosensation in associated muscles and joints, primarily through tactile (such as massage, tapping to mechanoreceptors of the skin and muscles) and proprioceptive stimulations (such as joint positions in a motion and changes in muscle length), could enhance the ascending neuromuscular pathways in the SMI process, together with the descending motor outputs of the affected W/H in repeated physical training (Papale and Hooks, 2018; Asan et al., 2021). Moreover, precise SMI neuroplasticity for targeted muscles might reduce learned disuse to achieve close-to-normal movement patterns in daily tasks (Lin et al., 2024a).

However, clinical practices usually skew attention towards motor parts, resulting in asynchronization between the motor retraining and therapeutic sensory feedback in the

rehabilitation process and hindering the neuroplasticity of the interrelated sensorimotor network for SMI after stroke (Lin et al., 2024c). Among the traditional therapies, Bobath therapy stands out as one that integrates sensorimotor interventions. Nonetheless, it is inferior to task-specific training in efficacy and does not outperform other interventions in enhancing arm activity, mainly because it relies on therapists providing passive movement guidance for stroke survivors with a focus on postural control (Dorsch et al., 2023). Some other adjuvant therapies, including various priming modalities, have been examined to modulate the CNS during traditional motor training for SMI rehabilitation. For example, somatosensory priming usually exerts electrical or vibratory stimulations (e.g., neuromuscular electrical stimulation (NMES) and focal vibratory stimulation (FVS)) on nerves or muscles to facilitate the neural processing of the somatosensory cortex prior to or concurrent with traditional motor-based interventions (Stoykov and Madhavan, 2015). It has been demonstrated to improve motor outcomes more efficiently than only motor-focused interventions, probably because of the closely linked somatosensory and motor networks (Stoykov et al., 2021). However, the effects on neuroplasticity after somatosensory priming remain unclear. Besides, these traditional therapies are all clinic-centered and labor-intensive, which necessitates new robotic technologies to integrate synchronous sensory feedback in motor interventions for better poststroke restoration.

1.3 Rehabilitation robots for W/H training after stroke

Rehabilitation robots have been developed to assist in labor-demanding physical training after stroke, with the main advantages of higher dosage and lower cost compared to manpower in long-term rehabilitation (Gassert and Dietz, 2018; Zhang et al., 2018; Zhang et al., 2019a). Robots with pure mechanical actuation (i.e., pure robots) simulate physical support provided by a human therapist in poststroke motor interventions (Zhang et al., 2019b; Lin et al., 2021). Rehabilitation robots could provide

intensive and repeated training for a long time with effective neuroplasticity for movement recovery of the UL (Xing and Bai, 2020). However, in the pure robots, it has been found that the recovery of the proximal joints, e.g., the shoulder/elbow (S/E), is much better than the distal, e.g., the W/H, in the long-term rehabilitative effects (Hu et al., 2009). The main possible reasons are: 1) The spontaneous motor recovery in the early stage after stroke is from the proximal to the distal; and 2) the proximal joints experienced more effective physical practices than the distal joints throughout the whole rehabilitation process since the proximal joints are more voluntarily controllable by most of stroke survivors (Raghavan, 2015). Neurological explanations are that stroke survivors usually develop ipsilateral compensatory strategies at the cortical level, while distal joints depend less on the ipsilateral projections than the proximal. However, improved proximal functions in the UL without the synchronized recovery at the distal make it hard to apply the improvements to meaningful daily activities, such as reaching out and grasping objects, which requires coordination among the joints of the UL, including the W/H (Rong et al., 2017). More effective rehabilitation methods that may benefit the functional restoration at the distal are desired for poststroke robot-assisted UL rehabilitation.

Besides, the current designs of robots follow repeated motor practices as in the traditional intervention. Current robots mainly emphasize the control precision on repetitive motor outputs but put little effort into achieving effective sensory responses in the desired ascending neural pathways, particularly related to the habitually disused muscles poststroke. Although proprioception experiences, e.g., joint motions and positions, could be provided even in movement assisted by pure robots, the neurological effectiveness of these afferent inputs has seldom been assessed and regulated in robot-assisted training (Lin et al., 2024c). Moreover, effective control of somatosensory stimulation to paretic muscles for SMI neuroplasticity is still lacking in current robots, which could be implemented via direct stimulation to peripheral muscles. Seldom do

robotic designs successfully recruit and/or control the somatosensory responses from targeted muscles in physical practices, which impedes the poststroke motor restoration requiring SMI compared to the interventions by human therapists who provide instructive pressing and tapping to muscles. It could be one of the major reasons that the rehabilitation effectiveness of robot-assisted physical training has not exceeded the traditional manual operations, even with higher repetitions (Rodgers et al., 2019). Incorporating somatosensory stimulation in robot-assisted practices has the potential to enhance poststroke motor relearning efficiency (Handelzalts et al., 2021). It has been found that the poststroke motor relearning process could be more efficient once somatosensory feedback was provided as tactile or proprioceptive cues in the practices (Handelzalts et al., 2021; Stoykov et al., 2021). The possible reason is that the stimulation paired with robot-assisted movement training, i.e., somatosensory priming, can generate a synergistic effect on neuroplasticity and offer afferent facilitation for SMI recovery than only movement intervention (Cordo et al., 2013; Stoykov and Madhavan, 2015; Asan et al., 2021). Precise integration and reinforcement of muscular somatosensory pathways from a target muscle paired with physical training in robotassisted rehabilitation require effective somatosensory stimulation eliciting simultaneously facilitated cortical responses in the sensorimotor cortex.

1.4 Hybrid robotic systems with stimulation on UL distal muscles

NMES and FVS are promising modalities for somatosensory priming on target muscles in robot-assisted motor training, mainly because of their ready-to-integrate platforms and noninvasive applications (Calabrò et al., 2017; Conforto et al., 2018).

The hybrid system of NMES and mechanical robot (NMES-robot) is a new trend in robotic design (Resquin et al., 2016) since the two technologies could complement each other: 1) Phasic NMES on a target muscle during a desired motion could improve the awareness of a patient on the muscular location, reducing compensation from

alternative muscular synergies (i.e., sensory guidance) (Chae and Yu, 2000; Shindo et al., 2011). 2) The robot could provide mechanical assistance to a paretic limb with precise kinematics. For example, Nam et al. (2020) designed a mobile exoneuromusculoskeleton (ENMS) for multi-joint UL telerehabilitation. The system integrated multi-channel NMES to UL muscles, together with pneumatic actuation to the elbow and fingers, to provide assistance in arm-reaching tasks. Residual electromyography (EMG) in the paretic muscles was detected as voluntary motor effort to control the NMES and mechanical supports from the system. The rehabilitative effects could be augmented when voluntory motor effort was involved in the training (Farmer et al., 2004; Nam et al., 2020). Patients with chronic stroke obtained significant motor gains in the UL after 20 sessions of self-help ENMS-assisted training in lab and home environments (Nam et al., 2020; Nam et al., 2021). The integrated NMES could provide additional afferent facilitation along with muscle force enhancement and atrophy prevention on paretic distal muscles due to learned disuse poststroke, e.g., the extensor digitorum (ED), in hand functions (Nam et al., 2020). However, the effects of somatosensory responses to NMES are generally ignored in the design of NMES-robot currently. Compared to NMES's direct application for muscle contractions with a high stimulation intensity, transcutaneous electrical nerve stimulation (TENS) is mainly adopted for peripheral pain relief but also could enhance the somatosensory input by stimulating target peripheral nerves. For example, the REINFORCE system was designed to complement an exosuit's assistance by providing TENS on the medial tibial nerve and sural nerve on the feet to enhance somatosensation under the foot sole during the stance phase of walking (Basla et al., 2023). However, muscle hypertonia always occurs on UL flexor, e.g., flexor digitorum (FD), poststroke, in which case NMES and TENS as electrical stimulations are not applicable to FD because it directly elicits wide recruitment of diverse sensory receptors and muscle fibers, leading to pain, muscle fatigue and higher muscle spasticity on FD in long-term usage (Insausti-Delgado et al., 2020; Lin et al., 2024b).

Even though less efficient in inducing muscular contraction than NMES, FVS, without causing muscle contraction, holds the potential to be more suitable for somatosensory priming on FD, which usually has sufficient residual voluntary force after stroke (Lan et al., 2011; Miller and Dewald, 2012). That is because FVS could provide somatosensory feedback with higher comfortability in the long term than NMES due to the selective activation of mechanoreceptors (Lapole and Tindel, 2015; Souron et al., 2017; Lin et al., 2024b). Similar to the NMES-robots, simple integration of FVS on target muscles and mechanical robots, i.e., FVS-robot, was proposed in the literature. For example, Calabrò et al. (2017) implemented on-and-off FVS on spastic UL muscles together with robot-assisted limb movement; and the related clinical trial showed additional release of spasticity in the muscles. However, different from NMES, whose motor effects could be easily inspected by the related muscle contractions, FVS mainly introduced sensations that have not been well evaluated in stroke survivors. Cortical response to FVS for effective stimulation in stroke patients has not been well investigated yet. Little is known about the differences between the transient neuromodulatory effects of FVS and NMES in stroke survivors (Corbet et al., 2018), which hinders their precise application in achieving effective neuroplasticity poststroke.

1.5 Objectives

As previously mentioned, SMI plays a crucial role in the motor recovery of the UL after stroke. Although proprioception experiences could be provided in movement assisted by pure robots, the rehabilitative effects on W/H are still limited. New technologies are urgently needed to integrate synchronous sensory feedback from target muscles in motor interventions for better functional recovery after stroke. Effective restoration of W/H function was achieved by EMG-driven NMES-robot. However, NMES is not applicable to FD because it leads to pain, muscle fatigue, and higher muscle spasticity in FD in long-term usage. FVS holds the potential to be more suitable for

somatosensory priming on FD with higher comfortability in the long term. However, the main obstacles in current rehabilitation techniques for successful sensorimotor-integrated UL rehabilitation after stroke are: (1) little was known about the transient neuromodulatory effects of FVS on somatosensory feedback after stroke compared with NMES, hindering their precise application in achieving effective neuroplasticity poststroke; (2) design and validation of electro-vibro-feedback (EVF) integrating FVS and NMES in the hybrid robotic system needs further investigation, because of the adverse effects of NMES on FD muscles in NMES-robot for W/H rehabilitation; (3) rehabilitative effects of somatosensory priming assisted by the hybrid robotic system with EVF on W/H motor functions are still unclear to understand its long-term effects on neuroplasticity and application merits for stroke survivors. Therefore, this study has three primary objectives:

- 1. to investigate the immediate neuromodulatory effects of FVS on forearm muscles compared with NMES for effective somatosensory stimulation in stroke survivors.
- 2. to integrate the FVS and NMES (i.e., EVF) with continuous voluntory motor effort involvement into a hybrid robotic system for somatosensory priming in W/H rehabilitation after stroke.
- 3. to evaluate the long-term effectiveness of the new system in W/H rehabilitation after stroke and analyze the effects on neuroplasticity related to functional outcomes.

CHAPTER 2

COMPARISON OF IMMEDIATE NEUROMODULATORY EFFECTS BETWEEN FOCAL VIBRATORY AND ELECTRICAL SENSORY STIMULATIONS AFTER STROKE

This chapter is adapted from

Lin, L., Qing, W., Huang, Y., Ye, F., Rong, W., Li, W., Jiao, J., & Hu, X. (2024). Comparison of Immediate Neuromodulatory Effects between Focal Vibratory and Electrical Sensory Stimulations after Stroke. *Bioengineering*, 11(3), 286. https://doi.org/10.3390/bioengineering11030286

2.1 Introduction

Over 50% of stroke survivors suffer from sensory impairments on the hemiplegic side (Kessner et al., 2016), which consequently disrupted the intricate process of SMI (Edwards et al., 2019) and exacerbated the impairments of motor function (Bolognini et al., 2016). NMES and FVS are the primary techniques used to deliver external somatosensory stimulation to specific muscles transcutaneously for sensorimotor rehabilitation after stroke (Sitaram et al., 2017; Conforto et al., 2018; Edwards et al., 2019). NMES or FVS, together with baseline motor rehabilitation, has demonstrated efficacy for stroke rehabilitation (Calabrò et al., 2017; Conforto et al., 2018; Fleury et al., 2020). This effectiveness could be attributed to the cortical process elicited through the integration of ascending sensory information from a targeted muscle to generate descending motor commands essential for motor initiation and planning, ultimately contributing to the enhancement of functional motor outcomes (Edwards et al., 2019). However, little is known about the differences between the transient neuromodulatory effects of these sensory stimulation techniques poststroke (Corbet et al., 2018), which hinders their precise application in achieving effective neuroplasticity poststroke.

As an electrical stimulation to excitable cells, motor-level NMES is a technique in which electricity is used to evoke muscle contractions through the depolarization of motor nerves or muscle fibers (Paillard, 2021). It has been applied in routine poststroke interventions for enhancing muscular force, preventing muscle atrophy, and reducing muscle spasticity (Bao et al., 2020; Huang et al., 2020b). Sensory-level NMES with lower stimulation intensities than motor-level NMES mainly depolarizes the sensory neurons in the skin and muscles without eliciting muscle contraction (Hautasaari et al., 2019). It could improve muscular proprioception after stroke and reduce compensation from alternative muscular synergies (Shindo et al., 2011; Corbet et al., 2018). Insausti-Delgado et al. reported that both motor- and sensory-level NMES applied to muscles

could evoke event-related (de)synchronization (ERD/ERS) in the alpha and beta bands detected by electroencephalography (EEG) in unimpaired persons (Insausti-Delgado et al., 2020).

In comparison with NMES, FVS applied to a target muscle is more acceptable for stroke survivors because mainly the mechanoreceptors in the skin and muscles are activated during stimulation without wide recruitment of other sensory receptors (e.g., nociceptors, as in NMES) (Hautasaari et al., 2019; Wang et al., 2020). FVS can activate primary afferent endings (i.e., Ia afferents) in a muscle through mechanical deformation of the muscle spindles (Souron et al., 2017), which can increase muscular proprioception and suppress antagonist co-contraction (Hautasaari et al., 2019). FVS has also been found to ameliorate muscular spasticity during rehabilitation after stroke (Calabrò et al., 2017; Amano et al., 2020), with effects similar to those of manual massage.

Moreover, FVS evoked cortical activation comparable to that evoked by NMES in unimpaired individuals. For example, Hautasaari et al. reported that vibratory stimulation in healthy participants could evoke cortical activations similar to those evoked by electrical stimulation but with larger cortical areas being activated (Hautasaari et al., 2019). Event-related potentials (ERPs) evoked by FVS were adopted to investigate cognitive and somatosensory processes (Alsuradi et al., 2020), e.g., P300, a positive wave with an onset ranging from 250 ms–800 ms after stimulation (Reuter et al., 2014). Bolton et al. reported that the P300 component evoked by vibratory stimulation was lower in amplitude with a longer latency in older adults than younger adults, mainly because of a slower cognitive response due to aging (Bolton and Staines, 2012). However, the understanding of the transient cortical responses of FVS applied to peripheral muscles is still lacking for stroke survivors, although preliminary rehabilitation effectiveness introduced by FVS has been reported in the literature (Yeh et al., 2021; Schranz et al., 2022). In this study, we aimed to investigate and compare

the immediate neuromodulatory effects of FVS and NMES at the cortical level in poststroke and unimpaired people. We hypothesized that FVS could effectively activate the sensorimotor cortex as well as sensory-level NMES but with different responses: FVS would elicit better somatosensory engagement, while NMES would foster motor-related responses.

2.2 Materials and Methods

The transient cortical responses of participants with chronic stroke and the unimpaired controls were captured by EEG during FVS and NMES with different intensities to the forearm muscles. EEG was adopted in this study because it can reveal transient cortical responses to sensory stimulation with the advantages of high temporal resolution and cost-effectiveness compared to other neuroimaging techniques (Huang et al., 2020a).

2.2.1 Participants

This study was approved by the Human Subjects Ethics Sub-Committee of the Hong Polytechnic University before commencement Kong (approval HSEARS20210320003). Participants after stroke were screened and recruited from local districts. The inclusion criteria were as follows: (1) at least 6 months after the onset of a unilateral lesion in the cortical or subcortical regions due to stroke (Hu et al., 2006); (2) sufficient cognition to follow experimental instructions (Mini-Mental State Examination (MMSE) score > 23 (Tombaugh and McIntyre, 1992)); (3) moderate-tosevere motor disability in the affected UL (15 < Fugl-Meyer assessment (FMA) < 45) (Sullivan et al., 2011; Nam et al., 2021); (4) muscle spasticity scores ≤ 3 at the wrist and fingers, as measured by the modified Ashworth scale (MAS) (Bohannon and Smith, 1987); (5) a normal-to-diminished protective sensation on the affected forearm under a threshold of 4.31 (2.0 g) as measured by the Semmes-Weinstein monofilament test (Perle et al., 1999; Suda et al., 2020) on the skin surface above the muscle union of the flexor carpi radialis (FCR) and FD (i.e., FCR-FD), and the muscle union of the extensor carpi ulnaris (ECU) and ED (i.e., ECU-ED) of the paretic forearm; (6) no neurological impairments except for stroke; and (7) right-handed before the stroke onset. The exclusion criteria for stroke participants were (1) poststroke pain, (2) epilepsy, (3) cerebral implantation, or (4) pacemaker implantation. Unimpaired participants were also recruited from the local districts; their inclusion criteria were right-handed and no history of neurological, psychiatric, cardiovascular, cognitive, or mental impairments. The clinical assessments mentioned above were carried out by an independent assessor who was blinded to the content of the study. Finally, 15 stroke participants (i.e., the stroke group) and 15 unimpaired participants (i.e., the control group) were recruited. All participants understood the study's research information and signed the consent form before the experiment. Table 2.1 provides an overview of the demographic information of all the individuals involved in the study. The clinical scores of the stroke participants are presented in Table 2.2.

Table 2.1 Demographic data of the participants.

Group	No. of participants	Stroke types (hemorrhage/ ischemic)	Affected arm (left/right)	Gender (male/female)	Age (years, mean ± SD)	Years after stroke (min/max years)
Stroke	15	9/6	10/5	8/7	53±11	2/18
Control	15	-/-	-/-	9/6	67±3	-/-

Table 2.2 Clinical scores of the stroke participants.

Clinical	FMA	MAS		Monofilament			
Clinical assessment	Upper	Wrist	Eingar	Affected	Affected	Unaffected	Unaffected
	Limb	Wrist	Finger	extensor	flexor	extensor	flexor
Score (mean	31.1±11.5	1.1±0.9	1.9±0.8	3.23±0.67	3.24±0.49	3±0.45	3.26±0.38
± SD)	31.1±11.3	1.1±0.9	1.9±0.8	3.23±0.0/	3.24±0.49	3±0.43	3.20±0.38

2.2.2 Experimental setup

The experiment was carried out in a quiet environment where the temperature and humidity levels were regulated at $18-20^{\circ}$ C and $60\% \pm 5\%$, respectively. The experimental setup is shown in Figure 2.1A. The participant was requested to take a comfortable seated position facing a table, approximately 10 cm from the table edge to their torso. The participant was provided with an eye mask and a pair of earplugs to further minimize visual and auditory interference during the EEG recording. Then, they were instructed to reach their testing forearm forward, with the elbow resting at approximately 170° and supported by a cushion. The wrist and finger joints remained in a relaxed position. The contralateral UL was positioned naturally on the participant's thigh. A 64-channel EEG cap was mounted on the scalp of the participant according to the standard 10-10 system (Figure 2.2A) (Seeck et al., 2017). The impedance between each EEG electrode and the scalp was maintained below 5 k Ω (Lou et al., 2013). The EEG electrode cap was connected to amplifiers (BrainAmp MR, Brain Products Inc., Herrsching, Germany) and subsequently linked to a desktop computer for real-time EEG monitoring on one screen. A user interface was developed (LabVIEW 2015) and visualized on another screen to control the stimulation process (Figure 2.1A).

To enhance motor unit recruitment, the NMES electrode pairs (5×5 cm², PALS Neurostimulation Electrodes, Axelgaard Manufacturing Co., Ltd., Fallbrook, CA, USA) were placed in the common area of the motor points for muscle bellies of the FCR-FD or ECU-ED muscle unions, given the close anatomical proximity of the two muscles in a muscle union (Figure 2.2B) (Muraoka, 2002; Nam et al., 2020). Before electrode attachment, the skin was prepared to lower the skin-electrode impedance below 5 k Ω (Lou et al., 2013). A miniature FVS vibration motor (model 310-122, Precision Microdrives, London, UK; 10 mm diameter, 3 mm height, 1.2 g weight; 11,500 rpm with 1.9 G amplitude at rated operating voltage 3V) was gently pressed against the

participant's skin using medical tape between the cathode and anode of the NMES electrodes to ensure vibration transmission, with care taken to avoid sharp edges and the sensation of the electrical wiring (Choi and Kuchenbecker, 2013). We integrated the one-channel FVS into an NMES control box developed previously (Nam et al., 2017; Nam et al., 2020; Nam et al., 2021). These NMES electrodes and FVS vibration motor were controlled by the control box, with the outputs of one-channel FVS in a range of amplitudes from 0.7 G to 1.9 G below the threshold of the tonic vibration reflex without involuntary muscle contraction (Murillo et al., 2014), and one-channel NMES generating alternating current in square pulses with a frequency of 40 Hz (i.e., 40 pulses per second), an amplitude of 70 V, and an adjustable pulse width ranging from 0 to 300 µs, allowing for different levels of stimulation intensity (Nam et al., 2017). These FVS and NMES intensities were reported for sensory rehabilitation poststroke (Insausti-Delgado et al., 2020; Wang et al., 2022).

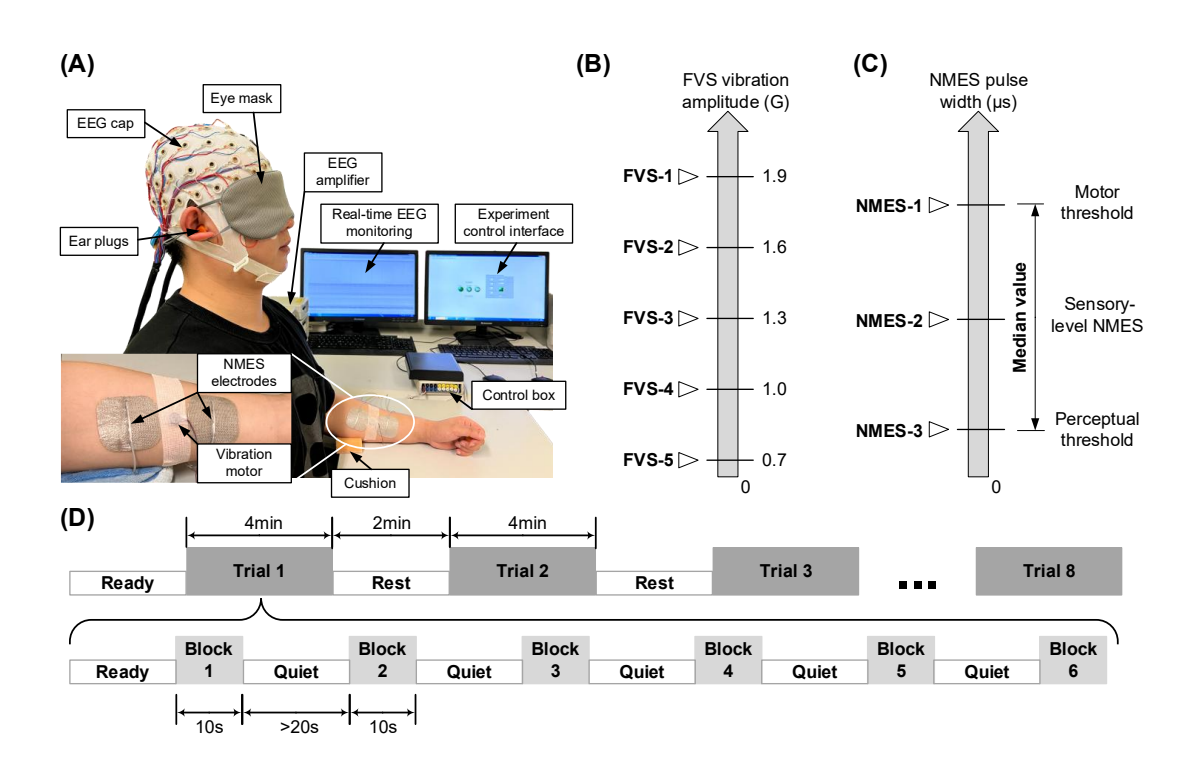


Figure 2.1 (A) Experiment setup. (B) Identification of 5 intensities in FVS schemes. (C) Identification of 3 intensities in NMES schemes according to the perceptual and

motor threshold. **(D)** Experimental protocol timing for a target muscle. The 8 different schemes of FVS and NMES were randomly delivered in 8 trials.

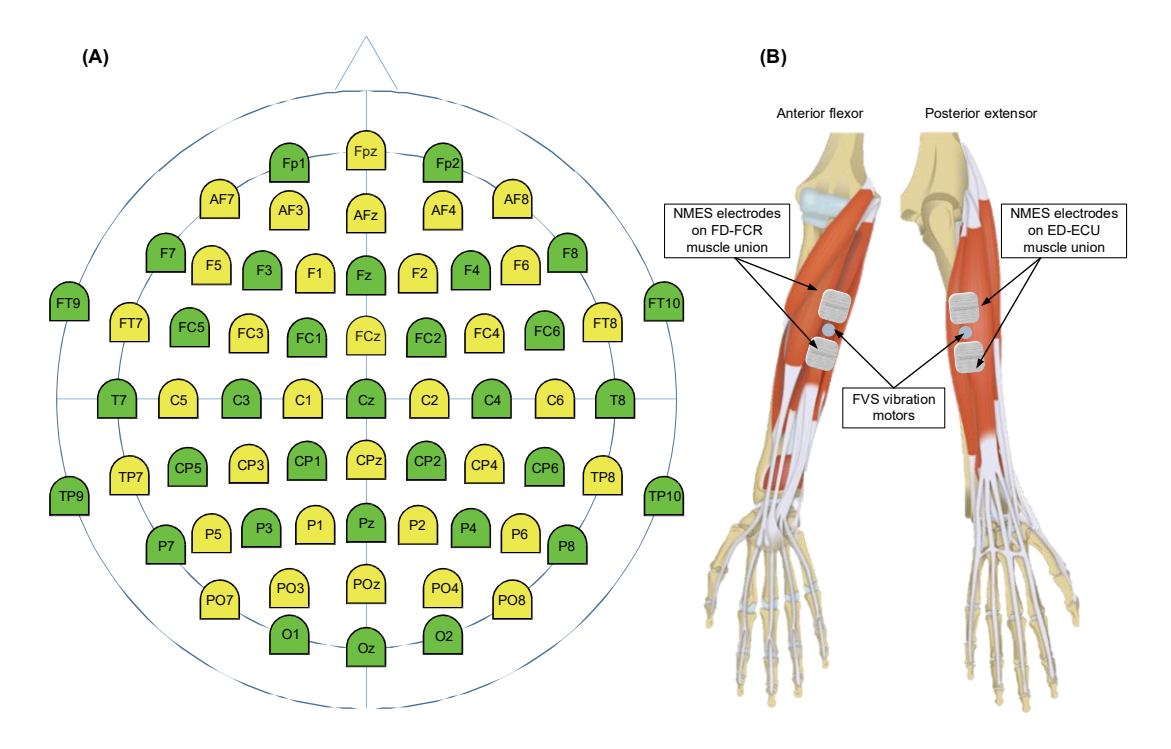


Figure 2.2. (**A**) EEG electrode layout and channel assignment according to the standard 10-10 system (Seeck et al., 2017). (**B**) Schematic placement of NMES electrodes and FVS vibration motors on the forearm.

2.2.3 Experimental protocol

Based on the above setup, we studied eight stimulating schemes, five FVS and three NMES schemes with different intensities. The FVS schemes had five intensities (Figure 2.1B): 1.9 G (FVS-1), 1.6 G (FVS-2), 1.3 G (FVS-3), 1.0 G (FVS-4), and 0.7 G (FVS-5); these intensities were reported to be effectively perceived and tolerable for the sustained stimulation of human participants (Seim et al., 2021). The NMES schemes had three intensities (Figure 2.1C): (1) the motor threshold (NMES-1), identified as the initial twitching of the fingers (Insausti-Delgado et al., 2020); (2) the representative sensory-level NMES (NMES-2), calculated as the median value between the perceptual and motor thresholds; and (3) the perceptual threshold (NMES-3), identified as the

initial tingling sensation on the forearm (Insausti-Delgado et al., 2020). Perceptual and motor thresholds were determined for each target muscle union by gradually increasing the NMES pulse width from 0 µs in steps of 1 µs. A duration of 10 s for sustained stimulation in all FVS and NMES schemes was selected as the stimulation block in this study (Figure 2.1D). Then, six stimulation blocks of the same scheme were arranged into a stimulation trial with a quiet period of at least 20 s between two consecutive blocks to minimize potential afferent adaptation (Genna et al., 2017). During a trial, a participant was required to avoid active mental tasks, maintain their posture still, and minimize head and neck motions, e.g., ocular and swallowing motions. There were eight trials associated with the eight stimulation schemes applied to a muscle union in random order, forming the stimulation protocol (Figure 2.1D, Table 2.3). A 2-minute interval between two consecutive trials was provided to a participant to move and rest. The stimulation protocol was applied sequentially to the four muscle unions of a participant in random order.

Table 2.3 Levels and abbreviation labels of the protocol.

Group	Target arm	Target muscle union	Stimulation scheme/trial	
	Nondominant/	Affected ECU-ED (AE)	FVS-1,2,3,4,5; NMES-1,2,3	
Stroke	Affected arm (A)	Affected FCR-FD (AF)	FVS-1,2,3,4,5; NMES-1,2,3	
group	Dominant/	Unaffected ECU-ED (UE)	FVS-1,2,3,4,5; NMES-1,2,3	
	Unaffected arm (U)	Unaffected FCR-FD (UF)	FVS-1,2,3,4,5; NMES-1,2,3	
	Nondominant/	Left ECU-ED (LE)	FVS-1,2,3,4,5; NMES-1,2,3	
Control	Left arm (L)	Left FCR-FD (LF)	FVS-1,2,3,4,5; NMES-1,2,3	
group	Dominant/ Right arm (R)	Right ECU-ED (RE)	FVS-1,2,3,4,5; NMES-1,2,3	
		Right FCR-FD (RF)	FVS-1,2,3,4,5; NMES-1,2,3	

During a stimulation trial, the EEG signals were amplified with a gain of 10,000, digitized at an analog-to-digital sampling rate of 1000 Hz. For monitoring EEG in the experiment, the signals were notch-filtered from 49 Hz to 51 Hz and bandpass-filtered from 1 Hz to 100 Hz in the real-time processing. Meanwhile, the raw EEG signals in

each stimulation trial were stored digitally after the sampling for later offline processing. The acquisition duration was 4 minutes for each trial, including the baseline and stimulation periods. The stimulation events were labeled by markers in the recorded EEG trials.

2.2.4 EEG analysis

In the offline EEG analysis (Figure 2.3), temporal, spectral, and spatial features were analyzed to evaluate the cortical responses to different stimulation schemes after signal pre-processing. EEG processing and analysis were conducted with the EEGLAB (version 2022.0) (*EEGLAB Toolbox*, 2023) and Fieldtrip (version 20220603) (*FieldTrip Toolbox*, 2023) toolboxes with the latest update (Delorme and Makeig, 2004; Oostenveld et al., 2011; Zhou et al., 2021a) using MATLAB R2019 (MathWorks, Natick, MA, USA).

In the offline processing, the recorded EEG signals in each stimulation trial were bandpass-filtered from 1 Hz to 100 Hz and notch-filtered from 49 Hz to 51 Hz digitally by a fourth-order Butterworth filter (Guo et al., 2020). Independent component analysis (ICA) was applied to all EEG signals to minimize potential muscular artifacts (Makeig et al., 1995; Pope et al., 2022). EEG signals were further screened by visual inspection to remove artifacts. The electrode positions of the EEG data were flipped along the midsagittal plane for participants with left-hemisphere lesions so that the affected hemisphere was on the right side for all stroke participants (Bao et al., 2021). The EEG signals of each trial were then segmented into six signal epochs with a duration of 15 s, corresponding to a 5 s baseline ahead of stimulation onset and a 10 s period during the stimulation block for later calculation (Delorme et al., 2007) (Figure 2.3). Each epoch contained the EEG episodes from the 62 channels. There were 178,560 EEG episode samples in the respective stroke and control groups (15 participants × 2 arms × 2 muscle unions × 8 schemes × 6 epochs × 62 episodes).

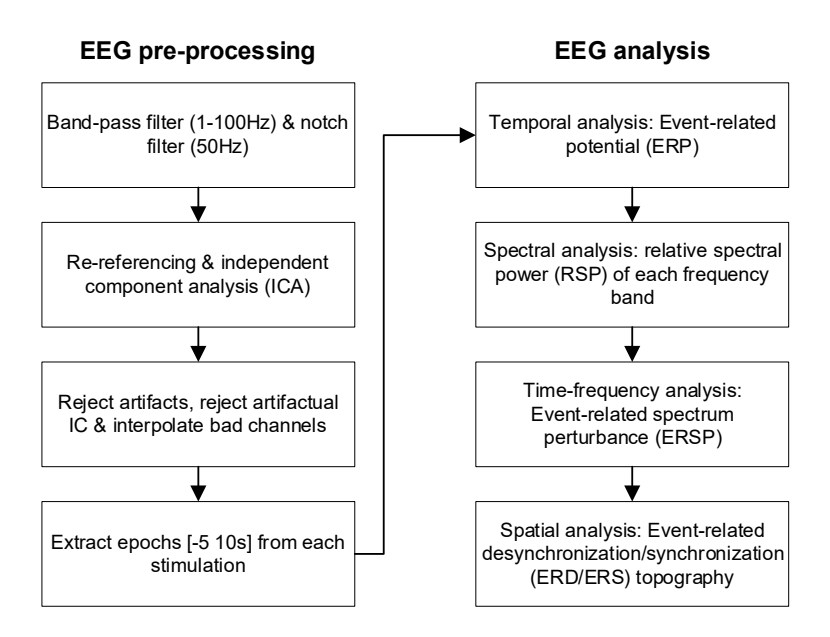


Figure 2.3 Flow chart of EEG pre-processing and analysis.

Four EEG features were used to investigate the cortical response: the ERP in the temporal domain, the relative spectral power (RSP) in the spectral domain, the event-related spectrum perturbation (ERSP) in the time-frequency domain, and the ERD/ERS topography in the spatial domain at the cortical level (Figure 2.3). These EEG features were calculated for each episode in an epoch. The ERP waveform of an episode was obtained from the baseline correction using Equation 2.1:

$$ERP(t) = p_{block}(t) - \overline{p_{baseline}(t)}$$
 (2.1)

where $p_{block}(t)$ is the EEG waveform during the stimulation block and $\overline{p_{baseline}(t)}$ is the mean value over the baseline period. The ERPs on the Fz, Cz, and Pz electrodes were averaged to obtain P300 (Reuter et al., 2014). To enable subsequent statistical analysis, the peak amplitude relative to the baseline and the peak latency after stimulation onset were computed for each participant's P300. The period of interest for RSP analysis was defined as the time window during which P300s were significantly different. The RSP of an episode was calculated by Equation 2.2:

$$RSP_{band} = \frac{\int_{F_1}^{F_2} p_{block}(f) df}{\int_{1}^{100} p_{block}(f) df} - \frac{\int_{F_1}^{F_2} p_{baseline}(f) df}{\int_{1}^{100} p_{baseline}(f) df}$$
(2.2)

where $p_{block}(f)$ is the power spectral density during the period of interest in the stimulation block; $p_{baseline}(f)$ is the power spectral density during the baseline; and F_1 and F_2 are the cutoff frequencies of the EEG frequency bands, which are the theta $(\theta, 4 \sim 8 \text{ Hz})$, alpha $(\alpha, 8 \sim 12 \text{ Hz})$, beta $(\beta, 13 \sim 30 \text{ Hz})$ and gamma $(\gamma, 30 \sim 100 \text{ Hz})$ bands in this study (Huang et al., 2020a). Then, the RSPs were averaged across the episodes from the whole-brain channels (i.e., whole-brain RSP) as practiced previously (Huang et al., 2020a) and across the episodes from channels on the sensorimotor cortex contralateral to the stimulated side (i.e., contralateral sensorimotor RSP) to quantify the response in the contralateral sensorimotor areas. The RSP was narrowed to the predefined period of interest and averaged on the frequency bands for quantification, while the ERSP was used to analyze the 2-dimensional cortical response with respect to continuous time and frequency. The ERSP of an episode for each EEG channel was obtained from baseline normalization using Equation 2.3:

$$ERSP(f,t) = \frac{S_{block}(f,t) - \mu_{baseline}(f)}{\sigma_{baseline}(f)}$$
(2.3)

where $S_{block}(f,t)$ is the time-frequency spectrum during the stimulation block, and $\mu_{baseline}(f)$ and $\sigma_{baseline}(f)$ are the mean and standard deviation, respectively, of the baseline spectrum. A baseline permutation statistical method (2000 times) with false discovery rate (FDR) correction for multiple comparisons was adopted, with a significance level of 0.05 (Grandchamp and Delorme, 2011). ERSPs of C3 and C4 were used as representative channels from the bilateral hemispheres (Insausti-Delgado et al., 2020; Remsik et al., 2022) to investigate lateralization of cortical activation during sensory stimulation to both arms. ERD/ERS topographies were used to evaluate the cortical distribution patterns of the peak values in each EEG band after the stimulations

for the two subject groups. Based on the ERSP, the ERD/ERS of each channel was calculated by Equation 2.4:

$$ERD/ERS = \frac{1}{K} \sum_{f \in F} \sum_{t \in T} EPSP(f, t)$$
 (2.4)

where F is the frequency band (i.e., theta, alpha, beta, or gamma bands); T is the analyzed latency within the stimulation block; and K is the total number of time-frequency bins within the time-frequency window (Grandchamp and Delorme, 2011). The FVS-1 and NMES-2 stimulation schemes were chosen as representative stimulations in the analyses of ERSP and ERD/ERS topography, as these two intensities evoked the strongest cortical ERPs in the sensory stimulations.

For each participant, an EEG feature was averaged across the six repeated blocks in a stimulation trial. This operation resulted in an averaged EEG feature with respect to a stimulation scheme on a muscle union of a participant, which was used as an experimental reading unit for statistical analysis.

2.2.5 Statistical analysis

The statistical analyses (Figure 2.4) were conducted for the monofilament scores, perceptual/motor NMES thresholds, ERPs, RSPs, and ERD/ERS topography. The features were first compared with respect to two independent factors: (1) the stimulation scheme (FVS-1,2,3,4,5, and NMES-1,2,3) or (2) the target muscle union (ECU-ED and FCR-FD muscle unions). The features were further combined and compared based on three factors: (1) the type of stimulation (FVS or NMES) used to determine the differences between the vibratory and electrical stimulation types; (2) the target arm (dominant or nondominant arm) used to determine the difference between the two sides; and (3) the group (control or stroke group) used to determine the changes in the cortical

response after stroke. The corresponding abbreviations of the five factors are listed in Table 2.3.

The Shapiro-Wilk normality test with Lilliefors correction was first performed. The amplitude and latency of the P300 peak and the RSP were normally distributed (p >0.05). Nonparametric tests were adopted for nonnormally distributed data so that Mann-Whitney U tests were conducted on the monofilament scores and perceptual/motor NMES thresholds for intra-group comparison between the two target muscle unions and two target arms, as well as Wilcoxon signed-rank tests for intergroup comparison based on the target muscle union. In addition, the ERP amplitudes during the stimulation blocks were compared using cluster-based permutation tests (2000 permutations) for intra-group comparisons among the eight stimulation schemes and between the two muscle unions, as well as inter-group comparisons among the four target arms. Paired and independent t-tests were applied to the respective intra-group and inter-group comparisons of the P300 peak's amplitude and latency between the FVS and NMES stimulation types and between the stroke and control groups. Moreover, the ERD/ERS topographies during representative FVS and NMES were compared between the stroke and control groups by cluster-based permutation tests (2000 permutations) to investigate poststroke spatial alterations during FVS and NMES.

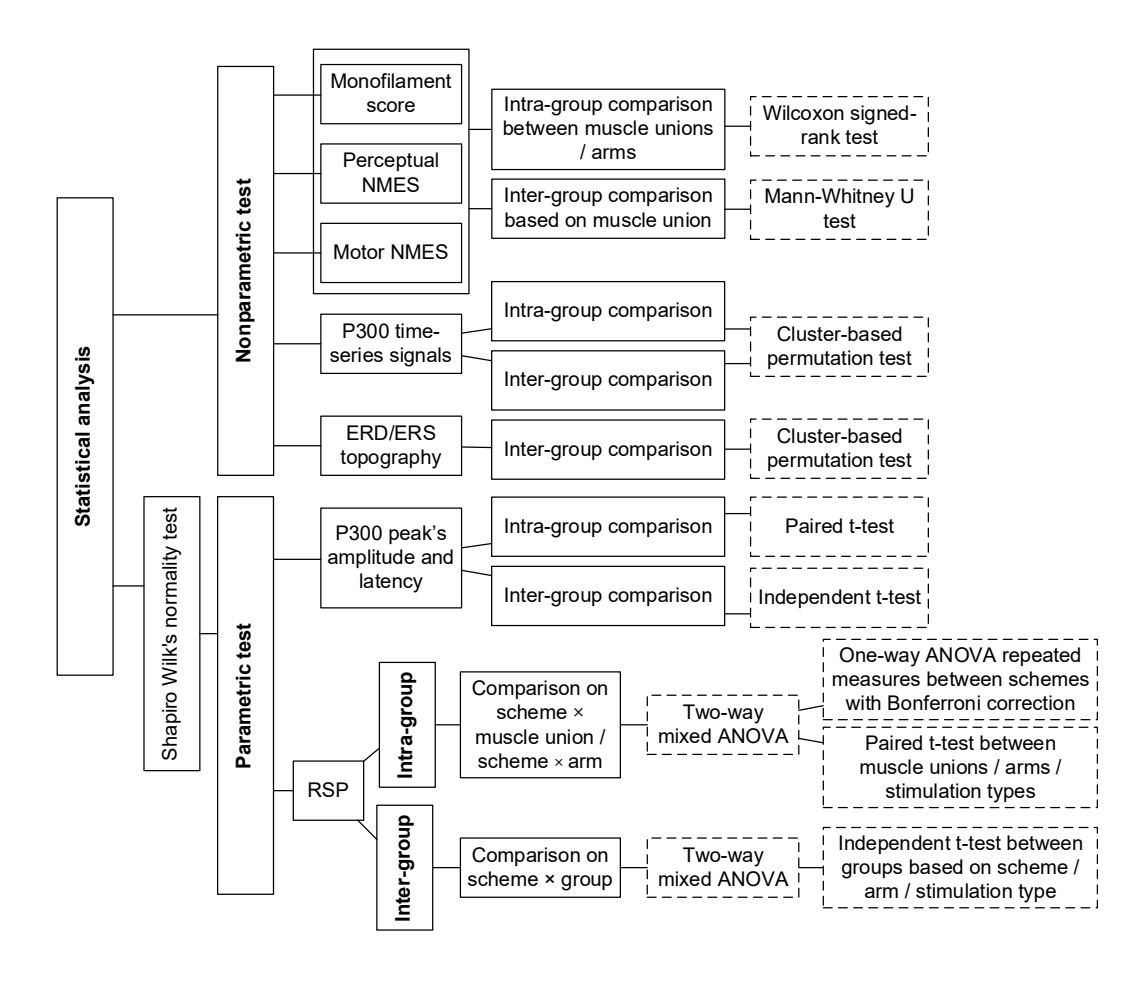


Figure 2.4 The logical flow of statistical analysis.

Parametric tests were adopted for RSP in each frequency band. Intra-group comparisons of the RSP were conducted for each group. Two-way mixed analyses of variance (ANOVAs) were used to evaluate the differences in RSP with respect to the factors of the stimulation scheme and target muscle union, as well as the stimulation scheme and target arm. Then, a one-way ANOVA with repeated measures (RM) was used to compare the RSP among the eight stimulation schemes with the Bonferroni post hoc test. Paired *t*-tests were used to compare the RSP between different target muscle unions, target arms, or stimulation types.

Next, inter-group comparisons of the RSP were conducted between groups. A two-way mixed ANOVA was conducted to evaluate the differences in RSP with respect to the factors of the stimulation scheme and group. Independent *t*-tests were subsequently

conducted to compare the RSP between the stroke and control groups based on the stimulation scheme, target muscle union, target arm, and stimulation type. The cluster-based permutation test was executed using the FieldTrip toolbox with the Monte Carlo method (Oostenveld et al., 2011). Other statistical analyses were performed utilizing SPSS 24.0 (2016). The statistical significance level was set at 0.05 in this work, with levels of 0.01 and 0.001 also indicated.

2.3 Results

2.3.1 Monofilament test and NMES thresholds

After the subject screening, 15 out of 17 stroke survivors (more than 88%) satisfied the criteria for a normal-to-diminished protective sensation (<4.31) in the monofilament test. Figure 2.5 shows the monofilament scores and perceptual/motor NMES thresholds of all muscle unions in the stroke and control groups. The detailed mean values and standard errors (SEs) are summarized in Table 2.4, Table 2.5 and Table 2.6, along with the Mann–Whitney U test or Wilcoxon signed-rank test probabilities and the estimated effect sizes (EFs) (Mastrich and Hernandez, 2021). The only significant finding in the monofilament score (Figure 2.5A) was that the sensitivity of the unaffected ECU-ED (UE) of the stroke group was significantly lower than that of the right ECU-ED (RE) of the control group (p = 0.009). No significant differences were observed in the intragroup comparisons between the target arms and target muscle unions within the stroke and control groups (p > 0.05).

According to the results of the inter-group comparison of NMES thresholds (Figure 2.5B, and C), the perceptual thresholds of the affected ECU-ED (AE) and FCR-FD (AF) muscle unions in the stroke group were significantly higher than those of the left ECU-ED (LE) and FCR-FD (LF) muscle unions in the control group (p = 0.009 and 0.037). The motor NMES threshold of AF muscle union in the stroke group was significantly

higher than that of the LF in the control group (p = 0.016). According to the intra-group comparisons, the perceptual and motor NMES thresholds of the RE muscle union were significantly higher than those of the RF muscle union in the control group (p = 0.010 and 0.004). The motor NMES thresholds of the UE muscle union were significantly higher than those of the unaffected FCR-FD (UF) muscle union in the stroke group (p = 0.002). Moreover, the perceptual and motor NMES thresholds of the affected arm (including AE and AF muscle unions) were significantly higher than those of the unaffected arm (including UE and UF muscle unions) in the stroke group (p < 0.001). In contrast, no significant difference was observed between the left and right arms in the control group (p = 0.160 and 0.246).

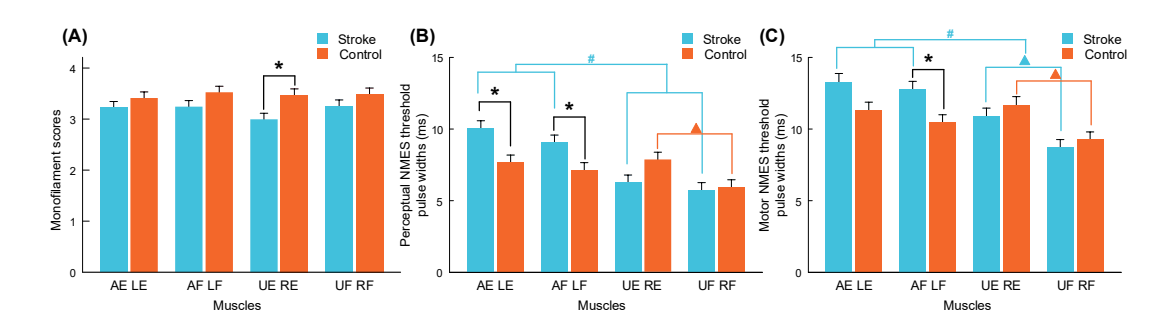


Figure 2.5 Monofilament scores (A), and pulse widths of perceptual (B) and motor (C) NMES thresholds on forearm muscle unions of the stroke and control groups, presented as the mean with SE (error bar). Significant inter-group differences based on muscle unions are indicated by "*" (p < 0.05, Mann-Whitney U test). Significant intra-group differences between ECU-ED and FCR-FD muscle unions, and between dominant and nondominant arms are indicated by " \blacktriangle " and "#" (p < 0.05, Wilcoxon signed-rank Test). (AE, affected ECU-ED; AF, affected FCR-FD; UE, unaffected ECU-ED; UF, unaffected FCR-FD for stroke group. LE, left ECU-ED; LF, left FCR-FD; RE, right ECU-ED; RF, right FCR-FD for control group).

Table 2.4 Monofilament scores on target muscle unions.

Test target		Stroke	Control	Mann-Whitney U test
Arm	Muscle union	Mean ± SE		p (A)
Nondominant	ECU-ED	3.23±0.18	3.41±0.10	0.412 (0.59)
	FCR-FD	3.24±0.13	3.53±0.10	0.137 (0.66)
Wilcoxon signed-rank test - p (r)		0.814(0.06)	0.129(0.39)	-
-	ECU-ED	3.00±0.12	3.47±0.10	0.009** (0.22)
Dominant	FCR-FD	3.26±0.10	3.49 ± 0.08	0.148 (0.66)
Wilcoxon signed-rank test - p (r)		0.068(0.47)	0.684(0.10)	-
Wilcoxon signed-rank test on arms - p (r)		0.162(0.26)	0.720 (0.07)	-

The superscript "*" denotes the significant inter-group difference based on muscle union pairs with 2 superscripts for p < 0.01.

Table 2.5 Pulse widths of perceptual NMES threshold on target muscle unions.

Stimulation target		Stroke	Control	Mann-Whitney U test
Arm	Muscle union	Mean ± SE		p (A)
Nondominant	ECU-ED	10.1±0.7	7.7 ± 0.5	0.009** (0.78)
	FCR-FD	9.1±0.6	7.1 ± 0.6	$0.037^* (0.72)$
Wilcoxon signed-rank test - p (r)		0.099(0.42)	0.233(0.31)	-
Daminant	ECU-ED	6.3±0.3	7.9 ± 0.6	0.07 (0.70)
Dominant	FCR-FD	5.7±0.3	5.9±0.3	0.775 (0.53)
Wilcoxon signed-rank test - p (r)		0.157(3.87)	0.010*(0.67)	-
Wilcoxon signed-rank test on arms - p (r)		0.000###(0.81)	0.160 (0.26)	-

The superscript "*", " \blacktriangle ", and "#" denotes the significant inter-group difference based on muscle union pairs, and the significant intra-group differences between ECU-ED and FCR-FD muscle unions and between dominant and nondominant arms, respectively, with 1 superscript for p < 0.05, 2 superscripts for p < 0.01, and 3 superscripts for p < 0.001.

Table 2.6 Pulse widths of motor NMES threshold on target muscle unions.

Stimulation target		Stroke	Control	Mann-Whitney U test
Arm	Muscle union	Mean ± SE		p (A)
Nondominant	ECU-ED	14.7±1.1	12.1±0.7	0.057 (0.72)
	FCR-FD	12.8±0.7	10.5±0.5	$0.016^* (0.75)$
Wilcoxon signed-rank test	Wilcoxon signed-rank test - p (r)		0.087(0.44)	
Dominant	ECU-ED	10.9±0.3	12.4±0.7	0.413 (0.59)
Dominant	FCR-FD	8.7 ± 0.4	9.3±0.4	0.486 (0.58)
Wilcoxon signed-rank test - p (r)		0.002▲▲(0.81)	0.004 • (0.74)	
Wilcoxon signed-rank test on arms - p (r)		0.000***** (0.76)	0.246 (0.21)	-

The superscript "*", " \blacktriangle ", and "#" denotes the significant inter-group difference based on muscle union pairs, and the significant intra-group differences between ECU-ED and FCR-FD muscle unions and between dominant and nondominant arms, respectively, with 1 superscript for p < 0.05, 2 superscripts for p < 0.01, and 3 superscripts for p < 0.001.

2.3.2 P300 in the ERP response to FVS and NMES

Figure 2.6A, and B display the P300 waveforms averaged across subjects with respect to the factors of the group, stimulation scheme, and target arm. No intra-group significance was found between the two target muscle unions on the same arm (p > 0.05). Figure 2.6C illustrates the comparison between the peak amplitude and latency of the P300 waves. The corresponding values for the amplitude and latency can be found in Table 2.7, along with the probability and EFs for both the paired and independent t-tests. According to the intra-group comparison of the eight stimulation schemes (Figure 2.6A), significant P300 differences in amplitude were found from 339 to 706 ms in the control group and from 375 to 688 ms in the stroke group (p < 0.05). P300 responses to FVS were activated earlier with a higher peak amplitude in the control group than NMES (p < 0.001, Figure 2.6C), and were activated earlier (p < 0.001).

0.001) without a significant difference in peak amplitude in the stroke group than NMES. There was also a "stimulation-intensity-dependent response" tendency in which a higher intensity evoked a quicker response and a higher amplitude of P300.

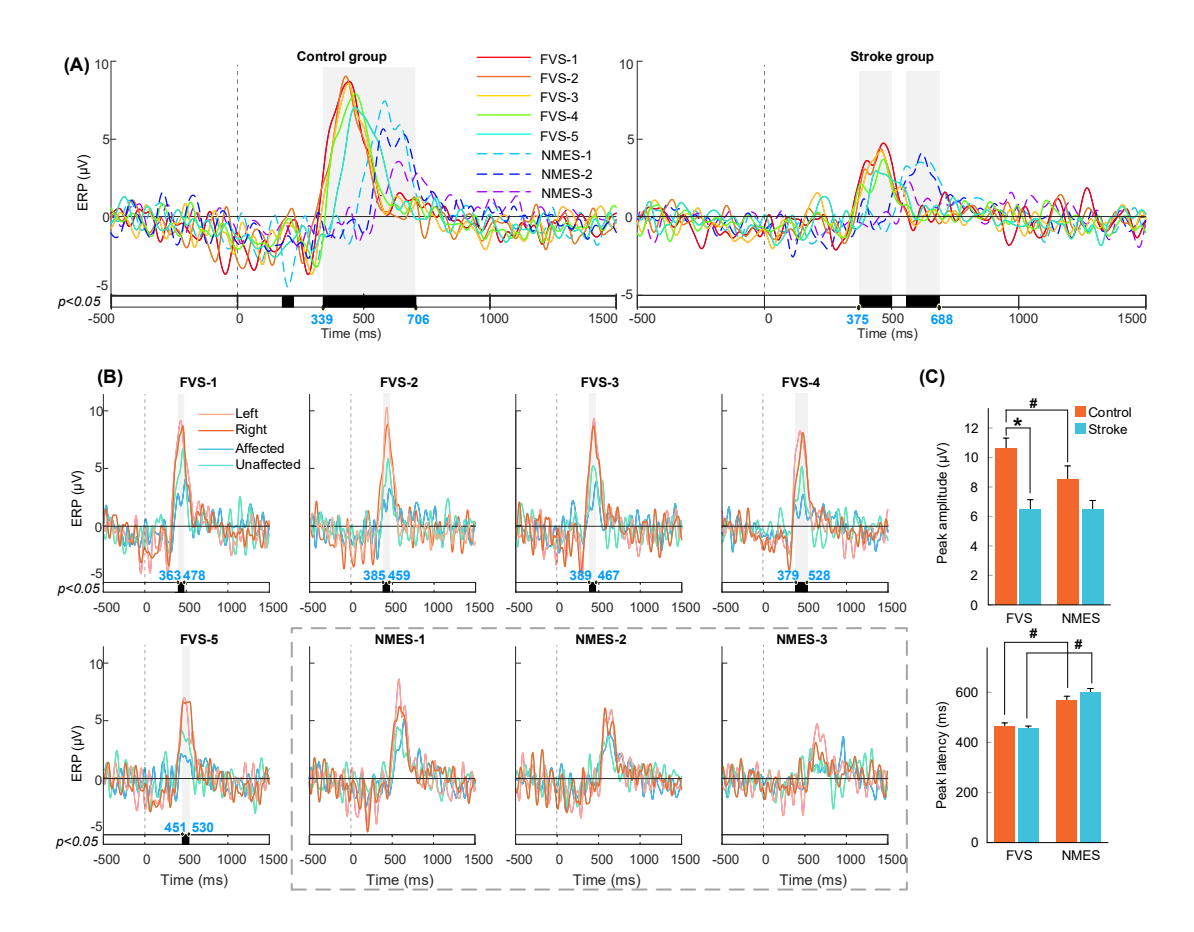


Figure 2.6 P300 in ERP averaged across subjects on the Fz, Cz, and Pz electrodes. The vertical dashed lines at 0s mean the onset of stimulations. (**A**) Intra-group comparisons among different schemes. (**B**) Inter-group comparisons among target arms of stroke and control groups based on stimulation scheme. The bold line means the significantly different periods between the amplitude of ERPs compared within a sliding time window (p < 0.05, cluster-based permutation test). The shading means P300 with statistical significance, of which the start and end time points were shown in blue. (**C**) Comparison of P300 peak amplitude and latency. Significant inter-group and intragroup differences are indicated by "*" and "#" (p < 0.05, independent t-test and paired t-test).

According to the inter-group comparison among the target arms of the stroke and control groups based on the stimulation scheme (Figure 2.6B), significant differences were observed from 363 to 478, 385 to 459, 389 to 467, 379 to 528, and 451 to 530 ms for responses to the FVS-1, 2, 3, 4, and 5 schemes, respectively (p < 0.05). The P300 peak amplitude in the control group during FVS was significantly higher than that in the stroke group (p < 0.001, Figure 2.6C). In contrast, no significant difference between the stroke and control groups was observed in all the NMES schemes (p > 0.05). Overall, the significant period of P300 was between 300 and 750ms, which was considered the period of interest in the RSP analysis.

Table 2.7 The amplitude and latency of P300 peaks.

		Stroke	Control	Independent t-test
Peak	Stimulation	Mean ± SE		p (Cohen's d)
A moralitando	FVS	6.45±0.69	10.60 ± 0.72	0.000*** (-1.52)
Amplitude	NMES	6.51±0.57	8.50±0.92	0.077 (-0.67)
Paired t-test - p (Cohen's d)		0.917(-0.03)	0.000### (1.08)	-
T stance	FVS	458.16±7.28	464.61±13.32	0.674 (-0.16)
Latency	NMES	599.24±16.24	569.09±15.66	0.192 (0.49)
Paired t-test - p (Cohen's d)		0.000### (-2.60)	0.000### (-1.32)	-

The superscript "*" and "#" denote the significant inter-group and intra-group differences of the P300 peak's amplitude and latency, respectively, with 3 superscripts for p < 0.001.

2.3.3 RSP response on the contralateral sensorimotor cortex

No significant differences among stimulation schemes were observed in the whole-brain RSP (p > 0.05). The RSP results reported here (Figure 2.7 and Figure 2.8) depict the contralateral sensorimotor RSP averaged across subjects during the period of interest. Appendix A, Appendix B, and Appendix C list the probability and EFs for the two-way mixed ANOVAs. No significant interaction was found in any of the frequency

bands, and no intra-group significant difference was found between the target muscle unions (p > 0.05). Appendix D, Appendix E, and Appendix F provide the detailed means and SEs of RSP with respect to the stimulation scheme, target muscle union, stimulation type, target arm, and group, in addition to the probabilities and EFs of the one-way ANOVA with repeated measures, as well as independent and paired t-tests.

Figure 2.7A shows the RSP comparison with respect to the stimulation scheme, target arm, and group. Intra-group significant differences in the beta and gamma bands were observed among stimulation schemes in the right arm of the control group (p < 0.001). According to the post hoc test, the NMES-3 scheme yielded significantly lower RSPs than did the FVS-1, 2, 3, and 4 schemes in the beta band (p < 0.05, adjusted by Bonferroni correction). In the gamma band, the NMES-3 scheme yielded significantly higher RSPs than did the FVS-1, 2, 3, 4, and 5 schemes, and the NMES-2 scheme yielded significantly higher RSPs than did the FVS-2 and 4 schemes (p < 0.05, adjusted by Bonferroni correction). No intra-group significant differences were found between the stimulation schemes for the control group in the theta or alpha band or for the stroke group in any band (p > 0.05). According to the results of the inter-group comparison, the overall RSP in the stroke group was significantly lower than that in the control group in the alpha and beta bands (p < 0.001 and = 0.012). In particular, the RSPs of the stroke group were significantly higher than those of the control group in the nondominant arms (i.e., A and L) during all stimulation schemes and in the dominant arms (i.e., U and R) during the FVS-1, 2, 4, 5, and NMES-1, 2 schemes in the alpha band (p < 0.05), as well as in the nondominant arms during the FVS-5 and NMES-2, 3 schemes and in the dominant arms during the NMES-3 scheme in the beta band (p <0.05). No inter-group significant differences based on the stimulation scheme or target arm were observed in the theta or gamma band (p > 0.05).

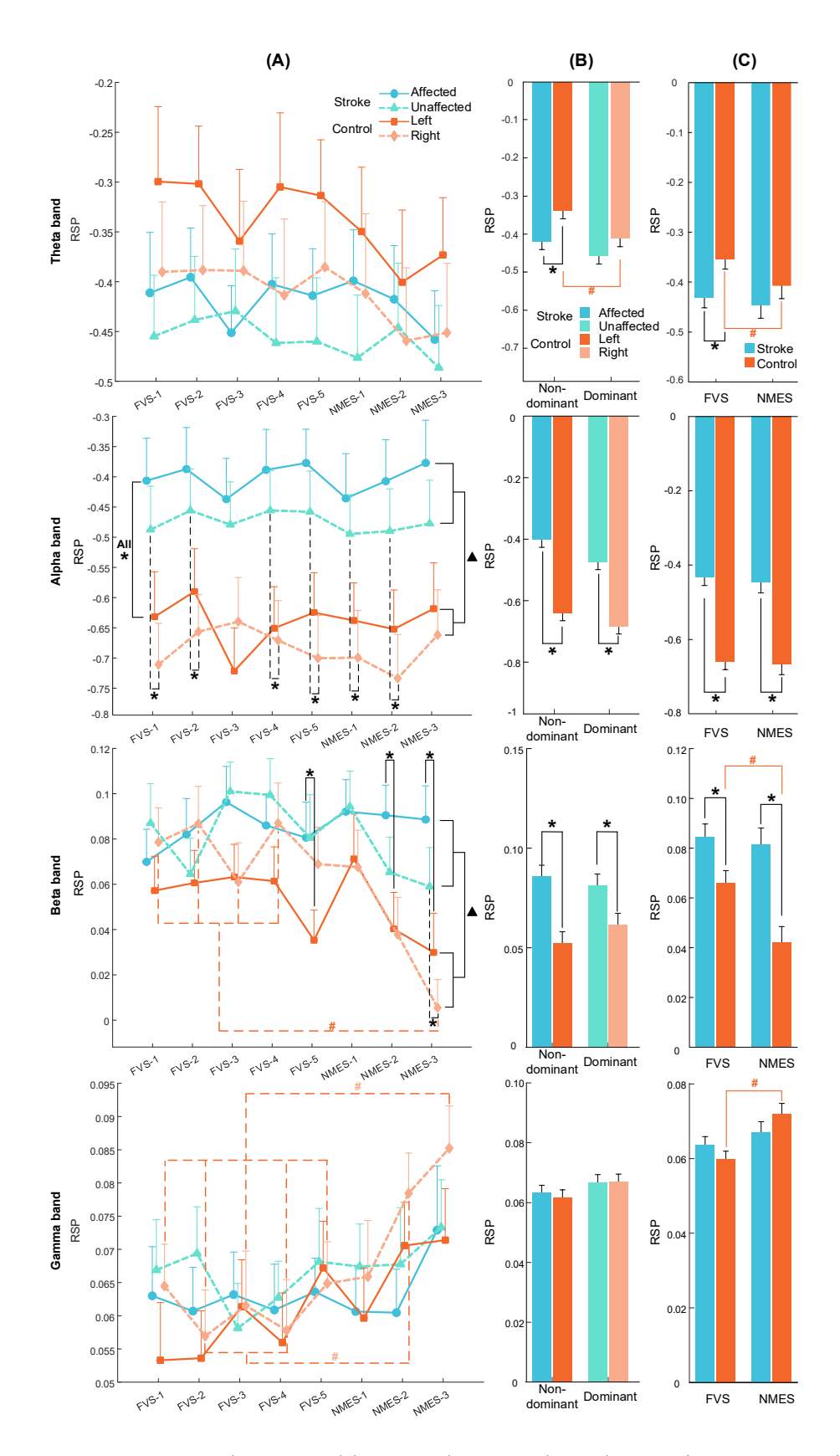


Figure 2.7 RSP averaged across subjects on the contralateral sensorimotor cortex in the theta, alpha, beta, and gamma bands during the period of interest. The RSP values are

presented as the mean with SE (error bar). RSP comparison with respect to (A) the stimulation scheme, target arm, and group. Significant intra-group differences between schemes are indicated by "#" (p < 0.05, one-way ANOVA repeated measures with Bonferroni post hoc tests). Overall, significant inter-group differences are indicated by " Δ " (p < 0.05, two-way mixed ANOVA). Significant inter-group differences based on the target arm are indicated by "*" (p < 0.05, independent t-test). RSP comparison with respect to (B) the target arm and group and (C) the stimulation type and group. Significant intra- and inter-group differences are indicated by "#" and "*" (p < 0.05, paired and independent t-test), respectively.

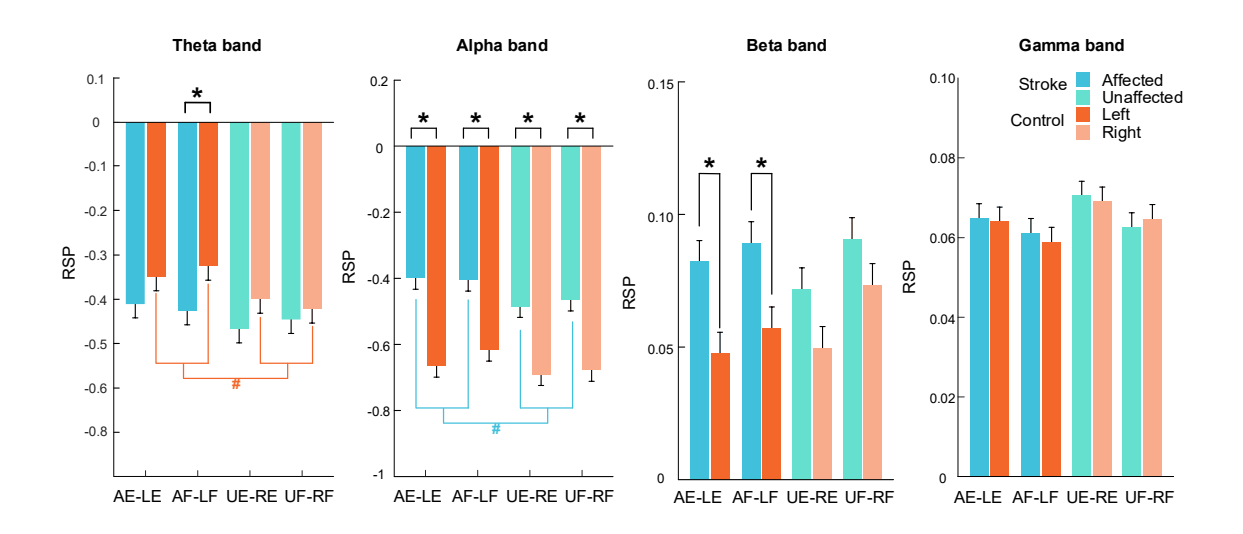


Figure 2.8 RSP comparison with respect to target muscle union. Significant inter-group differences based on target muscle union are indicated by "*" (p<0.05, independent t-test). No significant intra-group difference between four muscle unions in each group (p > 0.05, two-way mixed ANOVA). Significant intra-group differences between arms in each group are indicated by "#" (p < 0.05, independent t-test).

Figure 2.7B shows the RSP comparison with respect to the target arm and group. According to the intra-group comparison, the RSP in the theta band was significantly higher in the nondominant arm than in the dominant arm in the control group (p = 0.004). No intra-group significant differences between the target arms were observed in the

alpha, beta, or gamma band (p > 0.05). According to the results of the inter-group comparison, the RSP in the theta band was significantly lower in the nondominant arm in the stroke group than in the control group (p = 0.009). In the alpha and beta bands, both arms of the stroke group had significantly higher RSPs than did those of the control group (p < 0.05). No inter-group significant differences based on the target arm were observed in the gamma band (p > 0.05).

Figure 2.7C shows the RSP comparison with respect to the stimulation type and group. According to the intra-group comparison, the RSP of the control group during FVS was significantly higher than that during NMES in the theta and beta bands (p < 0.001 and = 0.023) but was significantly lower than that during NMES in the gamma band (p < 0.001). No intra-group significant differences between FVS and NMES were observed for the control group in the alpha band or for the stroke group in any of the bands (p > 0.05). According to the results of the inter-group comparison, the RSP during FVS in the theta band was significantly lower in the stroke group than in the control group (p = 0.005). In the alpha and beta bands, the RSP of the stroke group during FVS and NMES was significantly higher than that of the control group (p < 0.01). No inter-group significant differences were observed in the gamma band (p > 0.05).

2.3.4 ERSP response on the bilateral sensorimotor cortex

Figure 2.9 shows the ERSP at C3/C4 averaged across subjects with respect to the stimulation scheme, target arm, and group. In the control group, compared with the resting baseline, FVS and NMES evoked significant ERD in the alpha and beta bands (i.e., α ERD and β ERD) and significant ERS in the theta band (i.e., θ ERS) after stimulation onset (p < 0.05). For both FVS and NMES, compared to those in the control group, the stroke group exhibited decreased amplitudes and restricted distributions in ERD/ERS across the frequency bands. In addition, bilateral ERD/ERS could be observed in the control group on both arms. However, when the affected arm of the

stroke group was stimulated, the ERD/ERS was more intensive in the ipsilateral/contralesional hemisphere (Figure 2.9C) than in the contralateral/ipsilesional hemisphere (Figure 2.9A).

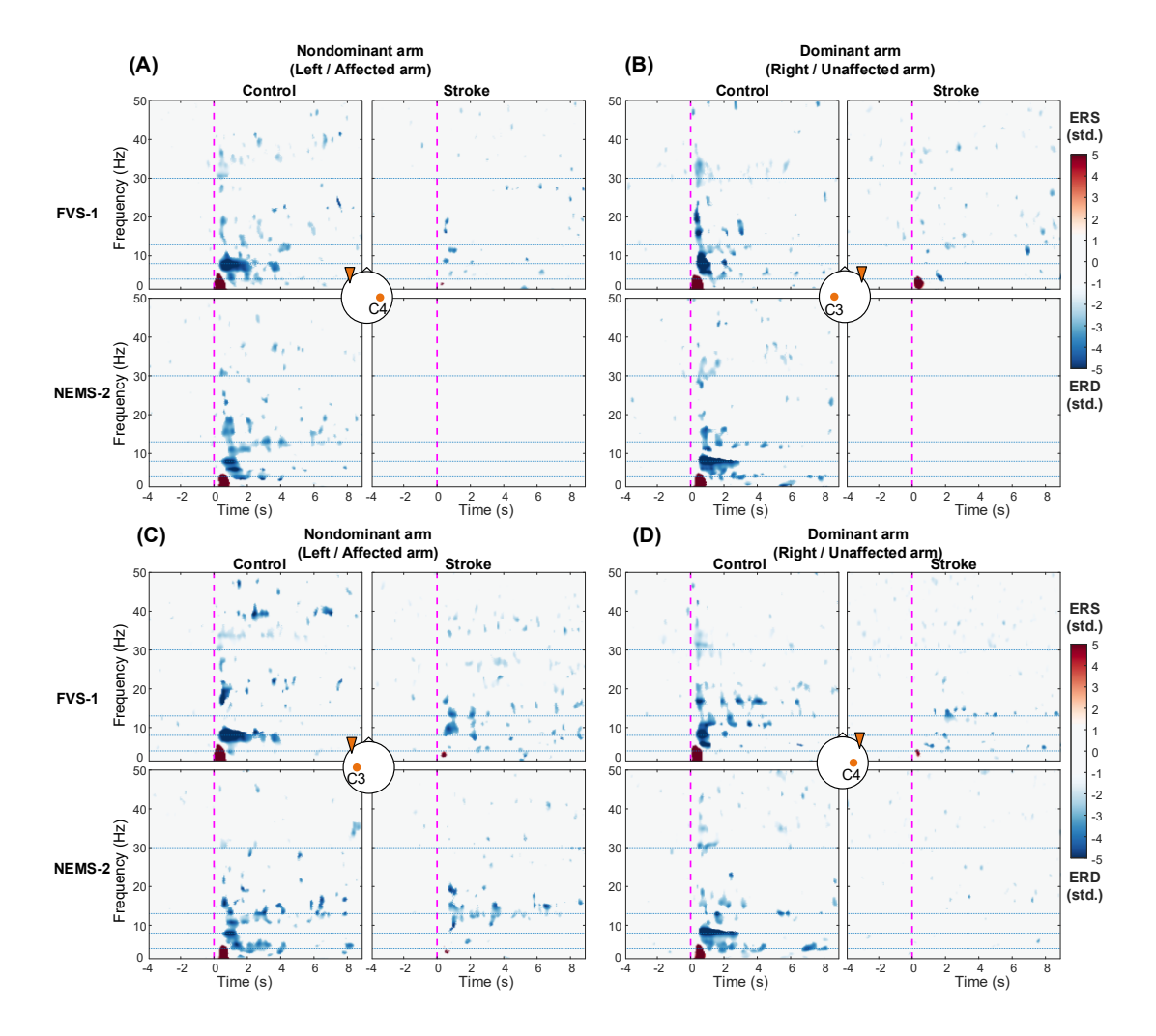


Figure 2.9 ERSP averaged across subjects in the C3/C4 channel contralateral (**A** and **B**) and ipsilateral (**C** and **D**) to the stimulated arms during representative FVS and NMES. The blue and red color schemes denote the ERD and ERS, respectively. Significant ERD/ERS in comparison with the resting baseline (p < 0.05, baseline permutation statistical method with FDR correction). The vertical dashed magenta lines at 0s mean the onset of stimulations. The horizontal dotted blue lines show the frequency band boundaries at 4, 8, 13, and 30 Hz. The brain icon at the center of each subfigure shows the stimulated nondominant/dominant arm by the orange triangle on

one side and the observed contralateral or ipsilateral channel by the C3/C4 label.

2.3.5 Spatial distribution of ERD/ERS topography

Figure 2.10 displays the averaged ERD/ERS topographies and comparisons between the stroke and control groups in response to FVS-1 and NMES-2. In Figure 2.10A, for both FVS and NMES, the stroke group showed lower holistic ERD/ERS in restricted cortical areas than did the controls. The θ ERS mainly occurred on the bilateral central area in the control group, and additional recruitment over the ipsilateral parietal area could be activated during FVS compared to NMES. No θ ERS was observed in the stroke group. The αERD occurred mainly on the bilateral central area in the control group but on the contralesional hemisphere in the stroke group. The aERD peaks in the stroke group shifted from the central area to the contralesional parietal-occipital area compared with those in the control group. The βERD occurred mainly on the bilateral central area in both subject groups. As shown in Figure 2.10B, in comparison with that in the control group, the θ ERS in the stroke group was significantly suppressed on the bilateral central-parietal-occipital area in response to FVS (p = 0.003) and mainly on the paramedian central area in response to NMES (p = 0.005). The α ERD was significantly weakened, mainly on the ipsilesional central-parietal area, during both FVS and NMES (p = 0.003). The β ERD was significantly diminished on the paramedian central-frontal area during FVS (p = 0.016) and on the ipsilesional centralfrontal area during NMES (p = 0.018).

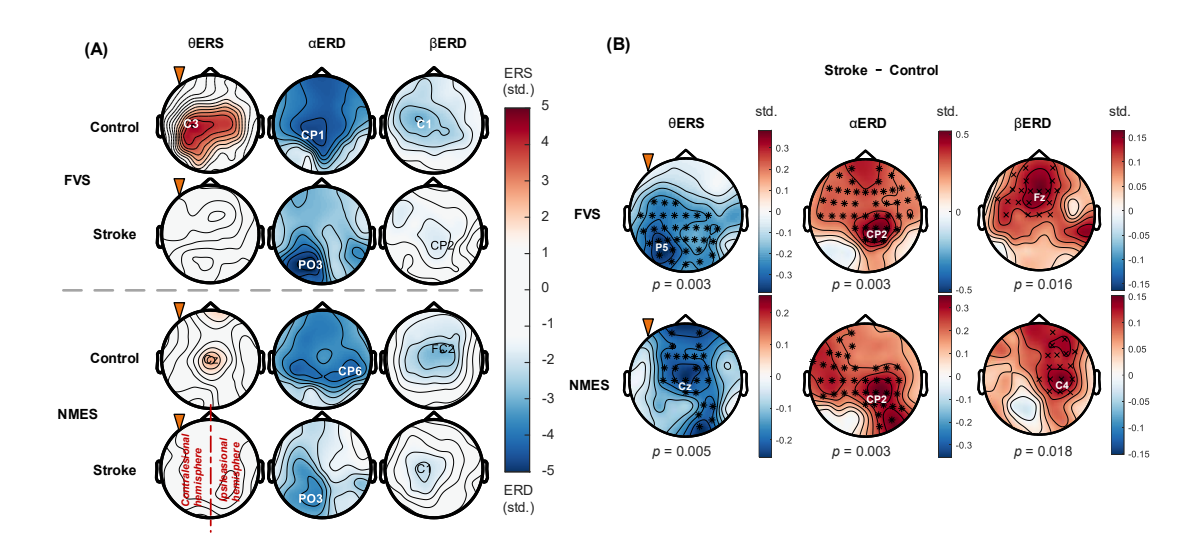


Figure 2.10 (A) ERD/ERS topographies when stimulating the nondominant arm. The blue and red color schemes denote the ERD and ERS, respectively. Peak channels are indicated by the labels. **(B)** Differences of the topography between stroke and control groups. The blue and red color schemes denote the negative or positive differences, respectively. Significant differences between stroke and control groups are indicated by "×" for p < 0.05 and "*" for p < 0.01 (cluster-based permutation test). The orange triangle indicates stimulating the nondominant (left/affected) arms. The right hemisphere is ipsilesional for the stoke group.

2.4 Discussion

By evaluating the immediate neuromodulatory effects of FVS and NMES via EEG, we found that both FVS at 1.9 G and sensory-level NMES effectively activated the sensorimotor cortex but with different responses. FVS was found to be particularly effective in eliciting transient involuntary attention, while sensory-level NMES primarily fostered cortical responses of the targeted muscles in the motor cortex.

2.4.1 Altered perceptual sensitivity after stroke

The monofilament test mainly assesses the tactile function of the skin. The increased perceptual sensitivity in the unaffected ED-ECU of stroke survivors revealed by the

monofilament results (Figure 2.5A) could be related to the sensory stimulation resulting from the habitually preferred use of the unaffected UL in chronic stroke. The lack of discrimination between the limbs and between the subject groups except UE vs. RE (Figure 2.5A) suggested that skin tactile function was basically preserved in the poststroke participants recruited in this work. In contrast to the preserved tactile function of the skin, combined sensorimotor impairment poststroke was revealed by the NMES evaluations. Both perceptual and motor thresholds in the affected arm were higher than those in the other arms, indicating weakened afferent and efferent functions in the target muscles after stroke (Figure 2.5B and C). The between-group differences in Figure 2.5B and C by sensory and motor NMES revealed combined effects of the skin and muscular functions on the impaired perceptual sensitivity after stroke when the differences in the skin tactile function were not significant. It implied that the sensory impairments after stroke in the targeted positions in this study could be mainly related to the sensory deficiency in muscles.

2.4.2 Earlier P300 evoked by FVS than NMES

For both subject groups, the P300 exhibited a stimulation-intensity-dependent trend at various intensities of FVS and NMES, respectively (Figure 2.6A). A direct quantitative association was demonstrated between brain activation and stimulation intensity, which was consistent with previous reports on the response to sensory stimulation in unimpaired persons measured by EEG (Insausti-Delgado et al., 2020), magnetoencephalography (Otsuru et al., 2011), functional magnetic resonance imaging (Backes et al., 2000; Smith et al., 2003), and transcranial magnetic stimulation (Fraser et al., 2002). Compared to NMES, the FVS in the control group evoked significantly higher peak amplitudes with shorter latencies in the P300 response (Figure 2.6A and C). This could be related to the fact that FVS can activate selective mechanoreceptors (mainly Ia afferent endings in the muscle spindles and Pacini receptors in the skin) with

synchronous action potential in the afferent pathway (Souron et al., 2017), while NMES can bypass mechanotransduction and directly elicit wider recruitment of diverse sensory receptors and nerve fibers, generating varying conduction velocities with receptor delays in the afferent pathway compared to FVS (Jousmäki, 2000; Kim et al., 2020). In addition, previous studies on sensory stimulation have suggested that a shorter latency in ERP is associated with less effort/attention to perform the sensation task (Ortiz Alonso et al., 2015), and a higher peak amplitude indicates more favorable skin interactions with fewer distractions to achieve better attention (Alsuradi et al., 2020). It indicated that FVS was a more favorable sensory stimulus than NMES in this study, requiring less effort of attention and fewer cognitive resources for perception. During FVS, P300 peaks were lower in the stroke group than in the control group (Figure 2.6B and C). This could be related to an impaired afferent pathway and reduced neural resources at the cortical level after stroke (Bolton and Staines, 2012; Reuter et al., 2014). However, FVS still demonstrated a faster response in evoking P300 than NMES in the stroke group (Figure 2.6A and C), mainly because of the homogeneous recruitment of mechanoreceptors in the skin and muscle spindles.

2.4.3 Spectral features of cortical responses to FVS and NMES

The power suppression (e.g., in RSP) or desynchronization (i.e., ERD) of alpha and beta rhythms over the sensorimotor cortex has been extensively employed as a characteristic of neural activation during somatosensory tasks in unimpaired participants (Corbet et al., 2018; Insausti-Delgado et al., 2020; Yakovlev et al., 2023). For example, NMES above the motor threshold has been reported to induce significant ERD in the alpha and beta bands over the sensorimotor cortex compared with the resting baseline (Insausti-Delgado et al., 2020; Carson and Buick, 2021). In addition, by depolarizing peripheral sensory neurons in the skin and muscles without causing muscular contraction, sensory-level NMES also effectively conveys proprioception and

induces significant ERD in the alpha and beta bands across sensorimotor areas through the afferent pathway (Corbet et al., 2018). In this study, the weakened activation level of the sensorimotor cortex in the alpha and beta bands (Figure 2.9) suggested stroke-induced sensory deficiency through the afferent pathway to the sensorimotor cortex. However, the ERD in the related bands in response to sensory-level NMES and FVS (1.9 G) still could be significantly differentiated from the baseline in the stroke group, with similar patterns between the two different stimulation types (Figure 2.9, stroke group). Similar to the ERD patterns, the alpha- and beta-RSPs over the contralateral sensorimotor cortex evoked by the FVS intensities had equivalent values to those by NMES, with the intensities above the perceptual threshold (Figure 2.7). These results suggested that FVSs could effectively evoke neural responses in the lesioned sensorimotor cortex through the afferent pathway in stroke survivors as NMESs above the perceptual threshold, which was considered the rehabilitative potential to induce neuroplastic modifications within the sensorimotor cortex poststroke (Corbet et al., 2018; Carson and Buick, 2021).

Compared to those in the control group, the holistic lowered alpha- and beta-RSP for both affected and unaffected arms of stroke survivors (Figure 2.7B) indicated bilaterally weakened sensorimotor activation after stroke. As indicated in the study by Genna et al., the cortical processing of sensory stimulation involves the bilateral hemispheres during tactile stimuli to unilateral arms, i.e., the sensory responses are fused through inter-hemispheric pathways in unimpaired persons (Genna et al., 2017). Similarly, in this study, the bilaterally weakened sensorimotor activation level in the stroke group also indicated the impact of impaired inter-hemisphere neural networks on the sensation of both affected and unaffected limbs, i.e., bilateral sensory deficiency, due to lesions in the ipsilesional hemisphere.

Moreover, the significant α ERD response induced by prolonged FVS and NMES, i.e., 10s, in this study mainly concentrated within the first 4 s after the stimulation onset in

the unimpaired controls but nonsignificant thereafter (Figure 2.9). It was related to the sensory adaptation to a sustained stimulus with attenuated cortical responses (Insausti-Delgado et al., 2020). In contrast to those in the control group, the shorter duration of α ERD in the stroke group suggested an earlier adaptation to external somatosensory stimuli poststroke because of a rapid neuronal desensitization in the afferent pathway (Graczyk et al., 2018). The neuronal desensitization in the sensory pathway covered more than the mechanotransduction stimulated by FVS, as the α ERD evoked by NMES of the stroke group also demonstrated similar shortened durations.

Significant θERS was observed in the control group upon the onset of both FVS and NMES (Figure 2.9). However, this response was weak in the stroke group. Theta-band oscillations could reflect changes in the attention given to new information/stimulation (Khajuria and Joshi, 2022). Several studies have reported that power enhancement or synchronization in theta rhythms within 500 ms after the onset of an external stimulus mainly indicates transient involuntary attention given to this new sensory stimulus (Wang et al., 2010; Genna et al., 2017). In the control group, the significantly higher theta RSP during FVS than those during NMES (Figure 2.7C) indicated that FVS was more effective at evoking involuntary attention than NMES. Similar findings of the distinctions between FVS and NMES in theta oscillations could be observed for the stroke group (Figure 2.7C and Figure 2.9). However, they were not statistically significant, primarily due to the diminished temporary involuntary attention allocated to these sensory inputs after stroke.

It was also observed that NMES could arouse higher gamma RSP than FVS in the control group (Figure 2.7C). This difference might be related to the extent of unpleasant perceptions associated with the different stimulation types (Michail et al., 2016). Even at the sensory levels, NMES could cause burning or tingling sensations; while the intensities of FVS in this work mainly achieved sensory feelings similar to those of manual stimulations, e.g., skin tapping or light pressing. The unpleasant perception

during NMES was related to the wide recruitment of diverse sensory receptors and nerve fibers, including nociceptors, which accounted for the significantly higher gamma RSP than that of FVS eliciting homogenous mechanoreceptors in the skin and muscle spindles.(Hautasaari et al., 2019).

2.4.4 Topographical patterns of cortical responses to FVS and NMES

Transient cortical modulation in the sensorimotor area has been found in unimpaired persons during transcutaneous electrical sensory stimulation to muscles (Hautasaari et al., 2019; Insausti-Delgado et al., 2020). The transmission of the stimulation inputs through the afferent pathway, from peripheral sensory neurons in the muscles and skin to the spinal cord, can activate the primary motor cortex (M1) via Brodmann's area 3a in the primary somatosensory cortex (S1) (Carson and Buick, 2021). In this study, compared to the sensory-level NMES, FVS (1.9 G) activated similar sensorimotor areas in the alpha and beta bands in both subject groups (Figure 2.10A). These findings suggested that FVS could achieve cortical recruitment in the sensorimotor cortex via the afferent pathway similar to those of NMES, with similar intensities of the RSPs in the alpha and beta bands (Figure 2.7).

However, the cortical areas recruited by FVS in the θ ERS topography were larger than those recruited by NMES in the control group, with additional recruitment covering the ipsilateral parietal area (Figure 2.10A). In a study of cortical somatosensory responses in unimpaired persons by Hautasaari et al., it was reported that brain activation on the sensorimotor cortex could be elicited more widely by mechanical stimulation than the electrical one (Hautasaari et al., 2019). This is mainly because the mechanical stimulation elicits more homogenous mechanoreceptors in the skin and muscle spindles and additionally activates the ipsilateral somatosensory cortex, drawing more involuntary attention compared to the electrical stimulation. In this study, the results of wider recruitment in the θ ERS topography, together with the higher theta RSP (Figure

2.7C) obtained in the control group over the sensorimotor cortex, suggested that FVS was a more effective stimulation to recruit cortical resources for transient involuntary attention than NMES. The additional recruitment over the ipsilateral parietal area suggested that the posterior association area was recruited for somatosensory perception of FVS, which indicated better spatial attention/awareness of the body elicited by FVS than by NMES. However, θ ERS in the cortex of the stroke group could not be significantly presented related to poststroke numbness, mainly because of the weakened afferent signals evoked by both stimulation types compared to the control group (Figure 2.10B, Figure 2.9, and Figure 2.7C).

The stroke group exhibited contralesional compensation and domination in the cortical responses compared to those of the control group. Consistent with previous findings in unimpaired individuals (Genna et al., 2017), bilateral activation of the sensorimotor cortex was observed in the control group during FVS and NMES (Figure 2.9 and Figure 2.10A, control group) because the sensory responses are normally fused through interhemispheric pathways. In contrast, the αERD over the contralesional hemisphere remained after stroke (Figure 2.9C, stroke group, and Figure 2.10A), but the αERD over the ipsilesional hemisphere was significantly weakened (Figure 2.10B). This observation agreed with previous findings that the reorganization of somatosensory neurocircuits after stroke involves cortical recruitment concentrated in contralesional cortical regions, i.e., contralesional compensation (Zhou et al., 2021b; Williamson et al., 2022). Furthermore, αERD peaks shifted to the contralesional parietal-occipital area in the stroke group (Figure 2.10A), which revealed that the contralesional somatosensory association cortex and visual cortex outside the S1 were involved in the sensory process poststroke (Bauer et al., 2006; Huang et al., 2020a). It implied that stroke survivors exerted additional effort in the somatosensory association cortex and engaged supramodal neural networks in the visual cortex related to spatial attention as

part of their contralesional compensation mechanism. This allowed them to process and analyze sensory information from S1 in response to sensory stimuli after stroke.

Significant attenuated βERD responses were observed in the stroke group over the frontal-parietal area, i.e., motor cortex including M1, supplementary motor area (SMA), and premotor cortex (PMC) (Figure 2.10B). Interestingly, asymmetric cortical responses were captured in response to NMES in contrast to FVS. Beta oscillations play a crucial role in the closed-loop neural network for the transmission of motor-related information from the M1 to the muscles and back to the M1 via somatosensory pathways in corticospinal communications (Aumann and Prut, 2015). Corbet et al. indicated that the beta oscillations enhanced by electrical sensory stimulation could be interpreted as stimulation-fostered muscle representation in the motor cortex according to the beta closed-loop neural network (Corbet et al., 2018). In this study, for the ipsilesional hemisphere, beta oscillations were significantly attenuated in response to both FVS and NMES after stroke (Figure 2.10B), indicating impaired beta close-loop neural network wiring the ipsilesional motor cortex after stroke in response to the two sensory stimulation types. However, in the contralesional hemisphere, in contrast to FVS eliciting significantly weakened beta oscillations after stroke, NMES could evoke comparable beta oscillations as the control group (Figure 2.10B). This finding suggested that the sensory-level NMES fostered cortical responses of the targeted muscles by recruiting additional contralesional pathways for motor enhancement in comparison with that of FVS. This observation might also indicate that NMES could be more prone to trigger contralesional compensation in motor restoration than FVS.

Understanding how FVS and NMES neuromodulatory effects differ could guide new rehabilitative strategies. NMES could enable compensatory patterns, supporting early inpatient discharge. FVS may activate the ipsilesional somatosensory cortex and manage brief involuntary attention efficiently, making it ideal for training tasks requiring near-normal motor function or somatosensory engagement.

2.4.5 Limitations and future work

One potential limitation of this study was the relatively small sample size. The recruitment of participants continued until significant differences in the key EEG parameters were observed between FVS and NMES among the groups. Fifteen participants were finally recruited in each group, and the statistical significance achieved in the study showed sufficient effect sizes to reach conclusions. Another limitation of this study was the age disparity between the stroke and control groups. Despite the control group having a higher mean age than the stroke group, the significant inter-group differences in the EEG patterns remain evident. The significant findings suggested that neurological impairments introduced by stroke were the dominant factors over aging (Tyson et al., 2008) on the cortical responses to these sensory stimuli.

In addition to focal stimulation on a single target muscle investigated in the study, the application of distributed electrical and vibratory stimulations to multiple muscles has also demonstrated rehabilitative effects in patients following neurological disorders, e.g., whole-body vibration (Celletti et al., 2020) and the Electrosuit (Perpetuini et al., 2023). Future studies will be conducted on developing selective stimulation techniques with distributed vibratory stimulation and investigating the related neuromodulatory effects on muscle groups (e.g., agonist and antagonist, proximal and distal, etc.) with larger sample sizes of participants.

2.5 Periodic Summary

In this study, the immediate neuromodulatory effects of FVS and NMES were compared by EEG measurement on the cortical responses in individuals with chronic stroke and unimpaired controls. The results in alpha and beta oscillations of the stroke group revealed that both FVS at 1.9 G and NMES above the perceptual threshold

effectively activated the sensorimotor cortex and showed similar patterns in impairment of somatosensory processing after stroke, characterized by bilateral sensory deficiency on both affected and unaffected sides, early adaptation to external somatosensory stimuli, and contralesional compensation additionally eliciting parietal-occipital cortex. However, FVS was found to be particularly effective in eliciting transient involuntary attention, as evidenced by faster response in P300 and higher theta oscillations, mainly because of the homogeneous recruitment of mechanoreceptors in the afferent pathway by FVS. In contrast, sensory-level NMES primarily fostered cortical responses of the targeted muscles in the motor cortex by recruiting additional contralesional pathways for motor enhancement, as observed through beta oscillations. Overall, by elucidating the specific cortical responses involved in FVS and NMES, this study contributes to our understanding of their potential applications in stroke rehabilitation and provides valuable insights for developing more tailored interventions in the future.

CHAPTER 3

HYBRID SOFT ROBOT WITH ELECTRO-VIBRO-FEEDBACK FOR SENSORIMOTOR-INTEGRATED WRIST/HAND REHABILITATION AFTER STROKE

This chapter is adapted from

Lin, L., Qing, W., Kuet, M.-T., Zhao, H., Ye, F., Rong, W., Li, W., Huang, Y., & Hu, X. (2025). Sensorimotor Integration (SMI) by Targeted Priming in Muscles with EMG-driven Electro-Vibro-Feedback in Robot-Assisted Wrist/Hand Rehabilitation after Stroke. *Cyborg and Bionic System*. Submitted.

and

<u>Lin, L.</u>, Kuet, M.-T., Qing, W., Zhao, H., Ye, F., Huang, Y., et al. (2024). "Effects of sensorimotor-integrated (SMI) wrist/hand rehabilitation assisted by a hybrid soft robot poststroke," in 2024 17th International Convention on Rehabilitation Engineering and Assistive Technology (i-CREATe) (IEEE), 1–4. https://doi.org/10.1109/i-CREATe62067.2024.10776482

3.1 Introduction

Stroke was one of the leading reasons for serious long-term disabilities, and more than 2% of people reported that they had disabilities because of stroke (Mane et al., 2020). Stroke causes impairments in both motor and sensory pathways, and loss of sensory function hinders motor restoration. Therefore, motor relearning after stroke depends on integrated sensorimotor practices in the paralyzed limbs with high repetitions. On the one hand, limb motions with voluntory motor effort could enhance the neuroplasticity in the CNS and the motor output in the peripheral muscles. On the other hand, sensory retraining by either mechanical (e.g., FVS) or electrical stimulation (e.g., NMES) to the skin over the target muscles could improve movement coordination in the UL after stroke (Turville et al., 2019), by increasing the awareness of a target muscle in contraction, as well as elevating the related cortical activation (Cauraugh et al., 2000; Lin et al., 2024b).

Rehabilitation robots have been developed to assist in labor-demanding physical training after stroke, with the main advantages of higher dosage and lower cost, compared to manpower in long-term rehabilitation (Zhang et al., 2018). Robots with pure mechanical actuation, i.e., pure robots, simulate physical support provided by a human therapist in poststroke motor interventions. However, although proprioception experiences, e.g., joint motions and positions, could be provided even in movement assisted by pure robots, they still focus on precise control of repetitive motor actions, often neglecting the modulation of somatosensory inputs from target muscles crucial for poststroke motor restoration (Gassert and Dietz, 2018; Lin et al., 2024c). Seldom do robotic designs successfully recruit and/or control the somatosensory responses from targeted muscles in physical practices, which impedes the poststroke motor restoration requiring SMI compared to the interventions by human therapists who provide instructive pressing and tapping to muscles. It could be one of the major reasons that

the rehabilitation effectiveness of robot-assisted physical training has not exceeded the traditional manual operations, even with higher repetitions (Rodgers et al., 2019).

Transcutaneous NMES has been widely applied in routine poststroke rehabilitation with the main purpose of improving muscular force and preventing atrophy (Maciejasz et al., 2014). Meanwhile, NMES also provides additional therapeutic sensory inputs. The hybrid systems of NMES and mechanical robot (NMES-robots) indicated the benefits of introducing NMES to target muscles in addition to the mechanical assistance in limb motions, improving muscular coordination and leading to faster motor relearning compared to the pure robot (Qian et al., 2019). As a kind of NMES-robot, a novel soft ENMS for multi-joint UL rehabilitation was developed by our team recently (Nam et al., 2020). The system integrated multi-channel NMES to UL muscles, together with pneumatic actuation to the elbow and fingers, to provide assistance in armreaching tasks. Residual EMGs in the paretic muscles were detected as voluntory motor effort to control the NMES and mechanical supports from the system, augmenting the rehabilitative effects (Farmer et al., 2004; Nam et al., 2020). The integrated NMES could provide additional afferent facilitation along with muscle force enhancement and atrophy prevention on paretic distal muscles due to learned disuse poststroke, e.g., the ED, in hand functions (Nam et al., 2020). The combined NMES-robot has been found to be more effective than either NMES or pure robot solo treatments in poststroke UL rehabilitation (Resquin et al., 2016). However, muscle hypertonia always occurs on UL flexor (e.g., FD) poststroke, in which case NMES is not applicable to FD because it directly elicits wide recruitment of diverse sensory receptors and muscle fibers, leading to pain, muscle fatigue, and higher muscle spasticity on FD in long-term usage (Insausti-Delgado et al., 2020; Lin et al., 2024b).

In comparison with NMES, FVS, without causing muscle contraction, is more acceptable for stroke survivors since mainly the mechanoreceptors in the skin are activated in the stimulation. More recently, FVS has been introduced in robotic design

(Calabrò et al., 2017; Amano et al., 2020) to enhance the sensation of target muscles in initiating the contraction during robot-assisted physical training. In a hybrid robotic system, even though less efficient in inducing muscular contraction than NMES, FVS is more suitable for somatosensory priming on FD, which usually has sufficient residual force after stroke (Lan et al., 2011; Miller and Dewald, 2012). That is because FVS could efficiently activate the sensorimotor cortex and increase corticospinal excitabilities by afferent facilitation from target muscles but with higher comfortability in the long term than NMES due to selective activation of mechanoreceptors (mainly Ia afferent endings in the muscle spindles and Pacini receptors in the skin) (Lapole and Tindel, 2015; Souron et al., 2017; Lin et al., 2024b). However, FVS cannot directly evoke the focal muscular contraction in motor retraining as NMES, which is still necessary for motor restoration, particularly for the muscles with weakness due to learned disuse, e.g., ED. Therefore, robot-assisted somatosensory priming by the coordination of NMES on ED and FVS on FD with movement assistance has the promise to preserve the advantage of NMES in motor retraining with minimized pain and maximized effective sensory feedback by FVS to the CNS. However, little work has been done on the optimized integration of FVS and NMES in robot design, which could coordinate integrated sensorimotor functions of target muscles in limb practice for optimal motor restoration after stroke.

In this study, we designed EVF in a hybrid soft robot system to foster W/H motor restoration after stroke. The robot system is an EMG-driven exoneuromusculoskeleton with EVF (ENMS-EVF) that integrates NMES on the ED and FVS on the FD into a wearable exoskeleton with soft pneumatic muscles for W/H training after stroke. We also investigated the feasibility and rehabilitative effects of the rehabilitation training assisted by ENMS-EVF after stroke in a preliminary training program. We hypothesized that the ENMS-EVF system could feasibly assist stroke patients in improving the sensorimotor functions of UL after the training program.

3.2 Methodology

In this study, we designed a novel ENMS-EVF system in Figure 3.1 for W/H rehabilitation after stroke. The ENMS is a system with leading NMES-soft robotic technology (Nam et al., 2020) invented by our team. It integrates NMES and pneumatic actuation to UL joints through a triggering control by residual voluntory motor effort from a person after stroke, represented by EMG in paretic muscles, i.e., triggered by voluntory motor effort but not continuously involved. A novel EVF hardware system and control method were designed based on the EMG-triggered ENMS W/H module by integrating and collaborating FVS and NMES in the phasic motions of hand opening and closing. The integrated ENMS-EVF system consisted of a control box, a wearable glove, and a smartphone installed with an application as a wireless user interface through Bluetooth. The control box contained a rechargeable 12V Li-ion battery for a maximum of 4h continuous usage. In the hardware design, an FVS vibration motor was integrated into the EMG channel on the FD muscle, with the FVS motor in the middle of the two EMG electrodes. In the control design, FVS was delivered to the target FD muscle after the voluntory motor effort could be detected by EMG. Then, novel continuous EMG-driven EVF control was designed to coordinate NMES, FVS and pneumatic actuation to assist the hand movements with NMES channels on ED and sensory feedback from FVS on FD to achieve effective rehabilitative outcomes for stroke survivors. The feasibility and rehabilitation effectiveness of the new design were evaluated by a preliminary test and a 20-session training program with a group of people suffering from chronic stroke.

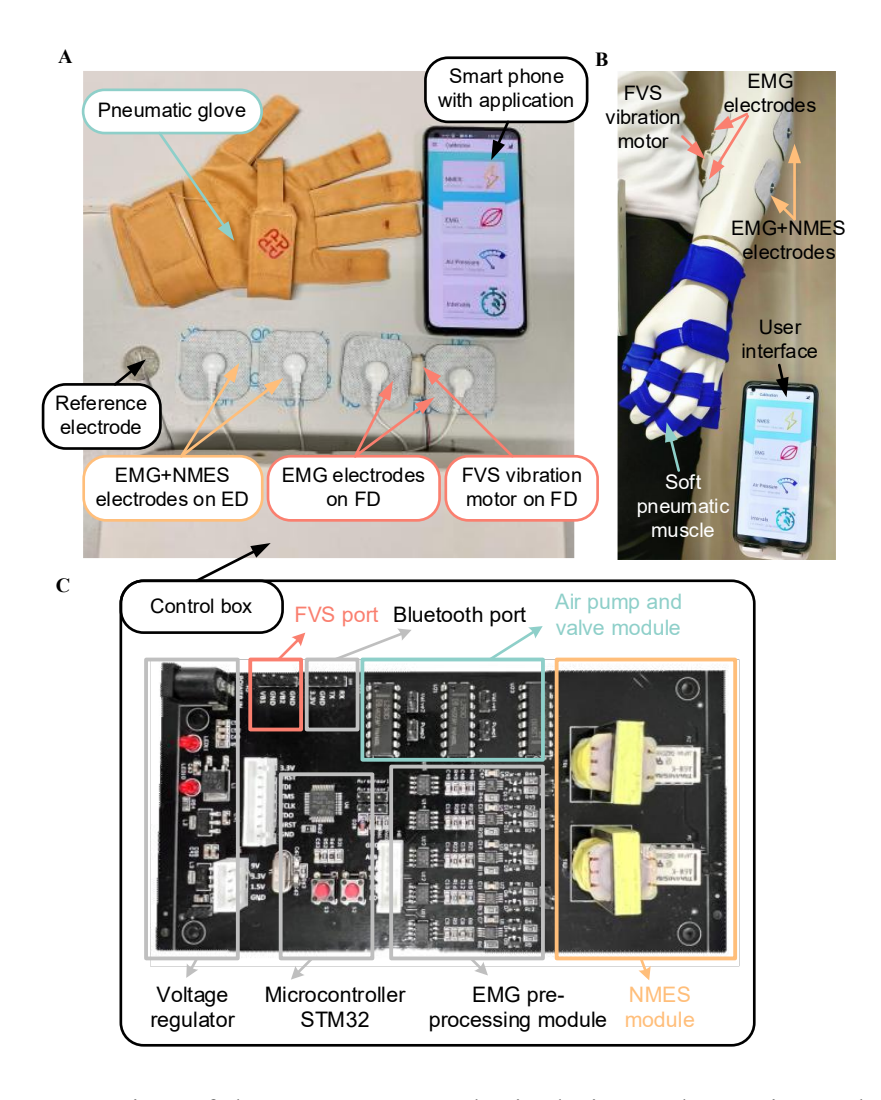


Figure 3.1 Overview of the ENMS-EVF robotic design and experimental setup. **(A)** ENMS-EVF system design. **(B)** ENMS-EVF worn on a mannequin. **(C)** The design of the PCB mounted in the control box.

3.2.1 System design of ENMS-EVF

The system diagram of the ENMS-EVF is illustrated in Figure 3.2. The microprocessor-based control unit (MCU, STM32F103C8T6 microprocessor, STMicroelectronics Inc.) coordinates with the voluntory motor effort detection via EMG, the ED unit, the FD unit, the musculoskeletal unit, and wireless communication with the smartphone (system of Android 10 with at least 3G network) via a Bluetooth module (HC-05, FEASYCOM. Co., Ltd).

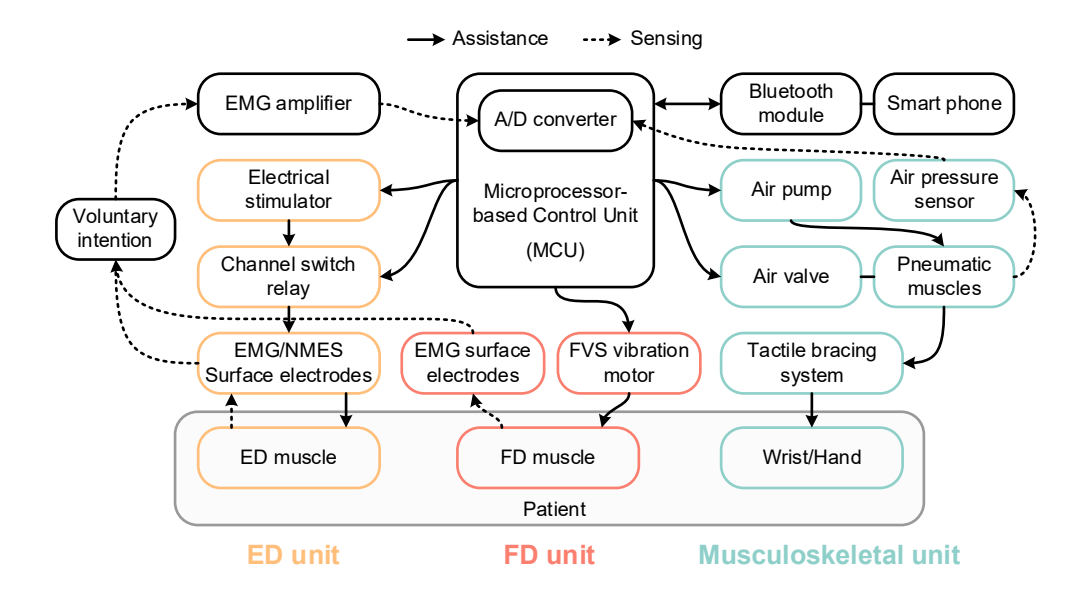


Figure 3.2 The design diagram of ENMS-EVF.

To detect voluntory motor effort, two pairs of EMG surface electrodes (5×5 cm², PALS Neurostimulation Electrodes, Axelgaard Manufacturing Co., Ltd.) were designed to be placed on the skin surface of the motor points of the W/H extensor and flexor, respectively. The extensor and flexor were, respectively, the muscle union of the ED and the ECU, i.e., ED-ECU, as well as the muscle union of the FD and the FCR, i.e., FD-FCR, given their close anatomical proximity in a muscle union. To avoid verbosity, we continue to use ED and FD to represent ED-ECU and FD-FCR muscle unions in the following text. The reference surface electrode (Ø2.5cm, PALS Neurostimulation Electrodes) was designed to be placed on the skin surface of the olecranon to attenuate the common mode noise. The EMG signals captured by the surface electrodes were first amplified 1000 times (INA 333 amplifier, Texas Instruments Inc.) and filtered from 10 to 500 Hz. These amplified and filtered signals were then sampled using the analog-to-digital (A/D) converter in the MCU with a sampling frequency of 1000 Hz for each EMG channel. After digitization, the EMG signals were full-wave rectified and moving-averaged with a 100-ms window to obtain the dynamic EMG levels (Nam et al., 2020).

In the ED unit, an NMES channel through the same EMG surface electrode pair on the ED was designed to assist muscle contraction and provide somatosensory feedback, i.e., somatosensory priming, during voluntary W/H extension. The NMES output was alternating current delivered in square pulses, with a frequency of 40 Hz (40 pulses per second) and an amplitude of 70 V. The pulse width was adjustable, ranging from 0 to 300 μs, which allowed for tailored levels of stimulation intensity that can achieve effective muscular contractions in paretic muscles after stroke (Rong et al., 2017). A channel switch relay was integrated into the channel control of electrodes on ED and used to alter the functions between the input of the EMG detection and the output of the NMES through the same electrode pair. This design also protected the EMG amplification circuit from the high stimulation voltage of NMES (Nam et al., 2020).

In the FD unit, the FVS vibration motor was designed to be attached between the EMG electrode pair on the FD to provide somatosensory priming during voluntary W/H flexion because of usually adequate muscle force on flexor preserved poststroke (Lan et al., 2011; Miller and Dewald, 2012). The vibration motor was a miniature encapsulated motor with eccentric rotating mass (E0716M, NFP-Motor Co., Ltd.), rotating at 14500rpm with a nominal amplitude of 5.1G, whose intensity was high enough to elicit the sensorimotor cortex (Lin et al., 2024b) without involuntary muscle contraction.

In the musculoskeletal unit of ENMS-EVF, 5 soft pneumatic muscles (polyvinyl chloride (PVC) membrane, 1-mm thick) with an exoskeleton extension (3D-printed by photopolymer) were covered by a textile glove (elastic bracing made of spandex) (Nam et al., 2020) for easy mounting to the W/H joints with Velcro tapes. The pneumatic muscles in the musculoskeletal were connected to a respective miniature air pump (WP27B-6D, Micro Energy, Co., Ltd) with an air valve (WV110A-3A, Micro Energy, Co., Ltd) and an air pressure sensor (MCP-H10, BOTLAND, Co., Ltd). The musculoskeleton unit was inflated by the air pump to provide extension torque to

individual digits as motor assistance during W/H extension and deflated when the valve was opened during W/H flexion. Additionally, the air pressure sensor connected to the pneumatic muscles fed back the real-time pressure to the MCU. The maximal inner pressure of the pneumatic muscles was set at <100 kPa to maintain the stability of the musculoskeletons under repeated inflations and deflations.

3.2.2 Control design of ENMS-EVF

The continuous EMG-driven EVF control in Figure 3.3 was designed to coordinate NMES in the ED unit, FVS in the FD unit, and pneumatic actuation in the musculoskeletal unit to assist the phasic motions of W/H extension and flexion with somatosensory priming. Voluntary EMG from a target driving muscle, i.e., EMG_{ED} or EMG_{FD} , was used to initiate assistance from the developed system. Once the EMG level of a driving muscle reached a preset EMG threshold, assistance from ENMS-EVF was initiated and continuously provided during an entire motion phase. In each motion phase, a patient was also required to exert the residual voluntary effort, together with the assistance to achieve the desired motion (Nam et al., 2020). The EMG threshold level in each motion phase was set as 10% maximal voluntary contraction (MVC) above the EMG baseline in the resting state.

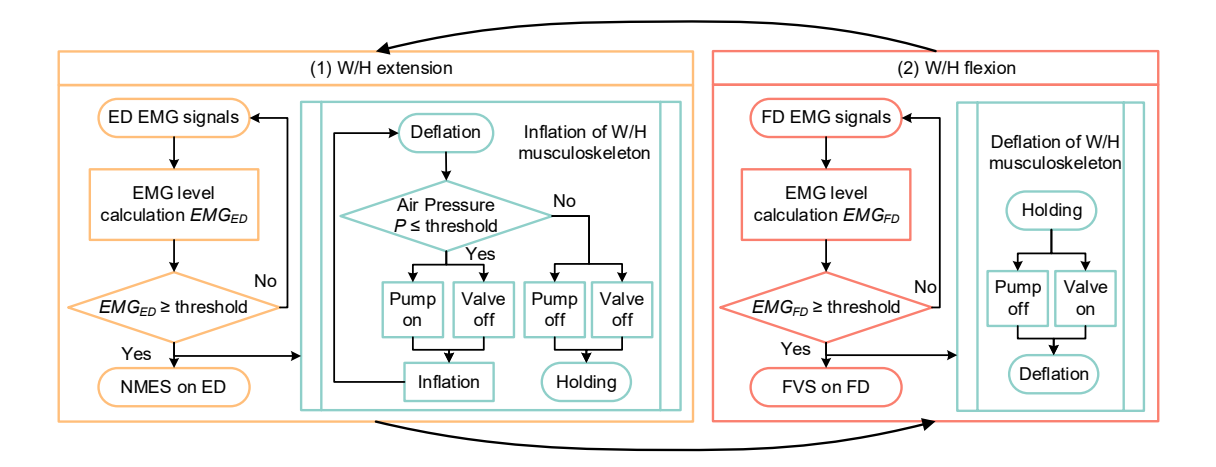


Figure 3.3 The control scheme diagram of the ENMS-EVF with voluntory motor effort

detection by EMG.

During the W/H extension phase, when the voluntary EMG activation level on the ED muscle EMGED reached the preset threshold, the ED received continuous NMES, and the fingers were mechanically assisted by the torque from the inflated musculoskeleton to aid in W/H extension throughout the motion phase. The air pressure P of pneumatic muscles was continuously monitored by the air pressure sensor during the inflation of the musculoskeleton. The air pump was on, and the air value was off to inflate the pneumatic muscles until the air pressure reached the preset threshold, which was determined when the user achieved maximal finger extension or when the air pressure P reached 100 kPa (Nam et al., 2020). When the air pressure P reached the preset threshold, the air pump stopped with the valve off to keep the musculoskeleton at holding status, requiring the patient to keep the residual voluntary effort of W/H extension. In the W/H flexion phase, as soon as the voluntary EMG activation level on the FD muscle EMG_{FD} reached the preset threshold, continuous FVS was provided to the FD of the paretic limb as somatosensory priming during the W/H flexion motion phase with torque propelled by residual contraction force from FD muscle of stroke patients without movement assistance, because of usually sufficient residual force in FD after stroke (Lan et al., 2011; Miller and Dewald, 2012). Meanwhile, the air valve was opened for passive pneumatic deflation of the musculolskeleton, during which the release of air from the pneumatic muscles was also facilitated by the residual voluntary effort from the FD.

3.2.3 Evaluation of ENMS-EVF

The assistive capability and rehabilitative effects of the ENMS-EVF were validated and evaluated on patients with chronic stroke. After the ethical approval of the Human Subjects Ethics Sub-Committee of the Hong Kong Polytechnic University before

commencement (approval number: HSEARS20210320003), a total of 7 chronic stroke participants were screened according to the following inclusion criteria:

- (1) at least 12 months after the onset of a unilateral lesion in cortical or subcortical regions due to stroke;
- (2) presence of no visual deficit and sufficient cognition to follow experimental instructions (MMSE score > 23) (Tombaugh and McIntyre, 1992);
- (3) moderate to severe motor disability in the affected UL (15 < FMA < 45) (Sullivan et al., 2011);
- (4) ≤ 3 spasticity at the wrist and fingers as measured by the MAS (Bohannon and Smith, 1987);
- (5) presence of detectable voluntary EMG signals from the ED and FD muscles on the affected arm (three times the standard deviation above the EMG baseline) (Nam et al., 2021);
- (6) presence of a passive range of motion (ROM) for the wrist from 45° extension to 60° flexion and the ability of the metacarpophalangeal (MCP) finger joints to be passively extended to 170°;
- (7) no neurological impairments except stroke; and
- (8) right-handed before the stroke onset.

The exclusion criteria for the stroke participants were (1) poststroke pain, (2) epilepsy, (3) cerebral implantation, and (4) pacemaker implantation. Before the commencement of the clinical trial, written informed consent was obtained from each participant.

3.2.3.1 Validation of ENMS-EVF configuration

A validation test was conducted to make sure the design parameters and task settings of the ENMS-EVF configuration were suitable for usage by the recruited participants. Before the validation test began, each participant received a tutorial that covered the process of donning and doffing the system, device operation, and the repetitive arm reaching and grasping tasks assisted by the ENMS-EVF. In the validation test of the ENMS-EVF configuration, each participant wore the ENMS-EVF on the paretic UL. Some configuration parameters were measured and tested to ensure that they were tailored to adapt to various spasticity levels of W/H joints and residual muscle force of ED and FD of each participant for feasible usage of the ENMS-EVF. These parameters included the EMG baseline in the resting state and MVC of the driving muscle unions to calculate 10% MVC above the EMG baseline for appropriate sensitivity of successful voluntory motor effort detection by EMG level, the applied FVS intensity for effective somatosensory stimulation, the applied pulse width of NMES for individual participants to open their wrists at 20°, and the maximum inner pressure of the pneumatic muscles for individual participants to passively open their MCP finger joints at a ROM of 170°.

After the test and setting of the parameters, participants had 10 minutes to get familiar with the respective assistance of FVS, NMES, and the musculoskeleton as a warm-up. Then, participants were instructed to sit at a table and maintain a distance of 30–40 cm between their shoulders and the table surface (as shown in Figure 3.4A). To begin, the smartphone with the app was placed on the table in front of the participant. Participants were then required to follow the instructions on the smartphone screen and complete 5 times of repetitive arm reaching and grasping tasks, assisted by the ENMS-EVF on the paretic UL. They were asked to complete horizontal tasks and vertical tasks at their natural speed while carrying a sponge (Nam et al., 2021), which is identical to those in the actual rehabilitation training. In the horizontal task (Figure 3.4A), the participant

was instructed to grasp a sponge near their affected side, move it 50 cm horizontally towards the other side, release it, then return it to the starting point and release it again. In the vertical task (Figure 3.4B), the participant was instructed to lift the sponge from the table to a shelf at 18cm height, release it, then bring it back down and place it on the table before releasing it again. Participants who successfully completed and passed the validation test on the ENMS-EVF configuration were invited to preliminary rehabilitation training.

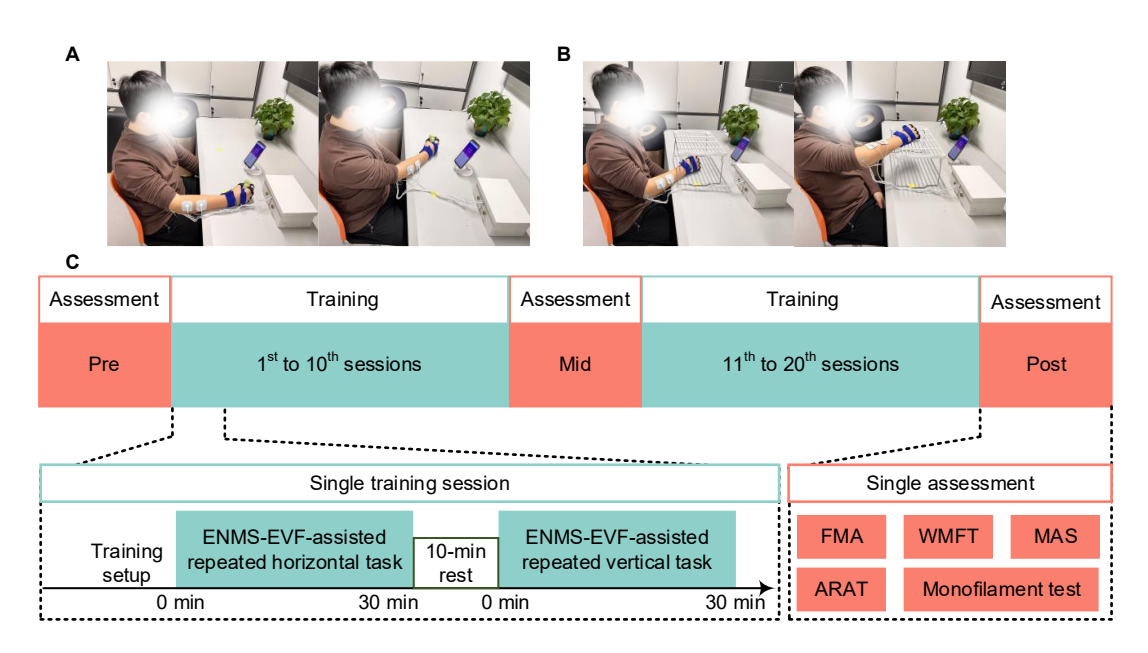


Figure 3.4 Evaluation of ENMS-EVF. **(A)** Horizontal task. **(B)** Vertical task. **(C)** Training program assisted by ENMS-EVF.

3.2.3.2 Rehabilitation training assisted by ENMS-EVF

A preliminary clinical trial with a single-group design was conducted to investigate the feasibility and rehabilitation effects of UL training assisted by the ENMS-EVF. The program for rehabilitation included 20 UL training sessions, all of which were assisted by ENMS-EVF and lasted at least 60 minutes per session (Figure 3.4C). The training sessions were scheduled at an intensity of 3-5 sessions per week for 7 consecutive

weeks, with no more than one session per day, as practiced before in robot-assisted W/H training (Nam et al., 2021).

The operator was responsible for instructing the participants and setting the training parameters for each training session according to the same procedures in the validation of the ENMS-EVF configuration mentioned above. These parameters included the EMG triggering levels of the driving muscles, the maximum inner pressure of the musculoskeleton, and the applied pulse width of NMES for individual participants. Prior to each training session, the operator would set these parameters to ensure that they were tailored to the needs of each participant. During each training session, participants were instructed according to the ENMS-EVF configuration and were asked to complete the repetitive arm reaching and grasping tasks, including a 30-minute horizontal task and a 30-minute vertical task at their natural speed while carrying a sponge (Nam et al., 2021). To prevent muscle fatigue during training sessions, a break of 10 minutes was permitted between two consecutive tasks (Figure 3.4B).

3.2.3.3 Evaluation of immediate training outcomes

The rehabilitation outcomes of UL training with assistance from ENMS-EVF were investigated by using clinical assessments on sensorimotor functional improvement. The adopted clinical assessments included (1) motor functional assessment in voluntary limb movements by the FMA with a total score of 66 for the UL assessment (Sullivan et al., 2011); (2) assessment of the UL voluntary functions focusing on the functional tasks by Action Research Arm Test (ARAT) (Carrol, 1965); (3) assessment of the functional ability and motion speed of the UL in daily tasks by Wolf Motor Function Test (WMFT) (Wolf et al., 1989); (4) sensation assessment on the affected arm measured by the Semmes-Weinstein monofilament test (Suda et al., 2020) on the skin surface above the ED and FD, and six sites on the ventral and dorsal side of the hand according to established protocol (Bowden et al., 2014); (5) muscle spasticity

assessment at the elbow, wrist, and finger joints measured by MAS (Bohannon and Smith, 1987). Both pre-training (Pre), mid-training (Mid), and post-training (Post) evaluations were conducted on all participants at time points before the 1st training session, immediately after the 10th training session, and immediately after the last training session, respectively (Figure 3.4C). The assessments were performed by an assessor who was blinded to the training.

3.2.4 Statistical analysis

The Shapiro-Wilk normality test was used to evaluate the normality of the clinical scores at a significance level of 0.05. Only MAS scores exhibited significance in the normality test (p < 0.05), meaning they were non-normally distributed. Other parameters were all normally distributed (p > 0.05). Thus, to investigate if there is a significant sensorimotor functional improvement immediately after 10-session or 20-session training, a paired test between the clinical scores at Mid or Post time points compared with those at Pre were conducted using Wilcoxon's signed-rank test on MAS and using paired t-test on other normally distributed scores. The statistical analysis in this study was performed by Matlab R2024a. The statistically significant level was set at 0.05 in this study. The significant level of 0.01 was also indicated.

3.3 Results

All the recruited participants successfully passed the validation test of the ENMS-EVF configuration and completed the rehabilitation training program assisted by ENMS-EVF. The demographic information of the recruited participants is shown in Table 3.1.

Table 3.1 Demographic information of participants.

Information	Value
Stroke Type	Hemorrhagic = 6, Ischemic = 1
Affected Arm	Left = 6 , Right = 1
Gender	Male = 4 , Female = 3
Age	Mean \pm SD = 53.29 \pm 12.68 years
Years after Stroke	$Mean \pm SD = 6.33 \pm 6.83 \text{ years}$

3.3.1 Validation test results of ENMS-EVF configuration

In the results of the ENMS-EVF configuration test in Table 3.2, the design parameters and task settings were all validated as feasible for usage by the recruited participants. Specifically, the EMG threshold for sensitive voluntory motor effort detection was set at 10% MVC above the EMG baseline, achieving a 100% success rate (7/7). The NMES intensity required for effective ED contraction to open the wrist at 20° was determined to be a mean of $18.29 \pm 12.19~\mu s$, also with a 100% success rate. For FVS intensity, a nominal amplitude of 5.1G was used to stimulate somatosensory feedback over the FD, again achieving full success. The inflation of pneumatic muscles assisted in achieving a ROM of MCP finger joints at 170°, with a maximum inner pressure maintained under 100~kPa, and all participants successfully completed this task. Additionally, both horizontal and vertical tasks involving carrying a sponge were completed with a 100% success rate, with participants moving the sponge 50cm horizontally and lifting it 18cm vertically.

Table 3.2 Validation of ENMS-EVF configuration.

Validation test	Parameter	Success rate
EMG threshold for sensitive voluntory motor effort detection	10% MVC above the EMG baseline	7/7
NMES intensity for ED contraction to open wrist at 20°	Mean \pm SD = 18.29 \pm 12.19 μ s	7/7
FVS intensity for somatosense over FD	Nominal amplitude of 5.1G	7/7
Inflation of pneumatic muscles to assist ROM of MCP finger joints at 170°	Maximum inner pressure under 100 kPa	7/7
Horizontal task while carrying a sponge	Moving 50cm	7/7
Vertical task while carrying a sponge	Lifting 18cm	7/7

3.3.2 Feasibility and effects of ENMS-EVF-assisted training

In the preliminary training program assisted by ENMS-EVF, the immediate changes in clinical scores over time in Pre, Mid, and Post assessments were shown in Figure 3.5. In Figure 3.5B and C, a significant improvement compared to Pre assessment was found at Mid timepoint in the ARAT scores and WMFT time consumption (p = 0.0394 and 0.0071, Conhen's d = 0.5343 and 0.7276, paired t-test). In Figure 3.5A and B, significant increases compared to Pre assessment were found at Post timepoint in the FMA UL full scores, FMA W/H scores, and ARAT scores (p = 0.0365, 0.0195 and 0.0247, Conhen's d = 0.5448, 0.6251 and 0.5962, paired t-test). In Figure 3.5D and E, although no significant change was found in all monofilament test scores and MAS scores (p > 0.05, paired t-test and Wilcoxon's signed-rank test), the monofilament test scores on sites 1, 2, 3, and 4 showed a continuous decrease along the training program and more participants achieved 0 level MAS scores on finger, wrist and elbow joints after training than Pre assessment.

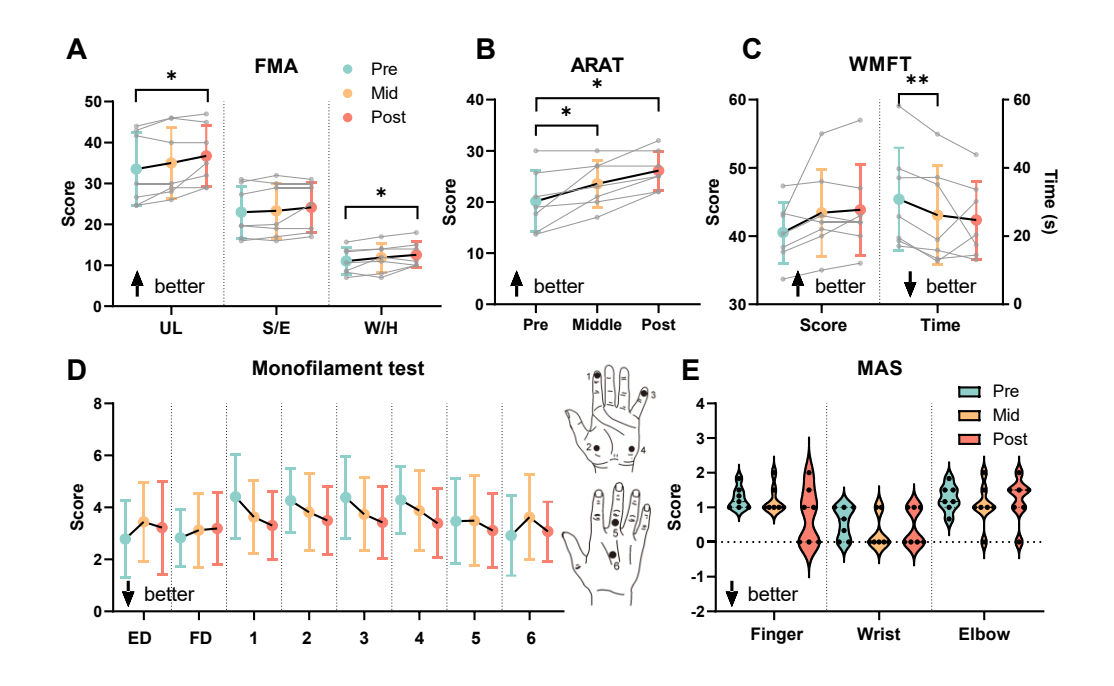


Figure 3.5 Immediate rehabilitation effects of ENMS-EVF assisted training on **(A)** FMA scores, **(B)** ARAT scores, **(C)** WMFT scores, and **(D)** Monofilament test scores. Sites 1–4 reflect glabrous skin and sites 5–6 hairy skin; sites 1–2 have median nerve innervation, 3–4 ulnar nerve, and 5–6 radial nerve (Bowden et al., 2014). **(E)** MAS scores. Pre assessments were conducted three times and averaged in statistical analysis. Results are presented as the means with standard deviations in **(A)**, **(B)**, **(C)**, and **(D)**, and violin plots with all data points in **(E)**. Significant differences are indicated as "*" for p < 0.05 and "**" for p < 0.01 (paired t-test in **(A)**, **(B)**, **(C)**, and **(D)**; Wilcoxon's signed-rank test in **(E)**).

3.4 Discussion

The ENMS-EVF system was developed to assist poststroke UL training with somatosensory priming. The configuration of the designed system was validated on patients with chronic stroke. A preliminary training program was also conducted to evaluate the feasibility of ENMS-EVF-assisted UL rehabilitation.

3.4.1 Design and validation of ENMS-EVF system

The ENMS-EVF is a hybrid soft robotic technology for W/H rehabilitation after stroke. It integrates NMES, FVS, and pneumatic actuation to W/H joints through a triggering control by residual voluntory motor effort from a person after stroke, represented by EMG in paretic muscles. Based on the validation test results, all parameters and tasks were successfully executed by the participants, indicating the feasibility of the ENMS-EVF design and configuration for rehabilitative training. In the ENMS-EVF design, the EMG electrode pairs were placed on the skin surface of the ED and FD for voluntory motor effort detection. NMES through the EMG electrode pairs on the ED assisted muscle contraction and provided sensory feedback during voluntary W/H extension, while FVS by the vibration motor between the EMG electrode pairs on the FD provided sensory feedback during voluntary W/H flexion because of usually adequate muscle force on FD preserved poststroke. The continuous EMG-driven EVF control was designed to coordinate NMES, FVS, and pneumatic actuation to assist hand movements with enhanced sensory feedback to achieve somatosensory priming in the phasic motions of hand opening and closing.

Specifically, in the parameter settings, the EMG threshold level in each motion phase was set as 10% MVC above the EMG baseline in the resting state. The validation results indicated that the voluntory motor effort of all stroke participants could be sensitively detected by the EMG threshold setting in the design of ENMS-EVF. During the extension phase, when the voluntary EMG signal on the ED reached the preset threshold, the ED received NMES while the fingers were mechanically assisted by an inflated pneumatic muscle to aid in W/H extension throughout the motion phase. The validation results showed that the mean NMES intensity required to achieve effective wrist extension at a 20° angle was $18.29 \pm 12.19~\mu s$, with a 100% success rate across all stroke participants, indicating the high reliability and efficacy of the NMES

parameters used in inducing wrist extension. Besides, the successful achievement of a 170° ROM in the MCP finger joints through the inflation of pneumatic muscles while maintaining a maximum inner pressure under 100 kPa demonstrates the feasibility of the musculoskeleton unit in facilitating finger extension without exceeding safe pressure limits, ensuring both efficacy and participant safety. In the flexion phase, as soon as the voluntary EMG on the FD muscle reached the preset threshold, passive pneumatic deflation and continuous FVS to the FD were provided throughout the voluntary W/H flexion. The validation results suggested that the use of a nominal amplitude of 5.1G for FVS successfully elicited somatosensory feedback over the FD, achieving a full success rate. This indicates that the chosen amplitude is effective in stimulating the desired sensory response, which is consistent with our previous study on the cortical response to FVS in stroke survivors (Lin et al., 2024b). Additionally, the completion of both horizontal and vertical tasks involving carrying a sponge with a 100% success rate, where participants moved the sponge 50 cm horizontally and lifted it 18 cm vertically, underscores the feasibility of the task setup for later rehabilitation training. Besides, the setup time for the ENMS-EVF was equivalent to the former ENMS system (Nam et al., 2020). These results collectively validate the effectiveness of the system's design parameters and task settings for the intended rehabilitative applications.

3.4.2 Short-term rehabilitative effects of ENMS-EVF

The results of this study support the hypothesis that the rehabilitation training assisted by ENMS-EVF could result in improved sensorimotor functions of UL for poststroke individuals. Significant motor functional improvements could be found after only 10 sessions, as shown in the ARAT and WMFT time consumption results (Figure 3.5B and C), suggesting an improvement in finger function and coordination for fine motor control during grasping, gripping, and pinching tasks and the efficiency to perform

daily activities. The significant increase in Post FMA scores (Figure 3.5A) showed improvement in voluntary motor functions of the entire UL, which indicated the rehabilitative effects of the ENMS-EVF on joint stability, coordination, and ROMs. The decreases in MAS scores on the elbow, wrist, and fingers (Figure 3.5E) indicated reduced spasticity and improved control of muscle synergy.

On the somatosensory part, the decreases in the monofilament test on the glabrous skin of the hand innervated by the median and ulnar nerves suggested an improvement in cutaneous sensitivity (Figure 3.5D, sites 1-4). These hand somatosensory improvements indicated the positive effects of somatosensory stimulation on the median and ulnar nerves of the dorsal forearm and repeated contact stimulation on the hand in the object-carrying tasks during the training. However, the differences are not significant, probably because of the relatively small sample size in the preliminary training trial. Nevertherless, joined with the motor functional effects mentioned above, these clinical assessment results highlighted the feasibility of ENMS-EVF in assisting poststroke W/H rehabilitation and its short-term rehabilitation effects in enhancing sensorimotor functions following stroke. Besides, monofilament test results on the skin over ED and FD muscles keep at the relatively same level as the Pre assessment (Figure 3.5D), which demonstrated no adverse effects remained on the cutaneous sensitivity of these sites after the repeated FVS and NMES stimulations.

3.5 Periodic Summary

In this study, a novel ENMS-EVF that integrates NMES on the ED and FVS on the FD into a wearable exoskeleton with soft pneumatic muscles was designed for supporting poststroke W/H rehabilitation with somatosensory priming. The developed system could assist intensive and repeated W/H practice under voluntory motor effort control by residual voluntary EMG signals from the affected UL. The participants with chronic stroke could complete the validation test and preliminary training program. The results

validated the effectiveness of the system's design parameters and task settings for the intended rehabilitative applications. The ENMS-EVF-assisted training program could facilitate sensorimotor improvement in the affected UL of the participants with chronic stroke. After 10-session training, significant motor improvements were achieved in finger function and coordination for fine motor control and efficiency to perform daily activities. Along the 20-session training, improved sensorimotor functions were observed in additon to finger function and corrdination, including improved voluntary motor functions in the entire UL and finger joints; improved cutaneous sensitivity innervated by median and ulnar nerves of the dorsal forearm; and released muscle spasticity at the elbow, wrist, and fingers.

CHAPTER 4

LONG-TERM EFFECTS OF SENSORIMOTORINTEGRATED WRIST/HAND REHABILITATION ASSISTED BY THE ENMS-EVF ON SENSORIMOTOR FUNCTIONS AND NEUROPLASTICITY AFTER STROKE

This chapter is adapted from

<u>Lin, L.</u>, Qing, W., Kuet, M.-T., Zhao, H., Ye, F., Rong, W., Li, W., Huang, Y., & Hu, X. (2025). Sensorimotor Integration (SMI) by Targeted Priming in Muscles with EMG-driven Electro-Vibro-Feedback in Robot-Assisted Wrist/Hand Rehabilitation after Stroke. *Cyborg and Bionic System*. Submitted.

and

Lin, L., Kuet, M.-T., Qing, W., Zhao, H., Ye, F., Huang, Y., & Hu, X. (2024). Effects of sensorimotor-integrated (SMI) wrist/hand rehabilitation assisted by a hybrid soft robot poststroke. In 2024 International Convention on Rehabilitation Engineering and Assistive Technology (i-CREATE 2024). https://doi.org/10.1109/i-CREATe62067.2024.10776482

4.1 Introduction

SMI plays a fundamental role in the purposeful movement of the UL. Pioneering research on the motor and sensory network mappings within the sensorimotor cortex has elucidated that precise interpretation of somatosensory information before and during movement is vital for proficient motor execution (Asan et al., 2021). The coordination between sensory and motor pathways in SMI facilitates the performance of specialized tasks, the acquisition of new abilities, or the retraining of skills through neuroplasticity following neurological disorders like stroke (Papale and Hooks, 2018; Lin et al., 2024c). Thus, disruption of SMI after stroke is a key barrier to motor restoration. More than 50% of stroke survivors experience sensory impairments on their hemiplegic side, which impedes SMI and exacerbates motor function impairments (Gopaul et al., 2018; Edwards et al., 2019). Based on the crucial rule of SMI in the movement of UL, the somatosensory function forms an essential factor within the neuroplasticity of motor re-learning after stroke (Asan et al., 2021; Lin et al., 2024c).

According to SMI principles, enhancement of somatosensory feedback fosters motor recovery after stroke (Aman et al., 2014; Asan et al., 2021; Filippi et al., 2023). In clinical practices, somatosensory priming has been examined to modulate the peripheral somatosensory nervous system when timed-paired with traditional motor training (Stoykov et al., 2021). Somatosensory priming usually adopts electrical or vibratory stimulations (e.g., NMES and FVS) on targeted peripheral nerves or muscles prior to or concurrent with motor-based interventions (Stoykov and Madhavan, 2015; Stoykov et al., 2021). It has been demonstrated to improve motor outcomes more efficiently than only motor-focused therapies, probably because it facilitated the neuroplasticity of the somatosensory cortex processing somatosensory feedback from target muscles in the ascending pathway during movement execution, i.e., afferent facilitation (Stoykov et al., 2021). Compared to clinic-centered and labor-intensive

traditional clinical practices, rehabilitation robots could provide intensive and repeated training for a long time with effective neuroplasticity for movement recovery of the UL (Gassert and Dietz, 2018; Xing and Bai, 2020). In the descending motor pathway, the rehabilitative neuroplasticity could be augmented when the voluntory motor effort was involved in robot-assisted training (Farmer et al., 2004; Nam et al., 2020). In the ascending sensory pathway, incorporating enhanced somatosensory inputs from target muscles via sensory stimulation in robot-assisted practices, i.e., robot-assisted somatosensory priming, has the potential to enhance the precise somatosense of target muscles via afferent facilitation and improve motor relearning efficiency poststroke (Yilmazer et al., 2019; Handelzalts et al., 2021; Stoykov et al., 2021; Lin et al., 2024c).

In robot-assisted rehabilitation, although proprioception experiences, e.g., joint motions and positions, could be provided in continuous passive movement by pure robots, they still focus on precise control of repetitive motor actions, often neglecting the modulation of somatosensory inputs from target muscles crucial for poststroke motor restoration (Gassert and Dietz, 2018; Lin et al., 2024c). Recently, NMES integrated into a rehabilitation robot could provide additional afferent facilitation along with muscle force enhancement and atrophy prevention on paretic distal muscles due to learned disuse poststroke, e.g., the ED, in hand functions (Nam et al., 2020). However, muscle hypertonia always occurs on UL flexor, e.g., FD, poststroke because of loss of cortical inhibition, spinal reflex hyperexcitability, and abnormal muscle synergy. Thus, NMES is not applicable to FD because it directly elicits wide recruitment of diverse sensory receptors and muscle fibers, leading to pain, muscle fatigue and higher muscle spasticity on FD in long-term usage (Insausti-Delgado et al., 2020; Lin et al., 2024b). Even though less efficient in inducing muscular contraction than NMES, FVS, without causing muscle contraction, is more suitable for somatosensory priming on FD, which usually has sufficient residual voluntary force after stroke (Lan et al., 2011; Miller and Dewald, 2012). That is because FVS could efficiently activate the sensorimotor cortex and increase corticospinal excitabilities by afferent facilitation from target muscles but with higher comfortability in the long term than NMES due to selective activation of mechanoreceptors (mainly Ia afferent endings in the muscle spindles and Pacini receptors in the skin) (Lapole and Tindel, 2015; Souron et al., 2017; Lin et al., 2024b). Therefore, robot-assisted somatosensory priming by the coordination of NMES for ED and FVS for FD with movement assistance has the promise to increase the awareness of the target muscle contraction through afferent facilitation in the ascending pathway and elevate synchronous activation in the related sensorimotor cortex, effectively contributing to the neuroplasticity for motor restoration (Conrad et al., 2011; Yilmazer et al., 2019; Asan et al., 2021; Stoykov et al., 2021; Lin et al., 2024b; Lin et al., 2024c).

The ENMS-EVF has been designed and validated in Chapter 3, and its short-term rehabilitation effects were evaluated by a preliminary training program assisted by the device (Lin et al., 2024a). However, we still don't know the long-term rehabilitative effects of the proposed ENMS-EVF on sensorimotor functions. More importantly, the long-term effects on cortical and pathway-specific corticomuscular neuroplasticity need to be further investigated to help understand the underlying mechanism of the intervention. In this study, we investigated the long-term rehabilitative effects and underlying neurological mechanisms of the rehabilitation training assisted by ENMS-EVF after stroke. We hypothesized that the robot-assisted somatosensory priming by the ENMS-EVF system could result in neuroplasticity of enhanced afferent sensory feedback from target muscles and benefit the functional recovery of UL movement for poststroke individuals.

4.2 Materials and Methods

4.2.1 Design of ENMS-EVF and experimental setup

The proposed ENMS-EVF in Figure 4.1A was an integrated hybrid soft robot system with somatosensory priming for W/H rehabilitation after stroke. It integrated NMES, FVS, and soft pneumatic muscles into wearable exoskeleton with voluntory motor effort detection by EMG as described in Chapter 3 (Hu et al., 2015; Nam et al., 2020; Lin et al., 2024b; Lin et al., 2024a). It consisted of a control box, a wearable glove, and a smartphone installed with an application as a wireless user interface through Bluetooth. The control box contained a rechargeable 12V Li-ion battery for a maximum of 4h continuous usage. The system can control the pneumatic muscles by an on/off switch of a set of air pumps and valves. It collects two-channel EMG inputs through two pairs of electrodes and outputs one-channel NMES through one pair of the same electrodes. Additionally, it manages the one-channel FVS delivery with a vibration motor.

In the robotic design of ENMS-EVF, the soft pneumatic muscles were covered by a textile glove. They inflated to provide extension torque to individual digits as motor assistance during hand opening, and they deflated when the valve in the control box was opened during hand closing. Two pairs of EMG electrodes (5 × 5 cm², PALS Neurostimulation Electrodes, Axelgaard Manufacturing Co., Ltd., Fallbrook, CA, USA) were placed on the skin surface of the motor points of the W/H extensor and flexor, respectively, for voluntory motor effort detection (Figure 4.1B and C). The extensor and flexor were, respectively, the muscle union of the ED and the ECU, i.e., ED-ECU, as well as the muscle union of the FD and the FCR, i.e., FD-FCR, given their close anatomical proximity in a muscle union. To avoid verbosity, we continue to use ED and FD to represent ED-ECU and FD-FCR muscle unions in the following text. The reference electrode (Ø2.5cm, PALS Neurostimulation Electrodes) was placed on the

skin surface of the olecranon (Figure 4.1B) to attenuate the common mode noise. The skin–electrode impedance of each electrode was lowered below 5 k Ω by skin preparation. The captured EMG signals were amplified, filtered, A/D converted, rectified, and moving-averaged to obtain the continuous EMG activation levels of ED and FD.



Figure 4.1 (A) Experimental setup for rehabilitation training assisted by ENMS-EVF. **(B)** Positions of EMG+NMES electrodes on ED and a reference electrode on the olecranon. **(C)** Positions of EMG electrodes on FD.

NMES through the EMG electrode pairs on the ED (Figure 4.1B) assisted muscle contraction and provided somatosensory feedback, i.e., somatosensory priming, during voluntary W/H extension, while FVS by the vibration motor between the EMG electrode pairs on the FD (Figure 4.1C) provided somatosensory priming during voluntary W/H flexion because of adequate muscle force on flexor preserved poststroke. The NMES output was alternating current delivered in square pulses, with a frequency

of 40 Hz (40 pulses per second) and an amplitude of 70 V. The pulse width was adjustable, ranging from 0 to 300 µs, which allowed for tailored levels of stimulation intensity. The vibration motor was a miniature encapsulated motor with eccentric rotating mass (E0716M, NFP-Motor Co., Ltd, Kowloon, Hong Kong, China), rotating at 14500rpm with a nominal amplitude of 5.1G, whose intensity was high enough to elicit the sensorimotor cortex (Lin et al., 2024b) without involuntary muscle contraction.

The continuous EMG-driven EVF control was designed to coordinate NMES, FVS, and pneumatic actuation to assist the phasic motions of W/H extension and flexion with somatosensory priming. The EMG threshold level in each motion phase was set as 10% MVC above the EMG baseline in the resting state. During the extension phase, when the voluntary EMG activation level on the ED reached the preset threshold, the ED received continuous NMES, and the fingers were mechanically assisted by the inflated pneumatic muscles to aid in W/H extension throughout the motion phase. In the flexion phase, as soon as the voluntary EMG activation level on the FD muscle reached the preset threshold, passive pneumatic deflation and continuous FVS to the FD were provided throughout the voluntary W/H flexion. The design parameters and configuration of the ENMS-EVF have been evaluated and validated in Chapter 3. A participant using the ENMS-EVF during training is shown in Figure 4.1A.

4.2.2 Rehabilitation assisted by ENMS-EVF

4.2.2.1 Participants

This study was approved by the Human Subjects Ethics Sub-Committee of the Hong Kong Polytechnic University before commencement (approval number: HSEARS20210320003). A total of 15 chronic stroke participants were screened according to the following inclusion criteria:

- (1) at least 12 months after the onset of a unilateral lesion in cortical or subcortical regions due to stroke;
- (2) presence of no visual deficit and sufficient cognition to follow experimental instructions (MMSE score > 23) (Tombaugh and McIntyre, 1992);
- (3) moderate to severe motor disability in the affected UL (15 < FMA < 45) (Sullivan et al., 2011);
- (4) ≤ 3 spasticity at the wrist and fingers as measured by the MAS (Bohannon and Smith, 1987);
- (5) presence of detectable voluntary EMG signals from the ED and FD muscles on the affected arm (three times the standard deviation above the EMG baseline) (Nam et al., 2021);
- (6) presence of a passive ROM for the wrist from 45° extension to 60° flexion and the ability of the MCP finger joints to be passively extended to 170°.
- (7) no neurological impairments except stroke; and
- (8) right-handed before the stroke onset.

The exclusion criteria for the stroke participants were (1) poststroke pain, (2) epilepsy, (3) cerebral implantation, and (4) pacemaker implantation. Before the commencement of the clinical trial, written informed consent was obtained from each participant.

4.2.2.2 Training program

The rehabilitation training program shown in Figure 4.2 included a tutorial prior to training and 20 UL training sessions, all of which were assisted by ENMS-EVF and contained 60-minute training tasks per session. The training sessions were scheduled at

an intensity of 3-5 sessions per week for seven consecutive weeks, with no more than one session per day.

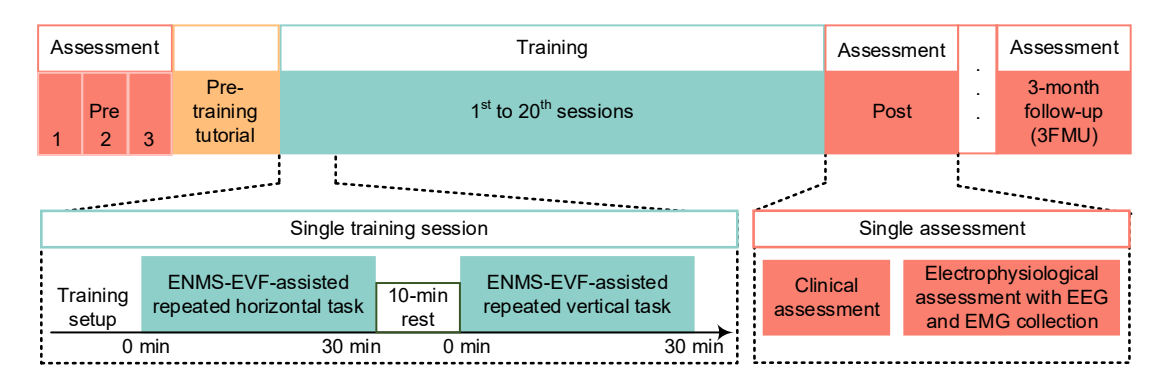


Figure 4.2 Timeline of the 20-session training program assisted by the ENMS-EVF and assessments before (Pre), after (Post), and 3 months after (3-month follow-up, 3MFU) the training sessions. In the Pre assessment, three times of clinical assessments were conducted over 2 weeks.

Each participant received a pre-training tutorial that covered the process of donning and doffing the system, device operation, and the training protocol before the training began. Prior to each training session, the operator was responsible for measuring and setting the training parameters to ensure that they were tailored to adapt to varying spasticity levels of W/H joints and residual muscle force of ED and FD of each participant along the program process. These parameters included the EMG baseline and MVC of the driving muscle unions for appropriate sensitivity of voluntory motor effort detection by EMG activation level, the maximum inner pressure of the pneumatic muscles for individual participants to passively open their MCP finger joints at 170°, and the applied pulse width of NMES for individual participants to open their wrists at 20°.

During each training session, participants were instructed to sit at a table and maintain a distance of 30–40 cm between their shoulders and the table surface (as shown in Figure 4.1A). To begin, the smartphone with the app was placed on the table in front of the participant. Participants were then required to follow the instructions on the smartphone screen and complete repetitive arm reaching and grasping tasks, assisted

by the ENMS-EVF on the paretic limb. They were asked to complete a 30-minute horizontal task and a 30-minute vertical task at their natural speed while carrying a sponge (Nam et al., 2021). In the horizontal task, the participant was instructed to grasp a sponge near their affected side, move it 50 cm horizontally towards the other side, release it, then return it to the starting point and release it again. In the vertical task, the participant was instructed to lift the sponge from the table to a shelf, release it, then bring it back down, and place it on the table before releasing it again. To prevent muscle fatigue during training sessions, a break of 10 minutes was permitted between two consecutive tasks.

4.2.3 Sensorimotor evaluation of training outcomes

The sensorimotor rehabilitation outcomes of UL training with assistance from ENMS-EVF were investigated by using clinical and electrophysiological assessments before (Pre), one day after (Post), and 3 months after (3MFU) the training sessions (Figure 4.2).

4.2.3.1 Clinical sensorimotor assessments on functional recovery

The sensorimotor functional improvement of each participant was evaluated using clinical assessments in this study. The adopted clinical assessments included (1) motor functional assessment in voluntary limb movements by the FMA with a total score of 66 for the UL assessment (Sullivan et al., 2011); (2) assessment of the UL voluntary functions focusing on the functional tasks by ARAT focusing on finger function and coordination for fine motor control including grasp, grip, pinch and gross sub-scores (Carrol, 1965); (3) assessment of the functional ability and motion speed of the UL in daily tasks by WMFT (Wolf et al., 1989); (4) sensation assessment on the affected arm measured by the Semmes-Weinstein monofilament test (Suda et al., 2020) on the skin surface above the ED and FD, and six sites on the ventral and dorsal side of the hand

according to established protocol (Bowden et al., 2014); (5) muscle spasticity assessment at the elbow, wrist, and finger joints measured by MAS (Bohannon and Smith, 1987). In the Pre assessment, three times of clinical assessments were conducted over 2 weeks before the training sessions started in order to make sure that participants had a steady functional rehabilitative baseline. After the training sessions, the same clinical assessments were also conducted in the Post and 3MFU assessments (Figure 4.2). All these clinical assessments were performed by an assessor who was blinded to the training.

4.2.3.2 Electrophysiological sensorimotor assessments on neuroplasticity changes

To trace the neuroplasticity changes and the neurological contribution to functional motor recovery after the ENMS-EVF-assisted training, EEG and EMG were collected to analyze corticomuscular coherence (CMC) and pathway-specific directed CMC (dCMC). The CMC is the coherence between EEG and EMG signals that shows timebased functional connections in the neuromuscular pathways between the cortex and target muscles when subjects perform specific motion tasks (Guo et al., 2020; Qing et al., 2024). It could be used to identify the location of cortical sources in the voluntary motor control of the target muscle through the corticospinal pathway (Mima and Hallett, 1999), associated with either cortical command to the muscle or afferent feedback from the contracting muscle (Mima et al., 2001). The dCMC was applicable to detect the pathway-specific (i.e., in descending or ascending pathway) corticomuscular interaction in voluntary movements (Lin et al., 2024a; Qing et al., 2024), where the descending dCMC reflects the strength of motor command from the cortex to the target muscle, and the ascending dCMC reflects the strength of somatosensory feedback from the target muscle to the cortex (Kristeva et al., 2007; Artoni et al., 2017; Zhou et al., 2021a).

In electrophysiological assessments, the EEG over sensorimotor cortex and EMG on target UL muscles, i.e., ED, FD, biceps brachii (BIC), and triceps brachii (TRI), were collected during 20% MVC of ED/FD according to a well-established setup and protocol achievable by the recruited stroke survivors (Guo et al., 2020; Zhou et al., 2021a). Each subject was required to perform three trials with a 2 min intertrial rest to avoid muscle fatigue. EEG and EMG signals were simultaneously recorded at a sample rate of 1200Hz. The subject was asked to minimize body movements, eye blinking, biting, and active mental tasks when conducting the target motion. Before the motion started in each trial, 10s rest-state signals were collected for EEG baseline correction in off-line analysis. After the motion started, participants were required to maintain the 20% MVC level of ED or FD for 35s. The same experimental protocol was applied for 20% MVC of ED during W/H extension and 20% MVC of FD during W/H flexion.

The procedures of off-line EEG/EMG pre-processing and further analysis are shown in Figure 4.3. For EEG pre-processing, the raw EEG data were retained [-10 30s], where 0s means the motion start mark. Next, EEG signals were band-pass filtered at 2-80 Hz, notch filtered at 50 Hz, corrected by the baseline period [-10 0s], re-referenced by the average of all channels, and analyzed by ICA to identify independent components with artifacts. Then, bad channels were interpolated by the surrounding channels. Artifactual periods and independent components were rejected to remove muscular/ocular artifacts and line noise. For EMG pre-processing, the raw EMG data during the motion period [0 30s] were band-pass filtered at 8-500 Hz and notch-filtered at 50 Hz. After pre-processing, EEG and EMG data were synchronized according to the motion start mark, went through visual inspection and rejection together, and segmented into epochs with 1s length for the motion period [0 30s]. These pre-processing and analysis followed the general procedures in FieldTrip (Oostenveld et al., 2011) and EEGLAB (Delorme and Makeig, 2004) toolboxes with the latest updates using Matlab 2022a (MathWorks, Natick, MA, USA).

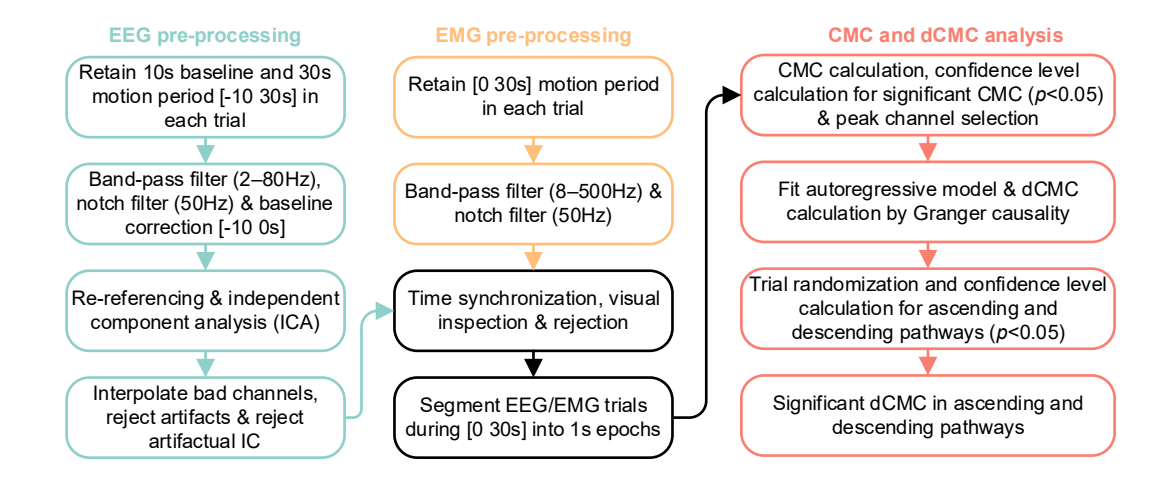


Figure 4.3 Signal processing flow chart.

The CMC in the beta band (13-30Hz) was analyzed for significant coherence between the 21 channels over the sensorimotor cortex (including CZ, CPZ, FCZ, C1-6, CP1-6, and FC1-6 channels) and target muscles (ED, FD, BIC, and TRI) in each participant. The CMC of each EEG-EMG pair was calculated by Equation 4.1:

$$CMC(\sigma) = \frac{|f_{xy}(\sigma)|^2}{f_{xx}(\sigma) \cdot f_{yy}(\sigma)}$$
(4.1)

where $f_{xx}(\sigma)$ and $f_{yy}(\sigma)$ represented the auto-spectrum of the EEG and EMG signals, respectively, and $f_{xy}(\sigma)$ represented the cross-spectrum of EEG and EMG (Zhang et al., 2024). The CMC amplitude above the 95% confidence level $CL_{95\%} = 1 - 0.05\frac{1}{n-1}$ was significant, where n is the number of the epochs for CMC calculation (Guo et al., 2020). To investigate the cortical reorganization after training, the laterality index (LI) of CMC topography was calculated by Equation 4.2:

$$LI = \frac{max(CMC_{contralateral}) - max(CMC_{ipsilateral})}{max(CMC_{contralateral}) + max(CMC_{ipsilateral})}$$
(4.2)

where $max(CMC_h)$ means the highest significant CMC (i.e., the peak CMC) amplitude of EEG channels on the specified h hemisphere (Wilkins et al., 2017). Positive LI means contralateral dominance and negative LI means ipsilateral dominance in CMC topography. The EEG channel with peak CMC in the topography

was identified as the channel of interest for the subsequent dCMC calculation (Zhou et al., 2021a).

In this study, the dCMC was calculated by Granger causality, which is a frequency-domain directional estimator based on the autoregressive (AR) modeling. A bivariate AR model with order k was first fitted at time t for each EEG-EMG pair based on Equation 4.3:

$$\sum_{\tau=0}^{k} A_{\tau} X_{t-\tau} = \boldsymbol{E}_{t} \tag{4.3}$$

where A_{τ} is the 2×2 coefficient matrix, X_t is the 2×1 signal matrix (EEG_t , EMG_t)^T, E_t is the temporally residual error with covariance matrix C, τ is the time delay (Brovelli et al., 2004). In this study, an AR model with sufficient order k = 60 was fitted and validated for necessary spectral resolution, consistency, stability, and whiteness of residuals (Delorme et al., 2011), as practiced in (Zhou et al., 2021a). Then, the frequency-domain transfer function of the system at frequency f was obtained by Equation 4.4:

$$H(f) = (\sum_{\tau=0}^{k} A_{\tau} e^{-2\pi i \tau f})^{-1}$$
 (4.4)

where i is the imaginary part (Brovelli et al., 2004). Finally, the dCMC from signal 1 to signal 2 of the signal matrix X_t at frequency f could be calculated by frequency-domain Granger causality in Equation 4.5:

$$dCMC_{1\to 2}(f) = -\ln\left(1 - \frac{\left(C_{11} - \frac{C_{12}^2}{C_{22}}\right)|H_{21}(f)|^2}{S_{22}(f)}\right)$$
(4.5)

where C_{11} , C_{12} , and C_{22} are elements of the covariance matrix C, $H_{21}(f)$ is the element of the transfer function H(f), representing the connection between the signal 1 input and the signal 2 output of the system, and $S_{22}(f)$ is the power spectrum of signal 2 at frequency f (Geweke, 1982; Brovelli et al., 2004). Similarly, the dCMC from signal 2 to signal 1 of X_t could be obtained by switching the subscript in Equation 4.5. The significant level of dCMC was determined using a nonparametric statistical test based

on the Monte Carlo simulation. The simulated data were obtained by randomly shuffling the trials of the original EEG and EMG signals for 1000 repetitions. Then, the 95th percentile of the dCMC distribution calculated from the simulated data was used as the confidence level of dCMC at a significant level of p < 0.05 to minimize false positive results (Babiloni et al., 2005; Witham et al., 2010). Non-significant dCMC was set as 0 in the subsequent statistical analysis.

4.2.4 Statistical analysis

The Shapiro-Wilk normality test was used to evaluate the normality of the clinical scores and dCMC parameters at a significance level of 0.05. Only MAS and dCMC amplitude exhibited significance in the normality test (p < 0.05), meaning they were non-normally distributed. Other parameters were all normally distributed (p > 0.05). Thus, the non-parametric Friedman test with FDR control for multiple comparison correction was used for MAS and dCMC amplitude, and One-way ANOVA with repeated measures and Turkey's post hoc test for multiple comparison corrections were adopted for other normally distributed parameters to determine whether they changed over time at Pre, Post, and 3MFU assessments. In addition, the scores among three Pre baseline assessments were also statistically analyzed. They showed no significant difference (p > 0.05), which means that participants had a steady functional rehabilitative baseline. Therefore, the baseline score value was averaged as a Pre score value in the pre-described analysis on changes over time. Correlation analysis was conducted between significant dCMC changes and clinical scores by Pearson's correlation to investigate the contribution of neuroplasticity to functional recovery. The statistical analysis in this study was performed by Matlab R2024a. The statistically significant level was set at 0.05 in this study. The significant level of 0.01 was also indicated.

4.3 Results

All the recruited participants (N = 15) completed the rehabilitation training assisted by the ENMS-EVF. The demographic information of the recruited participants is shown in Table 4.1.

Table 4.1 Demographic information of participants.

Information	Value
Stroke Type	Hemorrhagic = 12, Ischemic = 3
Affected Arm	Left = 10 , Right = 5
Gender	Male = 7, Female = 8
Age	Mean \pm SD = 52.93 \pm 11.25 years
Years after Stroke	$Mean \pm SD = 7.42 \pm 6.92 \text{ years}$

4.3.1 Sensorimotor functional changes in clinical assessments

The changes in clinical scores over time in Pre, Post, and 3MFU assessments were shown in Figure 4.4. In Figure 4.4A and B, significant increases were found after the training in the FMA UL total scores, FMA S/E, FMA W/H, ARAT total score, and ARAT grasp, and grip subscale scores (corrected p = 0.0023, 0.0464, 0.0320, 0.0485, 0.0465, and 0.0292, One-way ANOVA with Turkey's post hoc test). Significant increases were preserved for 3 months after the training in FMA UL, FMA W/H, and ARAT total and pinch scores (corrected p = 0.0367, 0.0360, 0.0133, and 0.0483, One-way ANOVA with Turkey's post hoc test). In Appendix G, averaged WMFT time decreased over time (p = 0.0548, One-way ANOVA), which was close to the significant level.

In Figure 4.4C, significant decreases in monofilament scores were found after the training on sites 2 and 4 and maintained after 3 months (Post vs. Pre: corrected p = 0.0190 and 0.0182; 3MFU vs. Pre: corrected p = 0.0059 and 0.0092, One-way ANOVA

with Turkey's post hoc test). Significant decreases could also be found over time on sites 1 and 3 (p = 0.0432 and 0.0263, One-way ANOVA) but not in Turkey's post hoc test after correction. Averaged Monofilament scores on site 5 decreased over time (p = 0.0503, One-way ANOVA), which was close to the significant level. In Figure 4.4D, significant decreases in MAS scores were found over time on the elbow joint (p = 0.0289, Friedmand test) but not in the post hoc test after FDR correction. Averaged MAS scores on the wrist joint decreased over time (p = 0.0548, Friedmand test), which was close to the significant level. Other parameters without marks in Figure 4.4 showed no significant change over time.

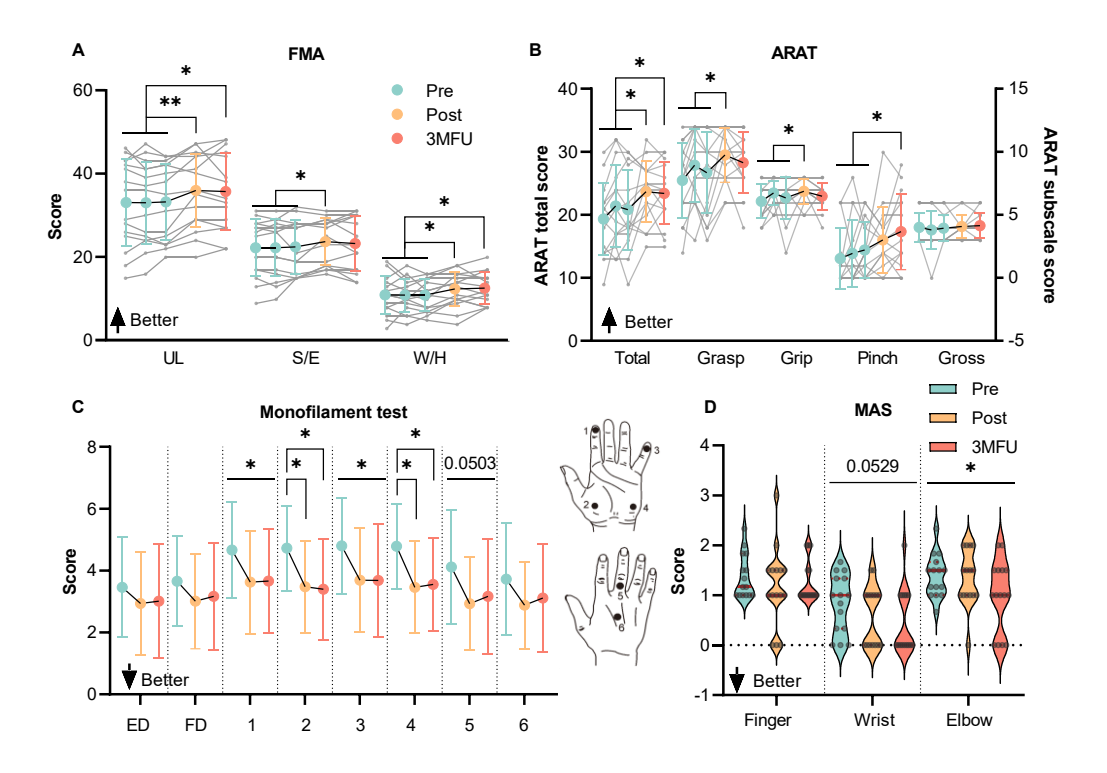


Figure 4.4 Results of clinical assessments on **(A)** FMA scores, **(B)** ARAT total and subscale scores, and **(C)** Monofilament test scores. Sites 1–4 reflect glabrous skin and sites 5–6 hairy skin; sites 1–2 have median nerve innervation, 3–4 ulnar nerve, and 5–6 radial nerve (Bowden et al., 2014). **(D)** MAS scores. Pre assessments were conducted three times and averaged in statistical analysis. Results are presented as the means with standard deviations in **(A)**, **(B)**, and **(C)**, and violin plots with all data points in **(D)**.

Significant differences are indicated as "*" for p < 0.05 and "**" for p < 0.01 (Oneway ANOVA with repeated measures and Turkey's post hoc test in (A), (B), and (C); Friedman test with FDR correction in (D)).

4.3.2 Sensorimotor neurological changes in corticomuscular coupling

Figure 4.5A shows the grand averaged topography changes of significant CMC between the sensorimotor cortex and the agonist muscles (i.e., ED/FD during extension/flexion) of all participants at the assessments of Post and 3MFU stages compared with the Pre stage. In the left two topography of significant CMC with ED during W/H extension, the CMC both increased on the bilateral hemispheres but with a peak CMC on the CP6 channel in the change of Post–Pre and on the C4 channel in the change of 3MFU–Pre. In the right two topography of significant CMC with FD during W/H flexion, the CMC increased on the contralateral/ipsilesional hemisphere with a peak CMC on the FC4 channel in the change of Post–Pre and increased on the bilateral hemispheres but with a peak CMC on the C6 channel in the change of 3MFU–Pre.

Figure 4.5B shows the LI changes of the significant CMC topography over time. Both LI of CMC with ED and FD showed a shift trend towards the contralateral/ipsilesional hemisphere in Post assessments. Significant LI shifts towards the contralateral hemisphere were found on the CMC with ED at the 3MFU stage compared with the Pre and Post stages, respectively (corrected p = 0.0107 and 0.0431, One-way ANOVA with repeated measures and Turkey's post hoc test).

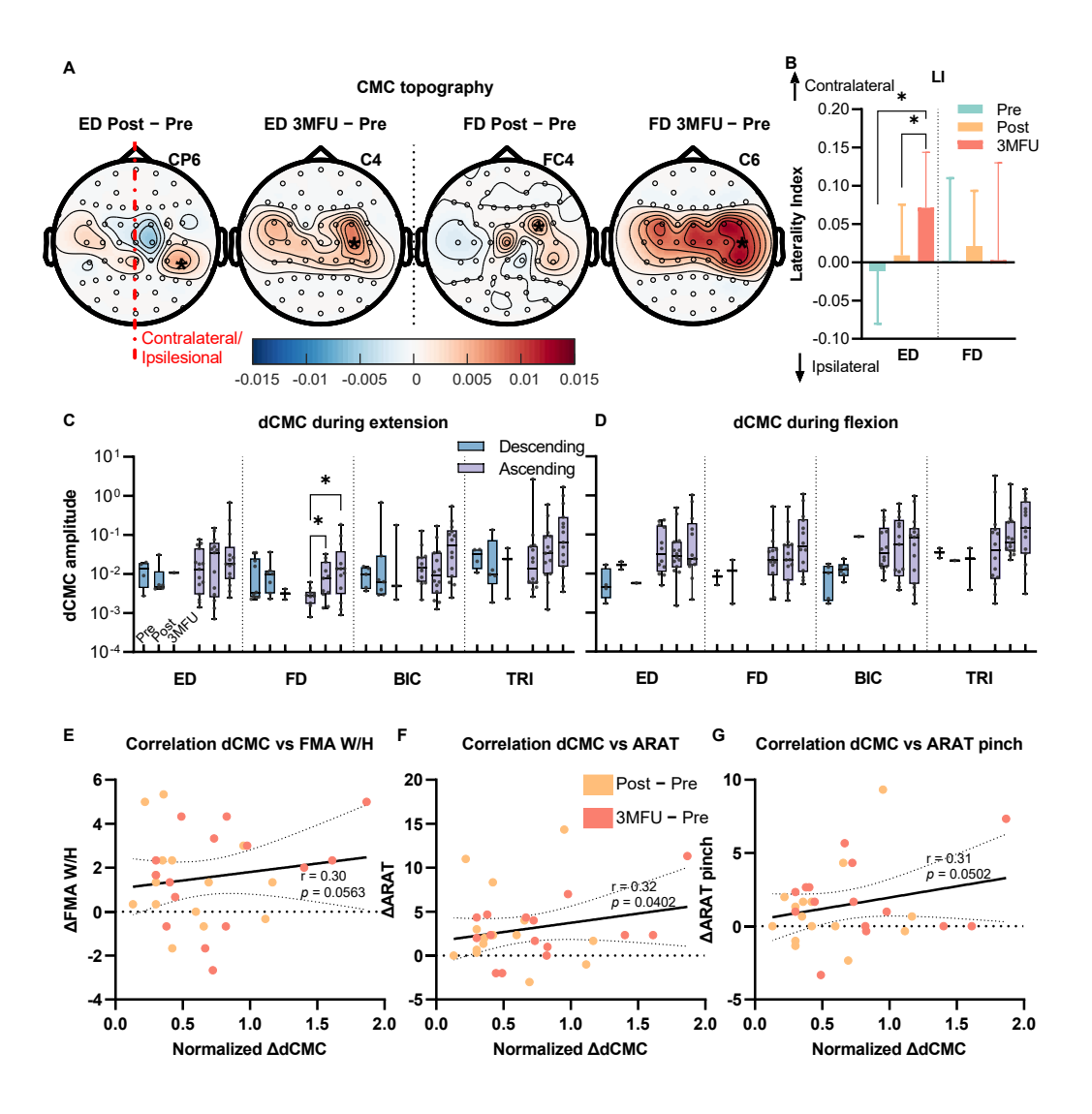


Figure 4.5 Results of corticomuscular assessments and their correlation with clinical assessments. **(A)** Grand averaged topography changes of significant CMC between sensorimotor cortex and ED/FD during extension/flexion of all participants (N = 15). Peak channels are indicated as "*" with corresponding labels on the top right corner of each topography. **(B)** LI changes of significant CMC topography with the agonist muscles. Results are presented as the means with standard deviations. Significant changes are indicated as "*" (p < 0.05, One-way ANOVA with repeated measures and Turkey's post hoc test). Significant dCMC between the peak CMC channel and four UL muscles during W/H extension **(C)** and felxion **(D)**. Results are presented as box and whisker plots with all data points. Significant changes are indicated as "*" (p < 0.05,

Friedman test with FDR correction). Pearson's correlation of changes of the significant ascending dCMC with FD during W/H extension (Post–Pre and 3MFU–Pre periods) vs. **(E)** FMA W/H sub-score, **(F)** ARAT total score, and **(G)** ARAT pinch sub-score, together with the least-squares fit line and its 95% confidence bands for both periods pooled (N = 30).

Figure 4.5C and D show the changes of significant dCMC amplitude over time during W/H extension and flexion, respectively. Less significant descending dCMC amplitude was observed than ascending dCMC in all conditions and stages. Improvements in dCMC mainly occurred on the ascending pathway. Significant increases in the ascending dCMCs with FD muscles during W/H extension were found after training and maintained after 3 months (corrected p = 0.0149 and 0.0004, Friedman test with FDR correction). The dCMC with other muscles in descending and ascending pathways showed no significant change during extension and flexion.

Figure 4.5E, F, and G exhibit the correlation between changes of the significant ascending dCMC with FD during W/H extension and FMA W/H sub-score, ARAT total score, and ARAT pinch sub-score, respectively, during Post–Pre and 3MFU–Pre periods. A significant correlation was found between the FD dCMC vs. ARAT total score (r = 0.32, p = 0.0402, Pearson's correlation). The correlations between the FD dCMC vs. FMA W/H and FD dCMC vs. ARAT pinch were both very close to the significant level (r = 0.30, p = 0.0563, and r = 0.31, p = 0.0502, Pearson's correlation). No significant correlation was found in the FD dCMC vs. other clinical scores.

4.4 Discussion

In this study, the EMG-driven ENMS-EVF that integrates NMES on the ED and FVS on the FD for somatosensory priming was developed to assist W/H training after stroke. The feasibility of the robot-assisted somatosensory priming was evaluated by a clinical

trial in which all 15 participants completed the training with minimal professional assistance in the laboratory without adverse effects. The results of the trial support the hypothesis that the robot-assisted somatosensory priming by the ENMS-EVF system could benefit the recovery of UL sensorimotor functions for poststroke individuals with maintained neuroplasticity through enhanced contralateral control and sensory feedback of the paretic limb.

4.4.1 Recovery of sensorimotor functions

The clinical assessment results demonstrated that the robot-assisted somatosensory priming jointly improved the motor and somatosensory functions of the UL with lasting effects after 3 months. The significant increase in FMA scores (Figure 4.4A) showed improvement in voluntary motor functions of the entire UL, especially the W/H joints, which indicated the rehabilitative effects of the ENMS-EVF on joint stability, coordination, and ROMs. The significant increase in ARAT scores (Figure 4.4B) indicated improvement in finger function and coordination for fine motor control during grasping, gripping, and pinching tasks. These motor function improvements of the entire UL, especially the W/H joint, were preserved at 3MFU, indicating an enduring rehabilitative effect 3 months after the training.

Even though the increased WMFT scores and decreased time consumption (WMFT time) (Appendix G) after training did not achieve a significant level, it still suggested an improvement trend in the ability to perform daily activities, especially the WMFT time, which kept at the same lower level after 3 months as the Post stage compared with the Pre stage. The significant decrease in MAS scores on the elbow (Figure 4.4D) indicated reduced spasticity and improved control of muscle synergy on the proximal joint. This result, along with the significant increase in FMA S/E (Figure 4.4A) after training, indicated the functional improvement in the proximal joints of UL due to

repeated vertical and horizontal tasks requiring the voluntary coordination of proximal joints.

On the somatosensory part, the significant decreases in the monofilament test on the glabrous skin of the hand innervated by the median and ulnar nerves suggested an improvement in cutaneous sensitivity (Figure 4.4C, sites 1-4). Especially these results were preserved at 3MFU on the proximal sites of the hand (Figure 4.4C, sites 2, 4). These hand somatosensory improvements indicated the positive effects of somatosensory stimulation on the median and ulnar nerves of the dorsal forearm and repeated contact stimulation on the hand in the object-carrying tasks during the training. Joined with the motor functional effects mentioned above, these clinical assessment results highlighted the benefits of robot-assisted somatosensory priming by ENMS-EVF in enhancing sensorimotor functions following stroke. Besides, monofilament results on the skin over ED and FD muscles did not show significant change but showed a decreasing trend after the training and 3 months (Figure 4.4C), which demonstrated no adverse effects remained on the cutaneous sensitivity of these sites after the repeated FVS and NMES stimulations.

4.4.2 Corticomuscular changes related to functional improvements

Accounting for the sensorimotor improvement, the CMC and dCMC results demonstrated that the robot-assisted somatosensory priming enhanced contralateral control of the agonist muscle and ascending sensory feedback from the antagonist muscle of the paretic limb with sustained positive neuroplasticity. The increase of CMC with the ED/FD muscles during 20% MVC motions in all topography changes (Figure 4.5A) indicated the effects of robot-assisted somatosensory priming on the improvement of corticomuscular functional coupling between sensorimotor cortex and the agonist muscles, which fostered a precise and agile motion control of the UL

functions (Guo et al., 2020), especially for the W/H joints, as exhibited in the FMA W/H and ARAT clinical assessments (Figure 4.4A and B).

Besides, the changes in interhemispheric asymmetry further indicated an enhanced contralateral dominance in the control of agonist muscles after the robot-assisted somatosensory priming by ENMS-EVF. A previous study also involving the CMC pattern reported that the brain-induced compensatory effects after stroke presented as the cortical location shift to the ipsilateral/contralesional hemisphere due to synaptic pruning and new synaptogenesis of neurons innervating the UL muscles (Guo et al., 2020). In this study, for the agonist muscles during W/H extension or flexion (i.e., ED or FD), the peak CMC (Figure 4.5A) and the increased LI (Figure 4.5B) shifting towards the contralateral/ipsilesional hemisphere after training indicated the rehabilitative effects on cortical reorganization back toward the ipsilesional hemisphere, i.e., a normal contralateral dominance. This intervention-induced cortical reorganization suggested enhanced recruitment of the ipsilesional CSTs, especially during W/H extension, as seen by the significant LI changes (Figure 4.5B, ED), which is supported by the results of other innervations on stroke patients, no matter revealed by functional magnetic resonance imaging (Carey et al., 2002) or CMC patterns (Wilkins et al., 2017). The sustained neuroplasticity changes of enhancement in contralateral activity after 3 months may allow for the long-lasting functional improvements reflected by FMA and ARAT clinical assessments (Figure 4.5A and B).

However, distribution and LI variances on the CMC topography showed different training effects on the ED and FD muscles partially due to the different properties of NMES and FVS in somatosensory priming. In this study, enhancement of CMC after training was observed on the bilateral sensorimotor cortex for ED, where NMES was applied, but on the contralateral sensorimotor cortex for FD, where FVS was applied (Figure 4.5A, topography 1 and 3). This was consistent with our previous finding about the immediate neuromodulatory effects of somatosensory stimulations that NMES tend

to foster the representation of forearm muscles on the contralesional motor cortex when compared with FVS (Lin et al., 2024b). It means that repeated NMES and FVS during training resulted in neuroplasticity changes similar to their immediate neuromodulatory effects. However, these cortical distribution variances did not sustain after 3 months, and the CMC topography with ED and FD converged to a similar pattern (Figure 4.5A, topography 2 and 4). Two potential mechanisms may underlie these findings. First, compensatory involvement of the contralesional hemisphere in controlling FX may have relapsed in the progress of generalization to daily activities after the intervention period. Second, the observed effects could reflect the development of a generalizable motor control strategy through neuroplasticity, which could generate coordinated motor commands across multiple forearm muscles during upper limb movements, as exemplified by the convergence of EX and FX CMC topography patterns in this study. Besides, after 3 months, the CMC enhancement of FD was still much higher than that of ED on the ipsilesional hemisphere (Figure 4.5A, topography 2 and 4), but the contralateral dominance was significantly enhanced for ED while reduced for FD (Figure 4.5B, 3MFU). The inconsistency of CMC topography and LI changes between ED and FD during the Post to 3MFU period may indicate that the neuroplasticity changes showed different post-intervention lasting effects on W/H extension and flexion in the progress of generalization to daily activities: The corticomuscular functional coupling with FD during flexion was bilaterally enhanced on the sensorimotor cortex (i.e., bilateral innervation enhancement) even though contralesional compensation relapsed, while the contralateral dominance for ED during extension was not only preserved but also significantly improved (i.e., contralateral dominance enhancement).

The dCMC was analyzed in this study to detect pathway-specific corticomuscular interaction in voluntary movements. Note that we applied nonparametric tests to include only the significant dCMC amplitude of each participant in the results for

minimizing false positive value and then conducted further statistical analysis over time (Figure 4.5C and D). The increase of significant descending dCMC reflects the enhancement of motor control from the cortex to the target muscle, and the increase of significant ascending dCMC reflects the enhancement of somatosensory feedback from the target muscle to the cortex. The overall dCMC pattern after stroke in this study presented as fewer numbers of significant descending dCMC with lower amplitude compared with more numbers of significant ascending dCMC with higher amplitude in all conditions and stages (Figure 4.5C and D). This result was partially supported by the finding of lower descending control (descending < ascending) on distal muscles of UL during W/H extension after stroke compared with unimpaired controls (descending > ascending) in a previous study because of the denervated CSTs with weakened monosynaptic connections after stroke (Zhou et al., 2021a). However, the poststroke descending dCMC pattern was not improved after the training (Figure 4.5C and D), which suggested challenges in the enhancement of descending control simultaneous with cortical reorganization, probably because of the still weak descending monosynaptic connection through the newly re-innervated CSTs in shifting toward contralateral dominance after the intervention (Figure 4.5A and B).

Surprisingly, the dCMC results on FD highlighted improved somatosensation conveyance/feedback up to the sensorimotor cortex and contributed to the finger function and coordination for fine motor control due to somatosensory priming of FVS on FD integrated into ENMS-EVF. As concluded in some reviews, somatosensory priming showed the ability to induce neuroplasticity and enhance the effects of rehabilitation because of the altered organization of the sensorimotor cortex (Stoykov and Madhavan, 2015; Stoykov et al., 2021). The robot-assisted somatosensory priming by ENMS-EVF resulted in the significantly increased ascending dCMC from the antagonist muscle (i.e., FD) to the sensorimotor cortex during W/H extension (Figure 4.5C). Previously, improvement of W/H extension functions was also found after

somatosensory priming on the antagonist muscle through muscle vibration, but the mechanism was not well explained (Cordo et al., 2013). In this study, the correlation results between ascending FD dCMC vs. FMA W/H, ARAT, and ARAT pinch (Figure 4.5E, F, and G) indicated the contribution of changes in neuroplasticity to the recovery of voluntary finger function and coordination for fine motor control, which uncovered the underlying mechanism that the functional improvement seen in clinical assessment (Figure 4.4) benefited from the neuroplasticity changes of improved somatosensation conveyance from the antagonist muscle to the sensorimotor cortex (Figure 4.5C) due to the afferent facilitation during the somatosensory priming by FVS on the antagonist muscle. That is because, in terms of immediate neuromodulatory effects, FVS effectively activated the sensorimotor cortex after stroke and was particularly good at eliciting transient involuntary attention (Lin et al., 2024b). The repetitive and synchronous pairing of the immediate effects with EMG-initiated robot-assisted movement in ENMS-EVF increased the strength of the somatosensory feedback in the ascending pathway to functionally interact with motor activities through afferent facilitation, thus enabling an improvement of movement functions (Stoykov and Madhavan, 2015; Asan et al., 2021). Moreover, the neuroplasticity effects lasted after 3 months and demonstrated that the effects persist after training has ceased. To sum up, the CMC and dCMC results in this study demonstrated that the robot-assisted somatosensory priming by ENMS-EVF achieved enduring positive neuroplasticity, benefiting UL sensorimotor functions by reorganizing interhemispheric dominance to contralateral control of agonist muscles and reinforcing the ascending somatosensory feedback from the antagonist muscle during W/H extension of the paretic limb.

4.4.3 Limitations and future works

There were several limitations of this study. The voluntary motor improvement of S/E joints cannot be maintained after 3 months, as indicated by FMA S/E (Figure 4.4A),

and the generalization of functional improvement to daily activities was also limited, as indicated by WMFT (Appendix G), both because the direct robotic assistance was only applied on W/H joints. Besides, the decreased MAS scores on the finger and wrist did not achieve a significant level (Figure 4.4D). A possible reason was that a few of the patients contracted their FD muscle overly when trying to trigger the EMG threshold due to impaired fine motor control, then hindered the significance of the spasticity improvement on these joints.

In the future, randomized clinical trials will be conducted to investigate the isolated effects of FVS and NMES and the effects of different priming methods paired with motor interventions (e.g., FVS on FD during W/H extension) in SMI rehabilitation. Besides, research is needed on clinical and neurological methods for assessing the collaborative magnitude of somatosensory and motor improvements. Moreover, future research on SMI rehabilitation should assert more efforts on the enhancement of descending pathways in corticomuscular coupling and investigation of the chronological differences between pathway-specific corticomuscular coupling and interhemispheric dominance shifting.

4.5 Periodic Summary

In this study, the long-term sensorimotor rehabilitative effects of the proposed ENMS-EVF and its underlying mechanisms related to cortical and pathway-specific corticomuscular neuroplasticity were investigated in a clinical trial. The results demonstrated that the system was feasible and effective for improving UL sensorimotor functions in robot-assisted somatosensory priming after stroke because of sustained neuroplasticity of enhanced contralateral control of ED and ascending somatosensory feedback from FD during W/H extension. This research sheds light on the rehabilitative effects of robot-assisted somatosensory priming on sensorimotor functions and its underlying cortical and pathway-specific corticomuscular mechanisms after stroke,

providing significant insights for developing more effective interventions toward SMI rehabilitation in the future.

CHAPTER 5

CONCLUSIONS

SMI plays a crucial role in the motor recovery of the UL after stroke. Although proprioception experiences could be provided in movement assisted by pure robots, the rehabilitative effects on W/H are still limited. New technologies are urgently needed to integrate synchronous sensory feedback from target muscles in motor interventions for better motor restoration after stroke. Effective restoration of W/H function was achieved by EMG-driven NMES-robot. However, NMES is not applicable to FD because it leads to pain, muscle fatigue, and higher muscle spasticity in FD in longterm usage. FVS, without causing muscle contraction, holds the potential to be more suitable for somatosensory priming on FD with higher comfortability in the long term. To explore the possibility of new robot-assisted rehabilitation techniques for successful sensorimotor-integrated UL rehabilitation after stroke, three experiments were conducted in this study: (1) comparison of immediate neuromodulatory effects between FVS and NMES on chronic stroke patients for effective somatosensory stimulation in W/H rehabilitation after stroke; (2) design and validation of ENMS-EVF integrating FVS and NMES in a hybrid robotic system for somatosensory priming in robot-assisted W/H rehabilitation training after stroke; (3) investigation of rehabilitative effects of somatosensory priming assisted by ENM-EVF on W/H sensorimotor functions, its long-term effects on neuroplasticity and application merits for stroke survivors.

In the first experiment, the immediate neuromodulatory effects of FVS and NMES were compared by EEG measurement on the cortical responses in individuals with chronic stroke and unimpaired controls. The results indicated that both FVS and NMES effectively activated the sensorimotor cortex after stroke. However, FVS was particularly effective in eliciting transient involuntary attention, while NMES primarily fostered the cortical responses of the targeted muscles in the contralesional motor cortex.

In the second experiment, a novel ENMS-EVF robotic system that integrates NMES on the ED and FVS on the FD into a wearable exoskeleton with soft pneumatic muscles was designed for somatosensory priming in poststroke W/H rehabilitation. Patients with chronic stroke were recruited to participate in the validation test and preliminary short-term training program. The results validated the effectiveness of the system's design and parameter and task settings for the intended rehabilitative applications. The ENMS-EVF-assisted training program could facilitate sensorimotor improvement in the affected UL of the participants with chronic stroke.

In the third experiment, the long-term rehabilitative effects of the proposed ENMS-EVF and its underlying mechanisms related to cortical and pathway-specific corticomuscular neuroplasticity were investigated in a clinical trial. The results demonstrated that the system was feasible and effective for improving UL sensorimotor functions in robot-assisted somatosensory priming after stroke because of sustained neuroplasticity of enhanced contralateral control of agonist muscles and ascending somatosensory feedback from antagonist muscles during W/H extension.

In conclusion (Figure 5.1), this study elucidated the specific cortical responses involved in FVS and NMES, which confirms the effectiveness of FVS for somatosensory stimulation, contributes to our understanding of their potential applications in stroke rehabilitation, and provides valuable insights for developing more tailored interventions in the future. In addition, this study designed and validated the novel ENMS-EVF system, which is feasible and effective for assisting stroke patients in improving sensorimotor functions of UL after the training program. Moreover, long-term rehabilitation effects and neuroplasticity changes after ENMS-EVF-assisted training sheds light on the rehabilitative effects of robot-assisted somatosensory priming on sensorimotor functions and its underlying cortical and pathway-specific corticomuscular mechanisms after stroke, providing significant insights for developing more effective interventions toward SMI rehabilitation in the future.

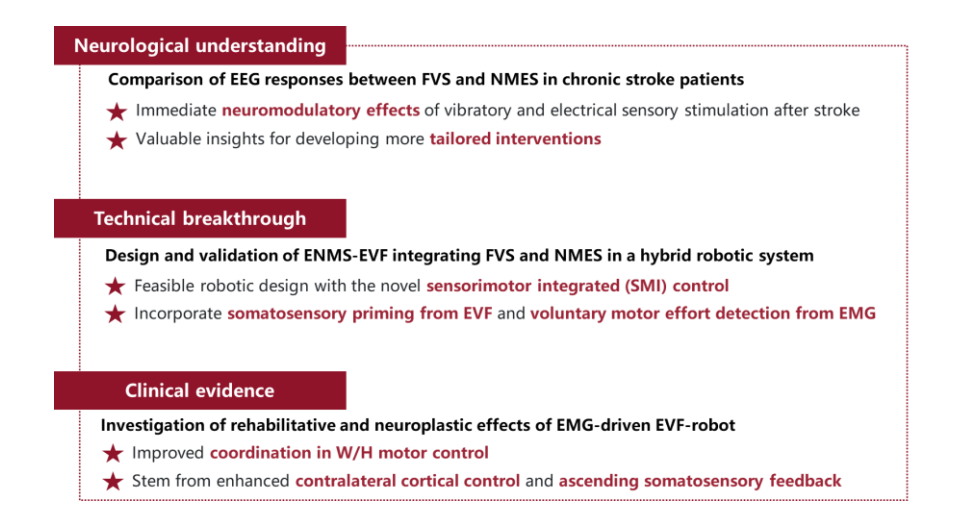


Figure 5.1 Diagram of the conclusion for SMI ENMS with EVF for W/H Rehabilitation after Stroke

In the future, further research will be conducted to:

- develop selective stimulation techniques with distributed vibratory stimulation and investigate the related neuromodulatory effects and interaction on muscle groups (e.g., agonist and antagonist, proximal and distal, etc.).
- (2) conduct randomized clinical trials to investigate the isolated effects of FVS and NMES and the effects of different priming methods paired with motor interventions (e.g., FVS on FD during W/H extension) in SMI rehabilitation.
- (3) research on clinical and neurological methods for assessing the collaborative magnitude of somatosensory and motor improvements.
- (4) Explore effective methods of pathway-specific reinforcement training, especially the enhancement of descending pathways in corticomuscular coupling during rehabilitation training.

(5) investigate the chronological differences between pathway-specific corticomuscular coupling and interhemispheric dominance shifting to help deepen our understanding of changing progress in neuroplasticity during rehabilitation.

APPENDICES

Appendix A: Comparison of RSP for the factors of the scheme and the stimulated muscle in Chapter 2.

		Two-way mixed ANOVA				
Frequency bands	Group	Scheme p (Partial η²)	Target muscle union p (Partial η²)	Scheme × Target muscle union p (Partial η²)		
T1 4	Stroke	0.431 (0.02)	0.957 (0.01)	0.510 (0.05)		
Theta	Control	0.007## (0.05)	0.871 (0.01)	0.969 (0.02)		
A 11	Stroke	0.304 (0.02)	0.889 (0.01)	0.780 (0.04)		
Alpha	Control	0.344 (0.02)	0.947 (0.01)	0.147 (0.07)		
D 4	Stroke	0.237 (0.02)	0.841 (0.02)	0.775 (0.04)		
Beta	Control	0.000### (0.08)	0.586(0.03)	0.766 (0.04)		
	Stroke	0.314 (0.02)	0.832 (0.02)	0.314 (0.06)		
Gamma	Control	0.000### (0.12)	0.870 (0.01)	0.954 (0.03)		

The superscript "#" denotes the significant difference with 2 superscripts for p < 0.01 and 3 superscripts for p < 0.001.

Appendix B: Comparison of RSP for the factors of the scheme and the target arm in Chapter 2.

	Two-way mixed ANOVA				
Frequency bands	Scheme Target arm		Scheme ×		
Trequency bunds	p (Partial η²)	p (Partial η²)	Target arm p (Partial η²)		
Theta	0.003##(0.03)	0.538 (0.02)	0.669 (0.02)		
Alpha	0.075 (0.02)	0.007## (0.10)	0.581 (0.02)		
Beta	0.000### (0.04)	0.082 (0.06)	0.098 (0.04)		
Gamma	0.000### (0.05)	0.881 (0.01)	0.397 (0.03)		

The superscript "#" denotes a significant difference with 2 superscripts for p < 0.01 and 3 superscripts for p < 0.001.

Appendix C: Comparison of RSP for the factors of the intensity and the group in Chapter 2.

	Two-way mixed ANOVA					
Frequency bands	Scheme Group		Scheme × Group			
	p (Partial η^2)	p (Partial η²)	p (Partial η²)			
Theta	$0.003^{\#\#}(0.03)$	0.278 (0.01)	0.245 (0.01)			
Alpha	0.076 (0.02)	0.000 * * (0.09)	0.877 (0.00)			
Beta	0.000### (0.04)	0.012 (0.05)	0.054 (0.02)			
Gamma	0.000### (0.05)	0.902 (0.00)	0.065 (0.02)			

The superscript "#" and " \blacktriangle " denotes the significant difference with 1 superscript for p < 0.05, 2 superscripts for p < 0.01, and 3 superscripts for p < 0.001.

Appendix D: RSP during stimulating by different intensities of FVS and NMES in Chapter 2.

Frequency bands		ľ	Nondominant arm			Dominant arm			
		Stroke affected arm (A)	Control	Independent t- test	Stroke unaffected arm (U)	Control	Independent t- test		
_	Sti	Mean ± SE		p (Cohen's d)	p (Cohen's d) Mean \pm SE		p (Cohen's d)		
	FVS-1	-0.41±0.06	-0.3±0.08	0.240 (-0.31)	-0.45±0.06	-0.39±0.07	0.490 (-0.18)		
	FVS-2	-0.4 ± 0.05	-0.3±0.06	0.215 (-0.32)	-0.44±0.06	-0.39±0.06	0.577 (-0.15)		
	FVS-3	-0.45 ± 0.05	-0.36±0.07	0.285 (-0.28)	-0.43±0.06	-0.39±0.07	0.661 (-0.11)		
Theta	FVS-4	-0.4±0.05	-0.3 ± 0.07	0.282 (-0.28)	-0.46±0.07	-0.41±0.07	0.629 (-0.13)		
band	FVS-5	-0.41 ± 0.05	-0.31±0.06	0.175 (-0.36)	-0.46 ± 0.06	-0.39±0.07	0.411 (-0.21)		
	NMES-1	-0.4 ± 0.05	-0.35±0.06	0.511 (-0.16)	-0.48 ± 0.06	-0.41±0.07	0.512 (-0.17)		
	NMES-2	-0.42 ± 0.05	-0.4 ± 0.07	0.847 (-0.05)	-0.45 ± 0.06	-0.46±0.07	0.892 (0.04)		
	NMES-3	-0.46 ± 0.05	-0.37±0.06	0.250 (-0.30)	-0.49 ± 0.06	-0.45±0.07	0.694 (-0.10)		
	y ANOVA (Partial η²)	0.346 (0.04)	0.074 (0.07)	-	0.667 (0.02)	0.199 (0.05)	-		
	FVS-1	-0.41±0.07	-0.63±0.07	0.032* (0.57)	-0.49±0.07	-0.71±0.07	0.028* (0.58)		

	FVS-2	-0.39±0.07	-0.59 ± 0.07	$0.045^*(0.53)$	-0.46 ± 0.07	-0.66±0.06	$0.034^*(0.56)$
	FVS-3	-0.44±0.07	-0.72 ± 0.07	$0.005^{**}(0.75)$	-0.48 ± 0.07	-0.64 ± 0.07	0.120 (0.41)
	FVS-4	-0.39±0.07	-0.65 ± 0.07	0.008** (0.70)	-0.46±0.07	-0.67±0.07	$0.024^* (0.60)$
Alpha band	FVS-5	-0.38±0.06	-0.62±0.07	0.006** (0.74)	-0.46±0.07	-0.7 ± 0.07	$0.016^* (0.64)$
ballu	NMES-1	-0.44 ± 0.07	-0.64 ± 0.06	$0.041^*(0.54)$	-0.49 ± 0.07	-0.7±0.08	$0.049^* (0.52)$
	NMES-2	-0.41±0.07	-0.65±0.06	0.012* (0.67)	-0.49 ± 0.07	-0.73±0.07	$0.019^* (0.62)$
	NMES-3	-0.38±0.07	-0.62 ± 0.08	$0.024^*(0.60)$	-0.48 ± 0.07	-0.66±0.07	0.081 (0.46)
•	ANOVA Partial η²)	0.360 (0.04)	0.213 (0.05)	-	0.885 (0.02)	0.241 (0.05)	-
	FVS-1	0.07±0.01	0.06±0.02	0.546 (0.16)	0.09±0.02	0.08±0.02	0.720 (0.09)
	FVS-2	0.08 ± 0.02	0.06 ± 0.01	0.323 (0.26)	0.06 ± 0.02	0.09 ± 0.02	0.333 (-0.25)
	FVS-3	0.1 ± 0.02	0.06 ± 0.01	0.126 (0.40)	0.1 ± 0.01	0.06 ± 0.02	0.069 (0.48)
Beta	Beta FVS-4 band FVS-5	0.09 ± 0.01	0.06 ± 0.02	0.235 (0.31)	0.1 ± 0.02	0.09 ± 0.02	0.606 (0.13)
band		0.08 ± 0.02	0.04 ± 0.01	$0.031^*(0.57)$	0.08 ± 0.02	0.07 ± 0.02	0.643 (0.12)
	NMES-1	0.09 ± 0.01	0.07 ± 0.02	0.394 (0.22)	0.09 ± 0.02	0.07 ± 0.02	0.241 (0.31)
	NMES-2	0.09 ± 0.01	0.04 ± 0.02	$0.019^* (0.62)$	0.07 ± 0.02	0.04 ± 0.02	0.228 (0.31)
	NMES-3	0.09±0.01	0.03 ± 0.02	$0.013^* (0.67)$	0.06 ± 0.02	0.01 ± 0.01	$0.015^* (0.65)$
One-way ANOVA RM - p (Partial η²)		0.821 (0.02)	0.230 (0.04)	-	0.091 (0.06)	0.000 ^{###} (0.13)	-
	FVS-1	0.06 ± 0.01	0.05 ± 0.01	0.385 (0.23)	0.07 ± 0.01	0.06 ± 0.01	0.807 (0.06)
	FVS-2	0.06 ± 0.01	0.05 ± 0.01	0.460 (0.19)	0.07 ± 0.01	0.06 ± 0.01	0.205 (0.33)
	FVS-3	0.06 ± 0.01	0.06 ± 0.01	0.846 (0.05)	0.06 ± 0.01	0.06 ± 0.01	0.745 (-0.08)
Gamma	FVS-4	0.06 ± 0.01	0.06 ± 0.01	0.631 (0.13)	0.06 ± 0.01	0.06 ± 0.01	0.596 (0.14)
band	FVS-5	0.06 ± 0.01	0.07 ± 0.01	0.677 (-0.11)	0.07 ± 0.01	0.06 ± 0.01	0.744 (0.09)
	NMES-1	0.06 ± 0.01	0.06 ± 0.01	0.923 (0.03)	0.07 ± 0.01	0.07 ± 0.01	0.882 (0.04)
	NMES-2	0.06 ± 0.01	0.07 ± 0.01	0.270 (-0.29)	0.07 ± 0.01	0.08 ± 0.01	0.289 (-0.28)
	NMES-3	0.07 ± 0.01	0.07 ± 0.01	0.900 (0.03)	0.07 ± 0.01	0.09 ± 0.01	0.195 (-0.34)
One-way ANOVA RM - p (Partial η²)		0.615 (0.02)	0.012# (0.08)	-	0.462 (0.03)	0.000 ^{###} (0.17)	-

The superscript "*" and "#" denotes the significant inter-group difference based on arm pairs and the significant intra-group difference between intensities, respectively, with 1 superscript for p < 0.05, 2 superscripts for p < 0.01, and 3 superscripts for p < 0.001.

Appendix E: RSP during stimulating each target arm of stroke and control groups in Chapter 2.

Danda	Stimulation target	Stroke	Control	Independent t-test
Bands	Stimulation target arm	Mea	n ± SE	p (Cohen's d)
	Nondominant	-0.42±0.02	-0.34±0.02	0.006** (-0.25)
Theta band	Dominant	-0.46±0.02	-0.4±0.02	0.162 (-0.13)
	Paired <i>t</i> -test p (Cohen's d)	0.330 (0.26)	0.004## (0.89)	-
	Nondominant	-0.4±0.02	-0.64±0.02	0.000*** (0.64)
Alpha band	Dominant	-0.47±0.02	-0.68±0.02	0.000*** (0.55)
	Paired <i>t</i> -test p (Cohen's d)	0.103 (0.45)	0.151 (0.39)	-
	Nondominant	0.09±0.01	0.05±0.01	0.000*** (0.40)
Beta band	Dominant	0.08 ± 0.01	0.06 ± 0.01	0.017* (0.22)
	Paired <i>t</i> -test p (Cohen's d)	0.706 (0.10)	0.217 (-0.33)	-
	Nondominant	0.06±0.002	0.06±0.003	0.665 (0.04)
Gamma band	Dominant	0.07±0.002	0.07 ± 0.002	0.959 (-0.01)
	Paired <i>t</i> -test p (Cohen's d)	0.445 (-0.20)	0.087 (-0.48)	-

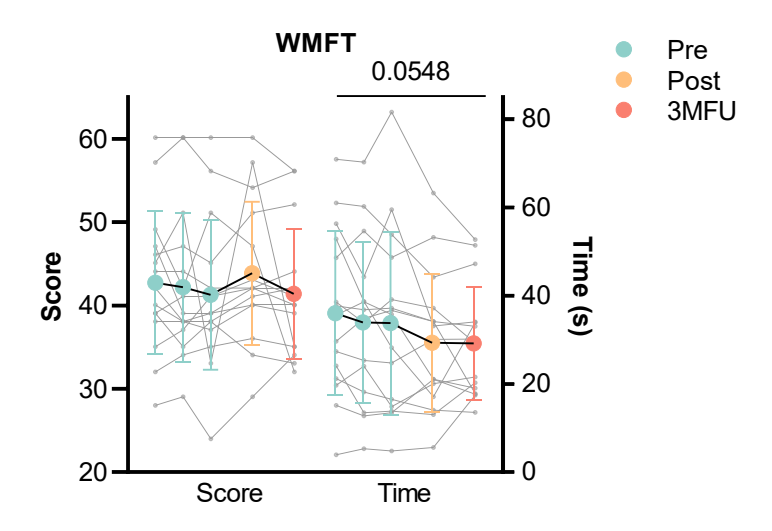
The superscript "*" and "#" denotes the significant inter-group difference based on muscle pairs and the significant intra-group difference between arms, respectively, with 1 superscript for p < 0.05, 2 superscripts for p < 0.01, and 3 superscripts for p < 0.001.

Appendix F: RSP of stroke and control group during FVS and NMES in Chapter 2.

Danda	Stimulation toma	Stroke	Control	Independent t-test
Bands	Stimulation type	Mea	n ± SE	p (Cohen's d)
	FVS	-0.43 ± 0.02	-0.35±0.02	0.005** (-0.23)
Theta band	NMES	-0.45±0.02	-0.41±0.03	0.266 (-0.12)
Theta band	Paired <i>t</i> -test p (Cohen's d)	0.376 (0.24)	0.000### (1.08)	-
	FVS	-0.43±0.02	-0.66±0.02	0.000*** (0.61)
Alpha band	NMES	-0.45±0.03	-0.67±0.03	0.000*** (0.57)
Агриа бани	Paired t-test p (Cohen's d)	0.340 (0.26)	0.565 (0.15)	-
	FVS	0.085±0.005	0.066±0.005	0.008** (0.22)
Beta band	NMES	0.082 ± 0.006	0.042 ± 0.007	0.000*** (0.45)
Deta band	Paired <i>t</i> -test p (Cohen's d)	0.340 (0.11)	0.023#(0.66)	-
	FVS	0.064±0.002	0.06±0.002	0.199 (0.11)
Gamma band	NMES	0.067±0.003	0.072 ± 0.003	0.249 (-0.12)
Gaiiiiia bailu	Paired <i>t</i> -test p (Cohen's d)	0.136 (-0.41)	0.000### (-1.55)	-

The superscript "*" and "#" denotes the significant inter-group difference and the significant intra-group difference based on stimulation types, respectively, with 1 superscript for p < 0.05, 2 superscripts for p < 0.01, and 3 superscripts for p < 0.001.

Appendix G: WMFT score and consumed time results in Chapter 4 (One-way ANOVA with repeated measures and Turkey's post hoc test).



Mini-Mental State Examination (MMSE)

Patient's Name:	Date:
-----------------	-------

<u>Instructions:</u> Ask the questions in the order listed. Score one point for each correct response within each question or activity.

Maximum Score	Patient's Score	Questions
5		"What is the year? Season? Date? Day of the week? Month?"
5		"Where are we now: State? County? Town/city? Hospital? Floor?"
3		The examiner names three unrelated objects clearly and slowly, then asks the patient to name all three of them. The patient's response is used for scoring. The examiner repeats them until patient learns all of them, if possible. Number of trials:
5		"I would like you to count backward from 100 by sevens." (93, 86, 79, 72, 65,) Stop after five answers. Alternative: "Spell WORLD backwards." (D-L-R-O-W)
3		"Earlier I told you the names of three things. Can you tell me what those were?"
2		Show the patient two simple objects, such as a wristwatch and a pencil, and ask the patient to name them.
1		"Repeat the phrase: 'No ifs, ands, or buts."
3		"Take the paper in your right hand, fold it in half, and put it on the floor." (The examiner gives the patient a piece of blank paper.)
1		"Please read this and do what it says." (Written instruction is "Close your eyes.")
1		"Make up and write a sentence about anything." (This sentence must contain a noun and a verb.)
1		"Please copy this picture." (The examiner gives the patient a blank piece of paper and asks him/her to draw the symbol below. All 10 angles must be present and two must intersect.)
30		TOTAL

(Adapted from Rovner & Folstein, 1987)

Instructions for administration and scoring of the MMSE

Orientation (10 points):

- Ask for the date. Then specifically ask for parts omitted (e.g., "Can you also tell me what season it is?"). One point for each correct answer.
- Ask in turn, "Can you tell me the name of this hospital (town, county, etc.)?" One point for each correct answer.

Registration (3 points):

- Say the names of three unrelated objects clearly and slowly, allowing approximately one second for
 each. After you have said all three, ask the patient to repeat them. The number of objects the
 patient names correctly upon the first repetition determines the score (0-3). If the patient does not
 repeat all three objects the first time, continue saying the names until the patient is able to repeat all
 three items, up to six trials. Record the number of trials it takes for the patient to learn the words. If
 the patient does not eventually learn all three, recall cannot be meaningfully tested.
- After completing this task, tell the patient, "Try to remember the words, as I will ask for them in a little while."

Attention and Calculation (5 points):

- Ask the patient to begin with 100 and count backward by sevens. Stop after five subtractions (93, 86, 79, 72, 65). Score the total number of correct answers.
- If the patient cannot or will not perform the subtraction task, ask the patient to spell the word "world" backwards. The score is the number of letters in correct order (e.g., dlrow=5, dlorw=3).

Recall (3 points):

 Ask the patient if he or she can recall the three words you previously asked him or her to remember. Score the total number of correct answers (0-3).

Language and Praxis (9 points):

- Naming: Show the patient a wrist watch and ask the patient what it is. Repeat with a pencil. Score
 one point for each correct naming (0-2).
- Repetition: Ask the patient to repeat the sentence after you ("No ifs, ands, or buts."). Allow only one trial. Score 0 or 1.
- 3-Stage Command: Give the patient a piece of blank paper and say, "Take this paper in your right hand, fold it in half, and put it on the floor." Score one point for each part of the command correctly executed.
- Reading: On a blank piece of paper print the sentence, "Close your eyes," in letters large enough
 for the patient to see clearly. Ask the patient to read the sentence and do what it says. Score one
 point only if the patient actually closes his or her eyes. This is not a test of memory, so you may
 prompt the patient to "do what it says" after the patient reads the sentence.
- Writing: Give the patient a blank piece of paper and ask him or her to write a sentence for you. Do
 not dictate a sentence; it should be written spontaneously. The sentence must contain a subject
 and a verb and make sense. Correct grammar and punctuation are not necessary.
- Copying: Show the patient the picture of two intersecting pentagons and ask the patient to copy the figure exactly as it is. All ten angles must be present and two must intersect to score one point. Ignore tremor and rotation.

(Folstein, Folstein & McHugh, 1975)

Interpretation of the MMSE

Method	Score	Interpretation		
Single Cutoff	<24	Abnormal		
Range	<21	Increased odds of dementia		
Range	>25	Decreased odds of dementia		
	21	Abnormal for 8 th grade education		
Education	<23	Abnormal for high school education		
	<24	Abnormal for college education		
	24-30	No cognitive impairment		
Severity	18-23	Mild cognitive impairment		
	0-17	Severe cognitive impairment		

Sources:

- . Crum RM, Anthony JC, Bassett SS, Folstein MF. Population-based norms for the mini-mental state
- examination by age and educational level. *JAMA*. 1993;269(18):2386-2391.

 Folstein MF, Folstein SE, McHugh PR. "Mini-mental state": a practical method for grading the cognitive state of patients for the clinician. J Psychiatr Res. 1975;12:189-198.
- Rovner BW, Folstein MF. Mini-mental state exam in clinical practice. Hosp Pract. 1987;22(1A):99, 103, 106,
- Tombaugh TN, McIntyre NJ. The mini-mental state examination: a comprehensive review. J Am Geriatr Soc. 1992;40(9):922-935.

The form adopted from:

http://www.heartinstitutehd.com/Misc/Forms/MMSE.1276128605.pdf

Appendix I: Modified Ashworth Scale (MAS)

Modified Ashworth Scale Instructions

General Information (derived Bohannon and Smith, 1987):

- · Place the patient in a supine position
- If testing a muscle that primarily flexes a joint, place the joint in a maximally flexed position and move to a position of maximal extension over one second (count "one thousand one")
- If testing a muscle that primarily extends a joint, place the joint in a maximally extended position and move to a position of maximal flexion over one second (count "one thousand one")
- Score based on the classification below

Scoring (taken from Bohannon and Smith, 1987):

- 0 No increase in muscle tone
- Slight increase in muscle tone, manifested by a catch and release or by minimal resistance at the end of the range of motion when the affected part(s) is moved in flexion or extension
- 1+ Slight increase in muscle tone, manifested by a catch, followed by minimal resistance throughout the remainder (less than half) of the ROM
- More marked increase in muscle tone through most of the ROM, but affected part(s) easily moved
- 3 Considerable increase in muscle tone, passive movement difficult
- 4 Affected part(s) rigid in flexion or extension

Patient Instructions:

The patient should be instructed to relax.

Modified Ashworth Scale Testing Form

Name:			Date:	
Muscle Tested	Score			
Reference for tes Bohannon, R. and Sr of muscle spasticity."	mith, M. (1987).	"Interrater i	reliability of a mo 06.	dified Ashworth sca
e form adopted fron	n:			
os://www.sralab.org	g/sites/default/	files/2017	=	
Modified%20Ashw	orth%20Scale	e%20Instru	actions.pdf	

Appendix J: Fugl-Meyer Assessment for UL (FMA-UL)

FMA-UE PROTOCOL

Rehabilitation Medicine, University of Gothenburg

FUGL-MEYER ASSESSMENT ID:
UPPER EXTREMITY (FMA-UE) Date:
Assessment of sensorimotor function Examiner:

Fugl-Meyer AR, Jaasko L, Leyman I, Olsson S, Steglind S: The post-stroke hemiplegic patient. A method for evaluation of physical performance. Scand J Rehabil Med 1975. 7:13-31

I. Reflex activity			none	can be	elicited
Flexors: biceps and finger flexors (at least one)		0	2		
Extensors: triceps	,	,	0	2	
		Subtotal I (max 4)			
				1	
		synergies, without gravitational help	none	partial	full
Flexor synergy: Hand from		Shoulder retraction	0	1	2
contralateral knee to ipsilate		elevation	0	1	2
From extensor synergy (sho		abduction (90°)	0	1	2
adduction/ internal rotation,		external rotation	0	1	2
extension, forearm pronation synergy (shoulder abduction		Elbow flexion	0	1	2
rotation, elbow flexion, forea		Forearm supination	0	1	2
supination).		Shoulder adduction/internal rotation	0	1	2
Extensor synergy: Hand from	om	Elbow extension	0	1	2
ipsilateral ear to the contrala		Forearm pronation	0	l i	2
ipsilateral car to the contrale	iterar knee	Subtotal II (max 18)	+ -		
		Subtotal II (Illax 10)			
III. Volitional movemen	nt mixing	synergies, without compensation	none	partial	full
Hand to lumbar spine		orm or hand in front of ant-sup iliac spine	0		
hand on lap	hand behin	d ant-sup iliac spine (without compensation)		1	
-	hand to lum	bar spine (without compensation)			2
Shoulder flexion 0°- 90°	immediate	abduction or elbow flexion	0		
elbow at 0°	abduction of	r elbow flexion during movement		1	
pronation-supination 0°	flexion 90°,	no shoulder abduction or elbow flexion			2
Pronation-supination		n/supination, starting position impossible	0		
elbow at 90°		ited pronation/supination, maintains starting position		111	
shoulder at 0°	full pronation	n/supination, maintains starting position			2
GOILD		Subtotal III (max 6)	91		7
IV Volitional moveme	nt with lit	,	none	nartial	full
IV. Volitional moveme		tle or no synergy	none	partial	full
Shoulder abduction 0 - 90°	° immedia	tle or no synergy tte supination or elbow flexion	none 0		full
Shoulder abduction 0 - 90° elbow at 0°	immedia supinati	tle or no synergy te supination or elbow flexion on or elbow flexion during movement		partial	
Shoulder abduction 0 - 90° elbow at 0° forearm neutral	immedia supination abduction	tle or no synergy te supination or elbow flexion on or elbow flexion during movement on 90°, maintains extension and pronation	0		full 2
Shoulder abduction 0 - 90° elbow at 0° forearm neutral Shoulder flexion 90° - 180°	immedia supination abduction immedia	tle or no synergy tte supination or elbow flexion on or elbow flexion during movement on 90°, maintains extension and pronation tte abduction or elbow flexion		1	
Shoulder abduction 0 - 90° elbow at 0° forearm neutral Shoulder flexion 90° - 180° elbow at 0°	immedia supinational abductional immedia abductional	tle or no synergy In the supination or elbow flexion In or elbow flexion during movement In 90°, maintains extension and pronation In the abduction or elbow flexion In or elbow flexion during movement	0		2
Shoulder abduction 0 - 90° elbow at 0° forearm neutral Shoulder flexion 90° - 180° elbow at 0° pronation-supination 0°	immedia supination abduction immedia abduction flexion 1	tle or no synergy In the supination or elbow flexion on or elbow flexion during movement on 90°, maintains extension and pronation of the abduction or elbow flexion on or elbow flexion during movement 80°, no shoulder abduction or elbow flexion	0	1	
Shoulder abduction 0 - 90° elbow at 0° forearm neutral Shoulder flexion 90° - 180° elbow at 0° pronation-supination 0° Pronation/supination	immedia supination abduction immedia abduction flexion 1	tle or no synergy In the supination or elbow flexion In 90°, maintains extension and pronation In the abduction or elbow flexion In or elbow flexion during movement In or elbow flexion during	0	1	2
Shoulder abduction 0 - 90° elbow at 0° forearm neutral Shoulder flexion 90° - 180° elbow at 0° pronation-supination 0° Pronation/supination elbow at 0°	immedia supination abduction immedia abduction flexion 1 no prona limited p	tle or no synergy In the supination or elbow flexion on or elbow flexion during movement on 90°, maintains extension and pronation of the abduction or elbow flexion on or elbow flexion during movement 80°, no shoulder abduction or elbow flexion ation/supination, starting position impossible pronation/supination, maintains start position	0	1	2
Shoulder abduction 0 - 90° elbow at 0° forearm neutral Shoulder flexion 90° - 180° elbow at 0° pronation-supination 0° Pronation/supination	immedia supination abduction immedia abduction flexion 1 no prona limited p	tle or no synergy Interest supination or elbow flexion Interest of the supination or elbow flexion or elbow flexion or elbow flexion or elbow flexion Interest of the supination or elbow flexion or elbow flexion during movement Interest of the supination or elbow flexion or	0	1	2
Shoulder abduction 0 - 90° elbow at 0° forearm neutral Shoulder flexion 90° - 180° elbow at 0° pronation-supination 0° Pronation/supination elbow at 0°	immedia supination abduction immedia abduction flexion 1 no prona limited p	tle or no synergy In the supination or elbow flexion on or elbow flexion during movement on 90°, maintains extension and pronation of the abduction or elbow flexion on or elbow flexion during movement 80°, no shoulder abduction or elbow flexion ation/supination, starting position impossible pronation/supination, maintains start position	0	1	2
Shoulder abduction 0 - 90° elbow at 0° forearm neutral Shoulder flexion 90° - 180° elbow at 0° pronation-supination 0° Pronation/supination elbow at 0° shoulder at 30°- 90° flexion V. Normal reflex activi	immedia supination abduction immedia abduction flexion 1 no prono limited prono full prono ity assesses	tle or no synergy Interest supination or elbow flexion Interest of the about the supination or elbow flexion and pronation Interest of the about the abou	0	1	2
Shoulder abduction 0 - 90° elbow at 0° forearm neutral Shoulder flexion 90° - 180° elbow at 0° pronation-supination 0° Pronation/supination elbow at 0° shoulder at 30°- 90° flexion V. Normal reflex activipart IV; compare with the un	immedia supination abduction of immedia supination of immedia abduction of immedia abd	tle or no synergy Interest supination or elbow flexion Interest of the about the supination or elbow flexion and pronation Interest of the about the abou	0 0	1 1	2 2 2
Shoulder abduction 0 - 90° elbow at 0° forearm neutral Shoulder flexion 90° - 180° elbow at 0° pronation-supination elbow at 0° shoulder at 30°- 90° flexion V. Normal reflex activity part IV; compare with the unbiceps, triceps,	immedia supination abductic immedia abductic flexion 1 no prona limited p full pron	tle or no synergy the supination or elbow flexion on or elbow flexion during movement on 90°, maintains extension and pronation the abduction or elbow flexion on or elbow flexion during movement 80°, no shoulder abduction or elbow flexion ation/supination, starting position impossible ironation/supination, maintains start position ation/supination, maintains starting position Subtotal IV (max 6) d only if full score of 6 points is achieved in e markedly hyperactive	0 0 0 hyper	1 1	2 2 2
Shoulder abduction 0 - 90° elbow at 0° forearm neutral Shoulder flexion 90° - 180° elbow at 0° pronation-supination elbow at 0° shoulder at 30°- 90° flexion V. Normal reflex activity part IV; compare with the unbiceps, triceps, finger flevors	immedia supination abductic immedia abductic flexion 1 no prona limited public full pron immedia absence full pron immedia abductic flexion 1 no prona limited public full pron immedia abductic full pron immedia	tle or no synergy Interest supination or elbow flexion Interest of the about the supination or elbow flexion and pronation Interest of the about the abou	0 0 0 hyper	1 1 lively	2 2 2
Shoulder abduction 0 - 90° elbow at 0° forearm neutral Shoulder flexion 90° - 180° elbow at 0° pronation-supination elbow at 0° shoulder at 30°- 90° flexion V. Normal reflex activity part IV; compare with the unbiceps, triceps, finger flevors	immedia supination abductic immedia abductic flexion 1 no prona limited public full pron immedia absence full pron immedia abductic flexion 1 no prona limited public full pron immedia abductic full pron immedia	Itle or no synergy Itle supination or elbow flexion It on or elbow flexion during movement Itle abduction or elbow flexion Itl	0 0 0 hyper	1 1 lively	2 2 normal
Shoulder abduction 0 - 90° elbow at 0° forearm neutral Shoulder flexion 90° - 180° elbow at 0° pronation-supination elbow at 0° shoulder at 30°- 90° flexion V. Normal reflex activity part IV; compare with the unbiceps, triceps, finger flevors	immedia supination abductic immedia abductic flexion 1 no prona limited public full pron immedia absence full pron immedia abductic flexion 1 no prona limited public full pron immedia abductic full pron immedia	tle or no synergy the supination or elbow flexion on or elbow flexion during movement on 90°, maintains extension and pronation the abduction or elbow flexion on or elbow flexion during movement 80°, no shoulder abduction or elbow flexion ation/supination, starting position impossible ronation/supination, maintains start position ation/supination, maintains starting position Subtotal IV (max 6) d only if full score of 6 points is achieved in e markedly hyperactive dly hyperactive or at least 2 reflexes lively reflex lively, none hyperactive	0 0 0 hyper	1 1 lively	2 2 normal

B. WRIST support may be provided at the elbow to take or hold the starting			partial	full
position, no support at wrist, check the passive range of motion prior testing			•	
Stability at 15° dorsiflexion	less than 15° active dorsiflexion	0		
elbow at 90°, forearm pronated	dorsiflexion 15°, no resistance tolerated		1	
shoulder at 0°	maintains dorsiflexion against resistance			2
Repeated dorsifexion / volar flexion	cannot perform volitionally	0		
elbow at 90°, forearm pronated	limited active range of motion		1	
shoulder at 0°, slight finger flexion	full active range of motion, smoothly			2
Stability at 15° dorsiflexion	less than 15° active dorsiflexion	0		
elbow at 0°, forearm pronated dorsiflexion 15°, no resistance tolerated			1	
slight shoulder flexion/abduction	maintains dorsiflexion against resistance			2
Repeated dorsifexion / volar flexion	cannot perform volitionally	0		
elbow at 0°, forearm pronated	limited active range of motion		1	
slight shoulder flexion/abduction	full active range of motion, smoothly			2
Circumduction	cannot perform volitionally	0		
elbow at 90°, forearm pronated	jerky movement or incomplete		1	
shoulder at 0°	complete and smooth circumduction			2
	Total B (max 10)			

C. HAND support may be provided at the elbow to keep 90° flexion, no support at		none	partial	full
the wrist, compare with unaffected hand, the objects are interposed, active grasp		Hone	partiai	Iuii
Mass flexion		0	1	2
from full active or passive extension		U	ı	2
Mass extension	C+GOTH	0	4	2
from full active or passive flexion	(A. C.)	U	1	2
GRASP				
a. Hook grasp	cannot be performed	0		
flexion in PIP and DIP (digits II-V),	can hold position but weak		1	
extension in MCP II-V	maintains position against resistance			2
b. Thumb adduction	cannot be performed	0		
1-st CMC, MCP, IP at 0°, scrap of paper	can hold paper but not against tug		1	
between thumb and 2-nd MCP joint	can hold paper against a tug			2
c. Pincer grasp, opposition	cannot be performed	0		
pulpa of the thumb against the pulpa of	can hold pencil but not against tug		1	
2-nd finger, pencil, tug upward	can hold pencil against a tug	CI		2
d. Cylinder grasp	cannot be performed	0		/
cylinder shaped object (small can)	can hold cylinder but not against tug		1	
tug upward, opposition of thumb and	can hold cylinder against a tug			2
fingers				
e. Spherical grasp	cannot be performed	0		
fingers in abduction/flexion, thumb	can hold ball but not against tug		1	
opposed, tennis ball, tug away	can hold ball against a tug			2
	Total C (max 14)			

D. COORDINATION/SPEED, sitting, after one trial with both arms, eyes closed, tip of the index finger from knee to nose, 5 times as fast as possible			slight	none
Tremor		0	1	2
Dysmetria	pronounced or unsystematic slight and systematic	0	1	
	no dysmetria	≥ 6s	2 - 5s	2 < 2s
Time start and end with the hand on the knee	6 or more seconds slower than unaffected side 2-5 seconds slower than unaffected side less than 2 seconds difference	0	1	2
	Total D (max 6)			

TOTAL A-D (max 6	5)
------------------	----

The form adopted from:

 $\underline{https://www.gu.se/en/neuroscience-physiology/fugl-meyer-assessment}$

Appendix K: Action Research Arm Test (ARAT)

ACT	ION Patient Name:	
RES	EARCH Rater Name:	
ARN	I TEST Date:	
Instru There a	etions e four subtests: Grasp, Grip, Pinch, Gross Movement. Items in each are ordered so that:	
•	if the subject passes the first, no more need to be administered and he scores top marks for that subtest	;
•	if the subject fails the first and fails the second, he scores zero, and again no more tests need to be performed in that subtest;	
•	otherwise he needs to complete all tasks within the subtest	
Activ	v S	core
Acur	,	core
Cross		
	x, wood, 10 cm cube (If score = 3, total = 18 and to Grip) up a 10 cm block	
	x, wood, 2.5 cm cube (If score = 0, total = 0 and go to Grip) up 2.5 cm block	
3. Blo	x, wood, 5 cm cube	
4. Blo	x, wood, 7.5 cm cube	
5. Ball	Cricket), 7.5 cm diameter	
6. Stor	10 x 2.5 x 1 cm	
Coeffic	ent of reproducibility = 0.98	
Coeffic	ent of scalability = 0.94	
Grip	water from close to close (If soons = 2, total = 12, and so to Binch)	
	water from glass to glass (If score = 3, total = 12, and go to Pinch) 2.25 cm (If score = 0, total = 0 and go to Pinch)	
	1 x 16 cm	
	er (3.5 cm diameter) over bolt	
	ent of reproducibility = 0.99 ent of scalability = 0.98	
Coemic	ent of scalability = 0.98	
Pinch	bearing, 6 mm, 3 rd finger and thumb (If score = 3, total = 18 and go to Grossmt)	
2. Mar	le, 1.5 cm, index finger and thumb (If score = 0, total = 0 and go to Grossmt)	
3. Ball	pearing 2 nd finger and thumb	
4. Ball	pearing 1st finger and thumb	
	le 3 rd finger and thumb	
	le 2 nd finger and thumb	
Coeffic	ent of reproducibility = 0.99	

Coefficient of scalability

= 0.98

		_
Crocemt	(Crose N	(fovement
CTLOSSIIIL	ULTI USS IV	iovement)

Place hand behind head (If score = 3, total = 9 and finish)

 (If score = 0, total = 0 and finish)

 Place hand on top of head

 Hand to mouth

Coefficient of reproducibility = 0.98

Coefficient of scalability = 0.97

References

Carroll D. "A quantitative test of upper extremity function." J Chronic Diseases. 1965;18:479-491.

Crow JL, Lincoln NNB, Nouri FM, De Weerdt W. "The effectiveness of EMG biofeedback in the treatment of arm function after stroke.

International Disability Studies. 1989;11:155-160.

De Weerdt WJG, Harrison MA. "Measuring recovery of arm-hand function in stroke patients: a comparison of the Brunnstrom-Fugl-Meyer test and the Action Research Arm test.

Physiotherapy Canada. 1985;37:65-70.

Lyle RC. "A performance test for assessment of upper limb function in physical rehabilitation treatment and research."

Int J Rehabil Res. 1981;4:483-492.

The form adopted from:

https://faculty.ksu.edu.sa/sites/default/files/action_research_arm_test.pdf

Appendix L: Wolf Motor Function Test (WMFT)

Type/Purpose of Test: The purpose of this test is to quantify upper extremity UE motor ability through a series of timed and functional tasks.

Population: Used primarily for stroke patients but could be used for people with impaired UE motor ability. *Limited usefulness for patients with chronic stroke and TBI who are lower functioning in motor deficit. Or for acute or sub-acute stroke before spontaneous recovery has completed.

Focus of measurement:		
Organic systems (X)Abiliti	esParticipation/life habits	Environmental Factors

Ease of Administration:

General Description of the WMFT

All tasks are performed as quickly as possible and are truncated at

120 seconds. Tasks are as follows:

- 1. Forearm to table (side): Subject attempts to place forearm on the table by abduction at the shoulder.
- 2. Forearm to box (side): Subject attempts to place a forearm on the box by abduction at the shoulder.
- Extend elbow (side): Subject attempts to reach across the table by extending the elbow (to the side).
- Extend elbow (to the side), with weight: Subject attempts to push the sandbag against outer wrist joint across the table by extending the elbow.
- 5. Hand to table (front): Subject attempts to place involved hand on the table.
- 6. Hand to box (front): Subject attempts to place hand on the box.
- 7. Reach and retrieve (front): Subject attempts to pull 1-lb weight across the table by using elbow flexion and cupped wrist.
- 8. Lift can (front): Subject attempts to lift can and bring it close to lips with a cylindrical grasp.
- 9. Lift pencil (front): Subject attempts to pick up pencil by using 3-jaw chuck grasp
- 10. Pick up paper clip (front): Subject attempts to pick up paper clip by using a pincer grasp.
- 11. Stack checkers (front): Subject attempts to stack checkers onto the center checker.
- 12. Flip cards (front): Using the pincer grasp, patient attempts to flip each card over.
- 13. Turning the key in lock (front): Using pincer grasp, while maintaining contact, patient turns key fully to the left and right.
- 14. Fold towel (front): Subject grasps towel, folds it lengthwise, and then uses the tested hand to fold the towel in half again.
- 15. Lift basket (standing): Subject picks up basket by grasping the handles and placing it on bedside table.

Clarity of Directions:

Very clear and easy to follow directions for the administrator of the test and the test taker.

Scoring Procedures:

The speed at which functional tasks can be completed is measured by performance time and the movement quality when completing the tasks is measured by functional ability.

Speed is measured by timing the task with a stopwatch from start to finish.

Movement quality during the task is measured by functional ability using a 6-point ordinal scale, where 0 = does not attempt with the involved arm and 5 = arm does participate/movement appears to be normal.

Examiner Qualification & Training

No qualification or training required.

	Standardization: Norms Criterion Referenced Other None were mentioned in the manual.
	Reliability: The inter-test and inter-rater reliability, and internal consistency and stability of the test is high for both the performance time and Functional Ability rating scale measures, ranging from .88 to .98, with most values \approx .95
	Validity: Construct validity, criterion validity
	Manual: Excellent Poor
	What is (are) the setting/s that you would anticipate using this assessment? I could see this used in any setting where a person with a stroke or UE motor impairment is being treated. Inpatient, outpatient, home health, related research, etc. (acute rehab might be a little premature for this type of test.)
	Summary of strengths and weaknesses: Weakness: I think that it is very easy for interraters to be consistent with the timing part of the test but I think there could be some difference of opinion for the movement quality assessment. A patient could become very frustrated if they were not able to do well in a timed test environment.
	Strength: There are mostly functional measurements of UE use. It is something that can be used to track progress of a patient. Very easy to learn and administer. Not expensive to simulate in a clinic or wherever you want to use it.
F	Form adopted from:

 $\underline{https://strokengine.ca/en/assessments/wmft/}$

Appendix M: Consent Form for Chapter 2, 3 and 4

I, ______ (name of subject), hereby consent to participate as a subject for the project entitled "Sensorimotor Integrated Exo-neuro-musculo-skeleton (ENMS) with Electro-vibro-feedback for Hand Rehabilitation after Stroke".

- I have understood the experimental procedures presented to me.
- I have given an opportunity to ask questions about the experiment, and these have been answered to my satisfaction.
- I have understood the information presented in the information sheet.
- I realize the experiment will possibly benefit my upper limb motor functions.
- The testing should not result in any undue discomfort, I realize that I can discontinue the experiment with no reasons given and no penalty received during the experiment.
- I realize that the results of this experiment may be published, but that my own results will be kept confidential.
- I realize that the results of this experiment are the properties of The Hong Kong Polytechnic University.
- I agree that the PI and the project research members, who obtained the authorization from the PI, can use my experimental data for this project study.

Subject name:	Signature:	Date:
Witness:	Signature:	Date:
Investigator:	Signature:	Date:
	 同意書	
我,	(受試者姓名),在此同意作為受試者參	加 "感知运动功能相结合
的外神经肌骨系统于中	风后手功能康复"。	

- 我已明白到該測試的步驟。
- 我已給予機會詢問有關該測試的問題,並已獲得滿意的回答。
- 我已明白在資料單張上所寫的所有內容
- 我已明白這個實驗有可能可以改善我的上肢運動功能
- 此實驗不會給您帶來不適,我已明白在實驗中我可以終止測試而無需給予任何理由,或 由此而受到任何懲罰。

- 我已知道這個測試的結果可被發表, 但有關我個人的結果將獲得保密。
- 我已知道這個測試的結果屬香港理工大 學 。
- 我同意本項目負責人及其受權的項目研究人員使用我的實驗記錄以作此項目的研究。

受試者姓名	簽署	_日期
作證人姓名	簽署	日期
研究員姓名	簽署	日期

REFERENCES

- Alsuradi, H., Park, W., and Eid, M. (2020). EEG-Based Neurohaptics Research: A Literature Review. *IEEE Access* 8, 49313–49328. doi: 10.1109/ACCESS.2020.2979855
- Aman, J. E., Elangovan, N., Yeh, I.-L., and Konczak, J. (2014). The effectiveness of proprioceptive training for improving motor function: a systematic review. *Front. Hum. Neurosci.* 8, 1075. doi: 10.3389/fnhum.2014.01075
- Amano, Y., Noma, T., Etoh, S., Miyata, R., Kawamura, K., and Shimodozono, M. (2020). Reaching exercise for chronic paretic upper extremity after stroke using a novel rehabilitation robot with arm-weight support and concomitant electrical stimulation and vibration: before-and-after feasibility trial. *Biomed. Eng. Online* 19. doi: 10.1186/s12938-020-00774-3
- Artoni, F., Fanciullacci, C., Bertolucci, F., Panarese, A., Makeig, S., Micera, S., et al. (2017). Unidirectional brain to muscle connectivity reveals motor cortex control of leg muscles during stereotyped walking. *NeuroImage* 159, 403–416. doi: 10.1016/j.neuroimage.2017.07.013
- Asan, A. S., McIntosh, J. R., and Carmel, J. B. (2021). Targeting Sensory and Motor Integration for Recovery of Movement After CNS Injury. *Front. Neurosci.* 15, 791824. doi: 10.3389/fnins.2021.791824
- Aumann, T. D., and Prut, Y. (2015). Do sensorimotor β-oscillations maintain muscle synergy representations in primary motor cortex? *Trends in neurosciences* 38, 77–85. doi: 10.1016/j.tins.2014.12.002
- Babiloni, F., Cincotti, F., Babiloni, C., Carducci, F., Mattia, D., Astolfi, L., et al. (2005). Estimation of the cortical functional connectivity with the multimodal integration of high-resolution EEG and fMRI data by directed transfer function. *NeuroImage* 24, 118–131. doi: 10.1016/j.neuroimage.2004.09.036
- Backes, W. H., Mess, W. H., van Kranen-Mastenbroek, V., and Reulen, J. P. (2000). Somatosensory cortex responses to median nerve stimulation: fMRI effects of current amplitude and selective attention. *Clin. Neurophysiol.* 111, 1738–1744. doi: 10.1016/S1388-2457(00)00420-X
- Bao, S.-C., Khan, A., Song, R., and Kai-Yu Tong, R. (2020). Rewiring the Lesioned Brain: Electrical Stimulation for Post-Stroke Motor Restoration. *Journal of stroke* 22, 47–63. doi: 10.5853/jos.2019.03027

- Bao, S.-C., Leung, K. W., and Tong, K.-Y. (2021). Cortico-muscular interaction to monitor the effects of neuromuscular electrical stimulation pedaling training in chronic stroke. *Comput. Biol. Med.* 137, 104801. doi: 10.1016/j.compbiomed.2021.104801
- Basla, C., Chee, L., Valle, G., Crema, A., Micera, S., Riener, R., et al. (2023). "Sensory-Motor Neurostimulation to Enhance Exosuit Performance," in *2023 International Conference on Rehabilitation Robotics (ICORR)* (IEEE), 1–6.
- Bauer, M., Oostenveld, R., Peeters, M., and Fries, P. (2006). Tactile spatial attention enhances gamma-band activity in somatosensory cortex and reduces low-frequency activity in parieto-occipital areas. *J. Neurosci.* 26, 490–501. doi: 10.1523/JNEUROSCI.5228-04.2006
- Bohannon, R. W., and Smith, M. B. (1987). Interrater reliability of a modified Ashworth scale of muscle spasticity. *Phys. Ther.* 67, 206–207. doi: 10.1093/ptj/67.2.206
- Bolognini, N., Russo, C., and Edwards, D. J. (2016). The sensory side of post-stroke motor rehabilitation. *Restor. Neurol. Neurosci.* 34, 571–586. doi: 10.3233/RNN-150606
- Bolton, D. A. E., and Staines, W. R. (2012). Age-related loss in attention-based modulation of tactile stimuli at early stages of somatosensory processing. *Neuropsychologia* 50, 1502–1513. doi: 10.1016/j.neuropsychologia.2012.03.002
- Bowden, J. L., Lin, G. G., and McNulty, P. A. (2014). The prevalence and magnitude of impaired cutaneous sensation across the hand in the chronic period post-stroke. *PLoS One* 9, e104153. doi: 10.1371/journal.pone.0104153
- Brovelli, A., Ding, M., Ledberg, A., Chen, Y., Nakamura, R., and Bressler, S. L. (2004). Beta oscillations in a large-scale sensorimotor cortical network: directional influences revealed by Granger causality. *Proceedings of the National Academy of Sciences of the United States of America* 101, 9849–9854. doi: 10.1073/pnas.0308538101
- Calabrò, R. S., Naro, A., Russo, M., Milardi, D., Leo, A., Filoni, S., et al. (2017). Is two better than one? Muscle vibration plus robotic rehabilitation to improve upper limb spasticity and function: A pilot randomized controlled trial. *PLoS One* 12, e0185936. doi: 10.1371/journal.pone.0185936
- Carey, J. R., Kimberley, T. J., Lewis, S. M., Auerbach, E. J., Dorsey, L., Rundquist, P., et al. (2002). Analysis of fMRI and finger tracking training in subjects with chronic stroke. *Brain* 125, 773–788. doi: 10.1093/brain/awf091

- Carrol, D. (1965). A quantitative test of upper extremity function. *Journal of chronic diseases* 18, 479–491. doi: 10.1016/0021-9681(65)90030-5
- Carson, R. G., and Buick, A. R. (2021). Neuromuscular electrical stimulation-promoted plasticity of the human brain. *The Journal of physiology* 599, 2375–2399. doi: 10.1113/JP278298
- Cauraugh, J., Light, K., Kim, S., Thigpen, M., and Behrman, A. (2000). Chronic motor dysfunction after stroke: recovering wrist and finger extension by electromyographytriggered neuromuscular stimulation. *Stroke* 31, 1360–1364. doi: 10.1161/01.str.31.6.1360
- Celletti, C., Suppa, A., Bianchini, E., Lakin, S., Toscano, M., La Torre, G., et al. (2020). Promoting post-stroke recovery through focal or whole body vibration: criticisms and prospects from a narrative review. *Neurol. Sci.* 41, 11–24. doi: 10.1007/s10072-019-04047-3
- Chae, J., and Yu, D. (2000). A critical review of neuromuscular electrical stimulation for treatment of motor dysfunction in hemiplegia. *Assist. Technol.* 12, 33–49. doi: 10.1080/10400435.2000.10132008
- Choi, S., and Kuchenbecker, K. J. (2013). Vibrotactile Display: Perception, Technology, and Applications. *Proc. IEEE* 101, 2093–2104. doi: 10.1109/JPROC.2012.2221071
- Conforto, A. B., Dos Anjos, S. M., Bernardo, W. M., Da Silva, A. A., Conti, J., Machado, A. G., et al. (2018). Repetitive Peripheral Sensory Stimulation and Upper Limb Performance in Stroke: A Systematic Review and Meta-analysis. *Neurorehabil. Neural. Repair.* 32, 863–871. doi: 10.1177/1545968318798943
- Conrad, M. O., Scheidt, R. A., and Schmit, B. D. (2011). Effects of wrist tendon vibration on arm tracking in people poststroke. *Journal of neurophysiology* 106, 1480–1488. doi: 10.1152/jn.00404.2010
- Corbet, T., Iturrate, I., Pereira, M., Perdikis, S., and Del Millán, J. R. (2018). Sensory threshold neuromuscular electrical stimulation fosters motor imagery performance. *NeuroImage* 176, 268–276. doi: 10.1016/j.neuroimage.2018.04.005
- Cordo, P., Wolf, S., Lou, J.-S., Bogey, R., Stevenson, M., Hayes, J., et al. (2013). Treatment of severe hand impairment following stroke by combining assisted movement, muscle vibration, and biofeedback. *Journal of neurologic physical therapy: JNPT* 37, 194–203. doi: 10.1097/NPT.00000000000000000

- Delorme, A., and Makeig, S. (2004). EEGLAB: an open source toolbox for analysis of single-trial EEG dynamics including independent component analysis. *J. Neurosci. Methods* 134, 9–21. doi: 10.1016/j.jneumeth.2003.10.009
- Delorme, A., Mullen, T., Kothe, C., Akalin Acar, Z., Bigdely-Shamlo, N., Vankov, A., et al. (2011). EEGLAB, SIFT, NFT, BCILAB, and ERICA: New Tools for Advanced EEG Processing. *Comput. Intell. Neurosci.* 2011, 1–12. doi: 10.1155/2011/130714
- Delorme, A., Westerfield, M., and Makeig, S. (2007). Medial prefrontal theta bursts precede rapid motor responses during visual selective attention. *J. Neurosci.* 27, 11949–11959. doi: 10.1523/JNEUROSCI.3477-07.2007
- Dorsch, S., Carling, C., Cao, Z., Fanayan, E., Graham, P. L., McCluskey, A., et al. (2023). Bobath therapy is inferior to task-specific training and not superior to other interventions in improving arm activity and arm strength outcomes after stroke: a systematic review. *J. Physiother.* 69, 15–22. doi: 10.1016/j.jphys.2022.11.008
- Edwards, L. L., King, E. M., Buetefisch, C. M., and Borich, M. R. (2019). Putting the "sensory" into sensorimotor control: the role of sensorimotor integration in goal-directed hand movements after stroke. *Front. Integr. Neurosci.* 13, 16. doi: 10.3389/fnint.2019.00016
- EEGLAB Toolbox (2023). Accessed October 24, 2023, https://sccn.ucsd.edu/eeglab/index.php
- Farmer, J., Zhao, X., van Praag, H., Wodtke, K., Gage, F. H., and Christie, B. R. (2004). Effects of voluntary exercise on synaptic plasticity and gene expression in the dentate gyrus of adult male Sprague-Dawley rats in vivo. *Neuroscience* 124, 71–79. doi: 10.1016/j.neuroscience.2003.09.029
- Feigin, V. L., Brainin, M., Norrving, B., Martins, S., Sacco, R. L., Hacke, W., et al. (2022). World Stroke Organization (WSO): Global Stroke Fact Sheet 2022. *International Journal of Stroke* 17, 18–29. doi: 10.1177/17474930211065917
- FieldTrip Toolbox (2023). Accessed October 24, 2023, https://www.fieldtriptoolbox.org/
- Filippi, G. M., Rodio, A., Fattorini, L., Faralli, M., Ricci, G., and Pettorossi, V. E. (2023). Plastic changes induced by muscle focal vibration: A possible mechanism for long-term motor improvements. *Front. Neurosci.* 17, 1112232. doi: 10.3389/fnins.2023.1112232

- Fleury, M., Lioi, G., Barillot, C., and Lécuyer, A. (2020). A Survey on the Use of Haptic Feedback for Brain-Computer Interfaces and Neurofeedback. *Front. Neurosci.* 14, 528. doi: 10.3389/fnins.2020.00528
- Fraser, C., Power, M., Hamdy, S., Rothwell, J., Hobday, D., Hollander, I., et al. (2002). Driving plasticity in human adult motor cortex is associated with improved motor function after brain injury. *Neuron* 34, 831–840. doi: 10.1016/s0896-6273(02)00705-5
- Gassert, R., and Dietz, V. (2018). Rehabilitation robots for the treatment of sensorimotor deficits: a neurophysiological perspective. *J Neuro Engineering Rehabil* 15, 46. doi: 10.1186/s12984-018-0383-x
- Genna, C., Oddo, C. M., Fanciullacci, C., Chisari, C., Jörntell, H., Artoni, F., et al. (2017). Spatiotemporal Dynamics of the Cortical Responses Induced by a Prolonged Tactile Stimulation of the Human Fingertips. *Brain topography* 30, 473–485. doi: 10.1007/s10548-017-0569-8
- Geweke, J. (1982). Measurement of Linear Dependence and Feedback between Multiple Time Series. *Journal of the American Statistical Association* 77, 304–313. doi: 10.1080/01621459.1982.10477803
- Gopaul, U., Carey, L., Callister, R., Nilsson, M., and van Vliet, P. (2018). Combined somatosensory and motor training to improve upper limb function following stroke: a systematic scoping review. *Phys. Ther. Rev.* 23, 355–375. doi: 10.1080/10833196.2018.1553668
- Graczyk, E. L., Delhaye, B. P., Schiefer, M. A., Bensmaia, S. J., and Tyler, D. J. (2018). Sensory adaptation to electrical stimulation of the somatosensory nerves. *J. Neural Eng.* 15, 46002. doi: 10.1088/1741-2552/aab790
- Grandchamp, R., and Delorme, A. (2011). Single-trial normalization for event-related spectral decomposition reduces sensitivity to noisy trials. *Front. Psychol.* 2, 236. doi: 10.3389/fpsyg.2011.00236
- Guo, Z., Qian, Q., Wong, K., Zhu, H., Huang, Y., Hu, X., et al. (2020). Altered Corticomuscular Coherence (CMCoh) Pattern in the Upper Limb During Finger Movements After Stroke. *Front. Neurol.* 11, 410. doi: 10.3389/fneur.2020.00410
- Handelzalts, S., Ballardini, G., Avraham, C., Pagano, M., Casadio, M., and Nisky, I.
 (2021). Integrating Tactile Feedback Technologies Into Home-Based
 Telerehabilitation: Opportunities and Challenges in Light of COVID-19 Pandemic.
 Front. Neurorobot. 15, 617636. doi: 10.3389/fnbot.2021.617636

- Hartmann, M. J. Z. (2009). Active touch, exploratory movements, and sensory prediction. *Integr. Comp. Biol.* 49, 681–690. doi: 10.1093/icb/icp107
- Hautasaari, P., Kujala, U. M., and Tarkka, I. M. (2019). Detecting differences with magnetoencephalography of somatosensory processing after tactile and electrical stimuli. *J. Neurosci. Methods* 311, 331–337. doi: 10.1016/j.jneumeth.2018.09.014
- Hu, X., Tong, K., Tsang, V. S., and Song, R. (2006). Joint-angle-dependent neuromuscular dysfunctions at the wrist in persons after stroke. *Arch. Phys. Med. Rehabil.* 87, 671–679. doi: 10.1016/j.apmr.2006.02.003
- Hu, X. L., Tong, K.-Y., Song, R., Zheng, X. J., and Leung, W. F. W. (2009). A comparison between electromyography-driven robot and passive motion device on wrist rehabilitation for chronic stroke. *Neurorehabil. Neural. Repair.* 23, 837–846. doi: 10.1177/1545968309338191
- Hu, X.-L., Tong, R. K., Ho, N. S. K., Xue, J., Rong, W., and Li, L. S. W. (2015). Wrist Rehabilitation Assisted by an Electromyography-Driven Neuromuscular Electrical Stimulation Robot After Stroke. *Neurorehabil. Neural. Repair.* 29, 767–776. doi: 10.1177/1545968314565510
- Huang, Y., Jiao, J., Hu, J., Hsing, C., Lai, Z., Yang, Y., et al. (2020a). Measurement of sensory deficiency in fine touch after stroke during textile fabric stimulation by electroencephalography (EEG). *J. Neural Eng.* 17, 45007. doi: 10.1088/1741-2552/aba160
- Huang, Y., Nam, C., Li, W., Rong, W., Xie, Y., Liu, Y., et al. (2020b). A comparison of the rehabilitation effectiveness of neuromuscular electrical stimulation robotic hand training and pure robotic hand training after stroke: A randomized controlled trial. *Biomed. Signal Process. Control* 56, 101723. doi: 10.1016/j.bspc.2019.101723
- Insausti-Delgado, A., López-Larraz, E., Omedes, J., and Ramos-Murguialday, A. (2020). Intensity and Dose of Neuromuscular Electrical Stimulation Influence Sensorimotor Cortical Excitability. *Front. Neurosci.* 14, 593360. doi: 10.3389/fnins.2020.593360
- Jones, T. A. (2017). Motor compensation and its effects on neural reorganization after stroke. *Nat Rev Neurosci* 18, 267–280. doi: 10.1038/nrn.2017.26
- Jousmäki, V. (2000). Tracking functions of cortical networks on a millisecond timescale. *Neural Netw.* 13, 883–889. doi: 10.1016/S0893-6080(00)00061-7

- Kessner, S. S., Bingel, U., and Thomalla, G. (2016). Somatosensory deficits after stroke: a scoping review. *Topics in stroke rehabilitation* 23, 136–146. doi: 10.1080/10749357.2015.1116822
- Khajuria, A., and Joshi, D. (2022). EEG-explained cortical correlates of transfemoral amputees during balancing with vibrotactile feedback: A pilot study. *Medical engineering & physics* 101, 103772. doi: 10.1016/j.medengphy.2022.103772
- Kim, M.-Y., Kwon, H., Yang, T.-H., and Kim, K. (2020). Vibration Alert to the Brain: Evoked and Induced MEG Responses to High-Frequency Vibrotactile Stimuli on the Index Finger of Dominant and Non-dominant Hand. *Front. Hum. Neurosci.* 14, 576082. doi: 10.3389/fnhum.2020.576082
- Kristeva, R., Patino, L., and Omlor, W. (2007). Beta-range cortical motor spectral power and corticomuscular coherence as a mechanism for effective corticospinal interaction during steady-state motor output. *NeuroImage* 36, 785–792. doi: 10.1016/j.neuroimage.2007.03.025
- Lan, Y., Yao, J., and Dewald, J. P. A. (2011). The impact of shoulder abduction loading on EMG-based intention detection of hand opening and closing after stroke. *Annual International Conference of the IEEE Engineering in Medicine and Biology Society. IEEE Engineering in Medicine and Biology Society. Annual International Conference* 2011, 4136–4139. doi: 10.1109/IEMBS.2011.6091027
- Lapole, T., and Tindel, J. (2015). Acute effects of muscle vibration on sensorimotor integration. *Neuroscience Letters* 587, 46–50. doi: 10.1016/j.neulet.2014.12.025
- Lawrence, E. S., Coshall, C., Dundas, R., Stewart, J., Rudd, A. G., Howard, R., et al. (2001). Estimates of the prevalence of acute stroke impairments and disability in a multiethnic population. *Stroke* 32, 1279–1284. doi: 10.1161/01.str.32.6.1279
- Lin, L., Kuet, M.-T., Qing, W., Zhao, H., Ye, F., Huang, Y., et al. (2024a). "Effects of Sensorimotor-Integrated (SMI) Wrist/hand Rehabilitation Assisted by a Hybrid Soft Robot Poststroke," in 2024 17th International Convention on Rehabilitation Engineering and Assistive Technology (i-CREATe) (IEEE), 1–4.
- Lin, L., Qing, W., Huang, Y., Ye, F., Rong, W., Li, W., et al. (2024b). Comparison of Immediate Neuromodulatory Effects between Focal Vibratory and Electrical Sensory Stimulations after Stroke. *Bioengineering* 11, 286. doi: 10.3390/bioengineering11030286
- Lin, L., Qing, W., Zheng, Z., Poon, W., Guo, S., Zhang, S., et al. (2024c). Somatosensory integration in robot-assisted motor restoration post-stroke. *Front. Aging. Neurosci.* 16. doi: 10.3389/fnagi.2024.1491678

- Lin, L., Zhang, F., Yang, L., and Fu, Y. (2021). Design and modeling of a hybrid soft-rigid hand exoskeleton for poststroke rehabilitation. *Int. J. Mech. Sci.* 212, 106831. doi: 10.1016/j.ijmecsci.2021.106831
- Lou, X., Xiao, S., Qi, Y., Hu, X., Wang, Y., and Zheng, X. (2013). Corticomuscular coherence analysis on hand movement distinction for active rehabilitation. *Comput. Math. Method Med.* 2013, 908591. doi: 10.1155/2013/908591
- Maciejasz, P., Eschweiler, J., Gerlach-Hahn, K., Jansen-Troy, A., and Leonhardt, S. (2014). A survey on robotic devices for upper limb rehabilitation. *J. NeuroEng. Rehabil.* 11, 3. doi: 10.1186/1743-0003-11-3
- Makeig, S., Bell, A., Jung, T.-P., and Sejnowski, T. J. (1995). Independent Component Analysis of Electroencephalographic Data. *Adv. Neural Inf. Process. Syst.* 8, 146–151.
- Mane, R., Chouhan, T., and Guan, C. (2020). BCI for stroke rehabilitation: motor and beyond. *J. Neural Eng.* 17, 41001. doi: 10.1088/1741-2552/aba162
- Mastrich, Z., and Hernandez, I. (2021). Results everyone can understand: A review of common language effect size indicators to bridge the research-practice gap. *Health psychology: official journal of the Division of Health Psychology, American Psychological Association* 40, 727–736. doi: 10.1037/hea0001112
- Michail, G., Dresel, C., Witkovský, V., Stankewitz, A., and Schulz, E. (2016). Neuronal Oscillations in Various Frequency Bands Differ between Pain and Touch. *Front. Hum. Neurosci.* 10, 182. doi: 10.3389/fnhum.2016.00182
- Miller, L. C., and Dewald, J. P. A. (2012). Involuntary paretic wrist/finger flexion forces and EMG increase with shoulder abduction load in individuals with chronic stroke. *Clinical neurophysiology : official journal of the International Federation of Clinical Neurophysiology* 123, 1216–1225. doi: 10.1016/j.clinph.2012.01.009
- Mima, T., and Hallett, M. (1999). Electroencephalographic analysis of cortico-muscular coherence: reference effect, volume conduction and generator mechanism. *Clin. Neurophysiol.* 110, 1892–1899. doi: 10.1016/S1388-2457(99)00238-2
- Mima, T., Matsuoka, T., and Hallett, M. (2001). Information flow from the sensorimotor cortex to muscle in humans. *Clin. Neurophysiol.* 112, 122–126. doi: 10.1016/S1388-2457(00)00515-0
- Muraoka, Y. (2002). Development of an EMG recording device from stimulation electrodes for functional electrical stimulation. *Front Med. Biol. Eng.* 11, 323–333. doi: 10.1163/156855701321138969

- Murillo, N., Valls-Sole, J., Vidal, J., Opisso, E., Medina, J., and Kumru, H. (2014). Focal vibration in neurorehabilitation. *Eur. J. Phys. Rehabil. Med.* 50, 231–242.
- Nam, C., Rong, W., Li, W., Cheung, C., Ngai, W., Cheung, T., et al. (2020). An Exoneuromusculoskeleton for Self-Help Upper Limb Rehabilitation After Stroke. *Soft Robot.* doi: 10.1089/soro.2020.0090
- Nam, C., Rong, W., Li, W., Xie, Y., Hu, X., and Zheng, Y. (2017). The Effects of Upper-Limb Training Assisted with an Electromyography-Driven Neuromuscular Electrical Stimulation Robotic Hand on Chronic Stroke. *Front. Neurol.* 8, 679. doi: 10.3389/fneur.2017.00679
- Nam, C., Zhang, B., Chow, T., Ye, F., Huang, Y., Guo, Z., et al. (2021). Home-based self-help telerehabilitation of the upper limb assisted by an electromyography-driven wrist/hand exoneuromusculoskeleton after stroke. *J. NeuroEng. Rehabil.* 18, 137. doi: 10.1186/s12984-021-00930-3
- Oostenveld, R., Fries, P., Maris, E., and Schoffelen, J.-M. (2011). FieldTrip: Open source software for advanced analysis of MEG, EEG, and invasive electrophysiological data. *Comput. Intell. Neurosci.* 2011, 156869. doi: 10.1155/2011/156869
- Ortiz Alonso, T., Santos, J. M., Ortiz Terán, L., Borrego Hernández, M., Poch Broto, J., and Erausquin, G. A. de (2015). Differences in Early Stages of Tactile ERP Temporal Sequence (P100) in Cortical Organization during Passive Tactile Stimulation in Children with Blindness and Controls. *PLoS One* 10, e0124527. doi: 10.1371/journal.pone.0124527
- Otsuru, N., Inui, K., Yamashiro, K., Urakawa, T., Keceli, S., and Kakigi, R. (2011). Effects of prior sustained tactile stimulation on the somatosensory response to the sudden change of intensity in humans: an magnetoencephalography study. *Neuroscience* 182, 115–124. doi: 10.1016/j.neuroscience.2011.03.019
- Paillard, T. (2021). Neuromuscular or Sensory Electrical Stimulation for Reconditioning Motor Output and Postural Balance in Older Subjects? *Front. Physiol.* 12, 779249. doi: 10.3389/fphys.2021.779249
- Pan, L.-L. H., Yang, W.-W., Kao, C.-L., Tsai, M.-W., Wei, S.-H., Fregni, F., et al. (2018). Effects of 8-week sensory electrical stimulation combined with motor training on EEG-EMG coherence and motor function in individuals with stroke. *Sci. Rep.* 8, 9217. doi: 10.1038/s41598-018-27553-4
- Papale, A. E., and Hooks, B. M. (2018). Circuit changes in motor cortex during motor skill learning. *Neuroscience* 368, 283–297. doi: 10.1016/j.neuroscience.2017.09.010

- Perle, S. M., Schneider, M. J., and Seaman, D. R. (1999). Chiropractic Management of Peripheral Neuropathy: Pathophysiology, Assessment, and Treatment. *Top. Clin. Chiropr.*
- Perpetuini, D., Russo, E. F., Cardone, D., Palmieri, R., Giacomo, A. de, Pellegrino, R., et al. (2023). Use and Effectiveness of Electrosuit in Neurological Disorders: A Systematic Review with Clinical Implications. *Bioengineering* 10, 680. doi: 10.3390/bioengineering10060680
- Pope, K. J., Lewis, T. W., Fitzgibbon, S. P., Janani, A. S., Grummett, T. S., Williams,
 P. A. H., et al. (2022). Managing electromyogram contamination in scalp recordings:
 An approach identifying reliable beta and gamma EEG features of psychoses or other disorders. *Brain and behavior* 12, e2721. doi: 10.1002/brb3.2721
- Qian, Q., Nam, C., Guo, Z., Huang, Y., Hu, X., Ng, S. C., et al. (2019). Distal versus proximal an investigation on different supportive strategies by robots for upper limb rehabilitation after stroke: a randomized controlled trial. *J. NeuroEng. Rehabil.* 16. doi: 10.1186/s12984-019-0537-5
- Qing, W., Song, H., Lin, L., Ye, F., and Hu, X. (2024). "Reorganization of Undirected and Directed Cortico-Muscular Connectivity After Exoneuromusculoskeleton-Assisted Telerehabilitation," in 2024 17th International Convention on Rehabilitation Engineering and Assistive Technology (i-CREATe) (IEEE), 1–5.
- Raghavan, P. (2015). Upper Limb Motor Impairment After Stroke. *Phys. Med. Rehabil. Clin. N. Am.* 26, 599–610. doi: 10.1016/j.pmr.2015.06.008
- Remsik, A. B., van Kan, P. L. E., Gloe, S., Gjini, K., Williams, L., Nair, V., et al. (2022). BCI-FES With Multimodal Feedback for Motor Recovery Poststroke. *Front. Hum. Neurosci.* 16, 725715. doi: 10.3389/fnhum.2022.725715
- Resquin, F., Cuesta Gomez, A., Gonzalez-Vargas, J., Brunetti, F., Torricelli, D., Molina Rueda, F., et al. (2016). Hybrid robotic systems for upper limb rehabilitation after stroke: A review. *Med. Eng. Phys.* 38, 1279–1288. doi: 10.1016/j.medengphy.2016.09.001
- Reuter, E.-M., Voelcker-Rehage, C., Vieluf, S., Winneke, A. H., and Godde, B. (2014). Extensive occupational finger use delays age effects in tactile perception-an ERP study. *Attention, perception & psychophysics* 76, 1160–1175. doi: 10.3758/s13414-014-0634-2
- Rodgers, H., Bosomworth, H., Krebs, H. I., van Wijck, F., Howel, D., Wilson, N., et al. (2019). Robot assisted training for the upper limb after stroke (RATULS): a

- multicentre randomised controlled trial. *Lancet (London, England)* 394, 51–62. doi: 10.1016/S0140-6736(19)31055-4
- Rong, W., Li, W., Pang, M., Hu, J., Wei, X., Yang, B., et al. (2017). A Neuromuscular Electrical Stimulation (NMES) and robot hybrid system for multi-joint coordinated upper limb rehabilitation after stroke. *J. NeuroEng. Rehabil.* 14, 34. doi: 10.1186/s12984-017-0245-y
- Schranz, C., Vatinno, A., Ramakrishnan, V., and Seo, N. J. (2022). Neuroplasticity after upper-extremity rehabilitation therapy with sensory stimulation in chronic stroke survivors. *Brain communications* 4, fcac191. doi: 10.1093/braincomms/fcac191
- Seeck, M., Koessler, L., Bast, T., Leijten, F., Michel, C., Baumgartner, C., et al. (2017). The standardized EEG electrode array of the IFCN. *Clin. Neurophysiol.* 128, 2070–2077. doi: 10.1016/j.clinph.2017.06.254
- Seim, C. E., Wolf, S. L., and Starner, T. E. (2021). Wearable vibrotactile stimulation for upper extremity rehabilitation in chronic stroke: clinical feasibility trial using the VTS Glove. *J. NeuroEng. Rehabil.* 18. doi: 10.1186/s12984-021-00813-7
- Shindo, K., Fujiwara, T., Hara, J., Oba, H., Hotta, F., Tsuji, T., et al. (2011). Effectiveness of hybrid assistive neuromuscular dynamic stimulation therapy in patients with subacute stroke: a randomized controlled pilot trial. *Neurorehabil. Neural. Repair.* 25, 830–837. doi: 10.1177/1545968311408917
- Sitaram, R., Ros, T., Stoeckel, L., Haller, S., Scharnowski, F., Lewis-Peacock, J., et al. (2017). Closed-loop brain training: the science of neurofeedback. *Nature reviews*. *Neuroscience* 18, 86–100. doi: 10.1038/nrn.2016.164
- Smith, G. V., Alon, G., Roys, S. R., and Gullapalli, R. P. (2003). Functional MRI determination of a dose-response relationship to lower extremity neuromuscular electrical stimulation in healthy subjects. *Exp. Brain Res.* 150, 33–39. doi: 10.1007/s00221-003-1405-9
- Souron, R., Besson, T., Millet, G. Y., and Lapole, T. (2017). Acute and chronic neuromuscular adaptations to local vibration training. *Eur. J. Appl. Physiol.* 117, 1939–1964. doi: 10.1007/s00421-017-3688-8
- Stoykov, M. E., Heidle, C., Kang, S., Lodesky, L., Maccary, L. E., and Madhavan, S. (2021). Sensory-Based Priming for Upper Extremity Hemiparesis After Stroke: A Scoping Review. *OTJR: Occupation, Participation and Health*, 15394492211032606. doi: 10.1177/15394492211032606

- Stoykov, M. E., and Madhavan, S. (2015). Motor priming in neurorehabilitation. *Journal of neurologic physical therapy : JNPT* 39, 33–42. doi: 10.1097/NPT.0000000000000065
- Suda, M., Kawakami, M., Okuyama, K., Ishii, R., Oshima, O., Hijikata, N., et al. (2020). Validity and Reliability of the Semmes-Weinstein Monofilament Test and the Thumb Localizing Test in Patients With Stroke. *Front. Neurol.* 11, 625917. doi: 10.3389/fneur.2020.625917
- Sullivan, K. J., Tilson, J. K., Cen, S. Y., Rose, D. K., Hershberg, J., Correa, A., et al. (2011). Fugl-Meyer assessment of sensorimotor function after stroke: standardized training procedure for clinical practice and clinical trials. *Stroke* 42, 427–432. doi: 10.1161/STROKEAHA.110.592766
- Timmermans, A. A. A., Spooren, A. I. F., Kingma, H., and Seelen, H. A. M. (2010). Influence of task-oriented training content on skilled arm-hand performance in stroke: a systematic review. *Neurorehabil. Neural. Repair.* 24, 858–870. doi: 10.1177/1545968310368963
- Tombaugh, T. N., and McIntyre, N. J. (1992). The mini-mental state examination: a comprehensive review. *J. Am. Geriatr. Soc.* 40, 922–935. doi: 10.1111/j.1532-5415.1992.tb01992.x
- Turville, M. L., Cahill, L. S., Matyas, T. A., Blennerhassett, J. M., and Carey, L. M. (2019). The effectiveness of somatosensory retraining for improving sensory function in the arm following stroke: a systematic review. *Clin Rehabil* 33, 834–846. doi: 10.1177/0269215519829795
- Tyson, S. F., Hanley, M., Chillala, J., Selley, A. B., and Tallis, R. C. (2008). Sensory loss in hospital-admitted people with stroke: characteristics, associated factors, and relationship with function. *Neurorehabil. Neural. Repair.* 22, 166–172. doi: 10.1177/1545968307305523
- Valery L Feigin, Benjamin A Stark, Catherine Owens Johnson, Gregory A Roth, Catherine Bisignano, Gdiom Gebreheat Abady, et al. (2021). Global, regional, and national burden of stroke and its risk factors, 1990-2019: a systematic analysis for the Global Burden of Disease Study 2019. *The Lancet Neurology* 20, 795–820. doi: 10.1016/S1474-4422(21)00252-0

- Wang, A. L., Mouraux, A., Liang, M., and Iannetti, G. D. (2010). Stimulus novelty, and not neural refractoriness, explains the repetition suppression of laser-evoked potentials. *Journal of neurophysiology* 104, 2116–2124. doi: 10.1152/jn.01088.2009
- Wang, H., Chandrashekhar, R., Rippetoe, J., and Ghazi, M. (2020). Focal Muscle Vibration for Stroke Rehabilitation: A Review of Vibration Parameters and Protocols. *Appl. Sci.-Basel* 10, 8270. doi: 10.3390/app10228270
- Wang, H., Ghazi, M., Chandrashekhar, R., Rippetoe, J., Duginski, G. A., Lepak, L. V., et al. (2022). User Participatory Design of a Wearable Focal Vibration Device for Home-Based Stroke Rehabilitation. *Sensors* 22, 3308. doi: 10.3390/s22093308
- Wilkins, K. B., Owen, M., Ingo, C., Carmona, C., Dewald, J. P. A., and Yao, J. (2017). Neural Plasticity in Moderate to Severe Chronic Stroke Following a Device-Assisted Task-Specific Arm/Hand Intervention. *Front. Neurol.* 8, 284. doi: 10.3389/fneur.2017.00284
- Williamson, J. N., Sikora, W. A., James, S. A., Parmar, N. J., Lepak, L. V., Cheema, C. F., et al. (2022). Cortical Reorganization of Early Somatosensory Processing in Hemiparetic Stroke. *J. Clin. Med.* 11. doi: 10.3390/jcm11216449
- Witham, C. L., Wang, M., and Baker, S. N. (2010). Corticomuscular coherence between motor cortex, somatosensory areas and forearm muscles in the monkey. *Front. Syst. Neurosci.* 4. doi: 10.3389/fnsys.2010.00038
- Wolf, S. L., Lecraw, D. E., Barton, L. A., and Jann, B. B. (1989). Forced use of hemiplegic upper extremities to reverse the effect of learned nonuse among chronic stroke and head-injured patients. *Experimental neurology* 104, 125–132. doi: 10.1016/S0014-4886(89)80005-6
- Wolpert, D. M., Diedrichsen, J., and Flanagan, J. R. (2011). Principles of sensorimotor learning. *Nat Rev Neurosci* 12, 739–751. doi: 10.1038/nrn3112
- Wolpert, D. M., Goodbody, S. J., and Husain, M. (1998). Maintaining internal representations: the role of the human superior parietal lobe. *Nat Neurosci* 1, 529–533. doi: 10.1038/2245
- Xing, Y., and Bai, Y. (2020). A Review of Exercise-Induced Neuroplasticity in Ischemic Stroke: Pathology and Mechanisms. *Mol. Neurobiol.* 57, 4218–4231. doi: 10.1007/s12035-020-02021-1
- Yakovlev, L., Syrov, N., Miroshnikov, A., Lebedev, M., and Kaplan, A. (2023). Event-Related Desynchronization Induced by Tactile Imagery: an EEG Study. *eNeuro* 10, 1–12. doi: 10.1523/ENEURO.0455-22.2023

- Yeh, I.-L., Holst-Wolf, J., Elangovan, N., Cuppone, A. V., Lakshminarayan, K., Cappello, L., et al. (2021). Effects of a robot-aided somatosensory training on proprioception and motor function in stroke survivors. *J. NeuroEng. Rehabil.* 18, 77. doi: 10.1186/s12984-021-00871-x
- Yilmazer, C., Boccuni, L., Thijs, L., and Verheyden, G. (2019). Effectiveness of somatosensory interventions on somatosensory, motor and functional outcomes in the upper limb post-stroke: A systematic review and meta-analysis. *NeuroRehabilitation* 44, 459–477. doi: 10.3233/NRE-192687
- Zhang, F., Lin, L., Yang, L., and Fu, Y. (2019a). Design of an Active and Passive Control System of Hand Exoskeleton for Rehabilitation. *Appl. Sci.-Basel* 9, 2291. doi: 10.3390/app9112291
- Zhang, F., Lin, L., Yang, L., and Fu, Y. (2019b). Variable impedance control of finger exoskeleton for hand rehabilitation following stroke. *Ind. Robot* 47, 23–32. doi: 10.1108/IR-02-2019-0034
- Zhang, J., Wang, M., Alam, M., Zheng, Y.-P., Ye, F., and Hu, X. (2024). Effects of non-invasive cervical spinal cord neuromodulation by trans-spinal electrical stimulation on cortico-muscular descending patterns in upper extremity of chronic stroke. *Front. Bioeng. Biotechnol.* 12, 1372158. doi: 10.3389/fbioe.2024.1372158
- Zhang, K., Chen, X., Liu, F., Tang, H., Wang, J., and Wen, W. (2018). System Framework of Robotics in Upper Limb Rehabilitation on Poststroke Motor Recovery. *Behavioural neurology* 2018, 6737056. doi: 10.1155/2018/6737056
- Zhou, S., Guo, Z., Wong, K., Zhu, H., Huang, Y., Hu, X., et al. (2021a). Pathway-specific cortico-muscular coherence in proximal-to-distal compensation during fine motor control of finger extension after stroke. *J. Neural Eng.* 18, 56034. doi: 10.1088/1741-2552/ac20bc
- Zhou, S., Huang, Y., Jiao, J., Hu, J., Hsing, C., Lai, Z., et al. (2021b). Impairments of cortico-cortical connectivity in fine tactile sensation after stroke. *J. NeuroEng. Rehabil.* 18, 34. doi: 10.1186/s12984-021-00821-7